TRANSCRIPTIONAL REGULATION OF AXONAL PATHFINDING: FOXB1 AND THE MAMMILLOTHALAMIC TRACT

Vom Fachbereich Chemie der Universität Hannover
zur Erlangung des Grades

Doktor der Naturwissenschaften
Dr. rer. nat.

genehmigte Dissertation
von

M.Sc. Biochemistry Qiuhong Jiang
geboren am 8.Dezember 1972 in Hunan Province, China

2004

Referent:

Prof. Dr. Walter Müller

Medizinische Hochschule Hannover

Korreferent:

Prof. Dr. Gregor Eichele

Max-Planck-Institut für experimentelle Endokrinologie, Hannover

Tag der Promotion: 15. November 2004

ACKNOWLEDGEMENTS

Before I start, I would like to acknowledge all those who have helped and supported me while I was working on this PhD:

First of all, I would like to thank Prof. Dr. Gregor Eichele for the opportunity to work in this Department, and for making available to me everything that was needed for my research. Above all, his personal interest in the process of the work, fruitful discussions and guidance for the independent scientific work contributed crucially to the successful execution of my project.

I am very grateful to Prof. Dr. Walter Müller for friendly accepting to assume the task of Official Supervisor of my work in representation of the Chemistry Department of the University of Hannover, and for his support in dealing with University bureaucracy.

I particularly appreciate Dr. Gonzalo Alvarez-Bolado for his excellent scientific supervision, and for offering me the opportunity to work in his group, as well as for proposing me such an intellectually stimulating subject for my PhD. His encouragement and guidance have been essential for me to take this difficult and fascinating project to good end. I will always remember his seminars on developmental neurobiology, which have been so important for me to enter into this exciting field.

The help, advice and friendship of Dr. Axel Visel have been very important to me in everyday life in the laboratory, in setting up difficult experiments, proofreading my thesis and in overcoming the bureaucratic difficulties as a foreigner student.

I would like to thank the administration, especially Carsten Gottschalk for patiently helping with formalities.

All through these years in Hannover I have received intelligent advice and kind assistance from Dr. Pablo Szendro, Dr. Xunlei Zhou, Dr. Miki Tsukada. I am indebted to them.

I thank Barbara Fischer, Uwe Grunenberg, Ana Martínez-Hernández, Kornelia Maslo, Polina Spies and Christine Zwingmann for their help with in situ hybridization work.

My friends and colleagues, the PhD students and postdocs of the Department, Dr. Henrik Oster, Diya Abraham, Carsten Möller (Dr. Möller), Murat Yaylaoglu (Dr. Yaylaoglu), Nora Szabó, Aravind Sekhar, Vladimira Jakubcakova, Frank Sacher, Judit Oldekamp (Dr. Oldekamp), Lars Geffers, Marei Warnecke (Dr. Warnecke), Judit Kovac, Christopher Esk, Stephan Busche, Murat Cankaya, Marían Comas, Jens Mittag, Katja Hübel, Johanna Rose, Andrew Titmus, and Tianyu Zhao, contributed their help to the pleasant working climate which I could enjoy at our Institute.

The present work would have been impossible without the support of the Mouse House personnel, Ina Klebba, Alexandra Meneking, Nadine Naujokat and Hans Peter Bader, working under the wise direction of Dr. Michael Leitges.

Claus Ebert, Sarah Herzog and Markus Uhr solved promptly and expertly all my frequent computer problems, and for this they deserve many thanks.

I thank Dr. T. Ciossek and Dr. P. Vanderhaeghen (Belgium) for kindly sharing the EphA7 mutant mouse line with us.

Finally, I am grateful to my husband, my parents, and my country, China, for all what they have done for me.

TABLE OF CONTENTS

ZUSAMMENFASSUNG

Der Einfluss von Transkriptionsfaktoren auf die Navigationsentscheidungen axonaler Wachstumskegel ist eine wichtige Fragestellung in der modernen Entwicklungsneurobiologie. In der vorliegenden Arbeit wurde die Gehirnentwicklung in einem transgenen Mausstamm mit einer Nullmutation des Transkriptionsfaktors Foxb1 untersucht. In diesen Mäusen liegt ein Navigationsdefekt eines spezifischen Axonbündels, des mammillothalamischen Traktes, vor, welcher eine markante anatomische Struktur des Diencephalons ist. In den Mutanten versagt das Wachstum der mammillothalamischen Axone zu ihrer eigentliche Zielregion, dem dorsalen Thalamus. Die Neuronen, in welchen der mammillothalamische Trakt entspringt, exprimieren Foxb1. Die Fragestellung der vorliegenden Arbeit war daher, wie Foxb1 die Navigationsentscheidungen mammillothalamischer Wachstumskegel beeinflußt.

Durch DNA-Microarrays wurden zunächst die Transkriptome im Wildtyp- und Mutantengehirn verglichen. Dieser Ansatz lieferte eine Reihe von Kandidatengenen, die potentiell durch Foxb1 reguliert werden. Diese Kandidatengene wurden anschließend durch *in situ*-Hybridisierung und quantitative PCR validiert. Durch Vergleich dieser Daten mit in der Literatur vorliegenden Angaben wurde für weitere Untersuchungen der vielversprechendste Kandidat ausgewählt, die Rezeptortyrosinkinase EphA7, für die bereits eine Beteiligung an der Lenkung von Axonen in anderen Gehirnbereichen beschrieben wurde. Anschließend wurde untersucht, ob und inwiefern EphA7 das Gen (oder eines der Gene) ist, das den biologischen Zusammenhang zwischen dem regulatorischen Protein Foxb1 und dem Phänotyp in der axonalen Navigation herstellt. Die vier bekannten Isoformen des Gens wurden kloniert und im Hinblick auf ihre Expression in den beteiligten Hirnregionen in Wildtyp und Foxb1-Mutante verglichen. Die Expressionsstärke aller vier Isoformen im Diencephalon war in der Mutante reduziert. Eine Expressionsanalyse aller bekannten potentiellen Liganden dieses Rezeptors ergab, dass einer von ihnen, Ephrin A5, zum richtigen Entwicklungszeitpunkt und in der richtigen Region exprimiert ist, um als Interaktionspartner für EphA7 in Frage zu kommen. Um eine direkte Kontrolle der EphA7-Expression durch Foxb1 zu untersuchen, wurden mögliche Fox-Bindungsstellen in Abschnitten des *EphA7*-Gens identifiziert, die zwischen Mensch und Maus konserviert sind. Zur Validierung dieser Bindungsstellen wurden *yeast-one-hybrid-* und *electrophoretic-mobility-shift*-Untersuchungen durchgeführt. Schließlich wurde untersucht, welche dieser Bindungsstellen in Säugetierzellen die Expression eines Reportergens steuern können. Unerwarteterweise bewirkte Foxb1 hierbei eine Repression statt – wie aufgrund der Microarray-, *in situ*-Hybridisierungs- und quantitativen PCR-Daten erwartet – einer Aktivierung des Reportergens. Die *electrophoretic-mobility-shift*-Untersuchungen wurden daher auf ein längeres genomisches Fragment ausgeweitet, ausgehend von der Annahme, dass in Nachbarregionen des ursprünglich gewählten Fragments bisher unbekannte regulatorische Kofaktoren eine Rolle für die Funktion von Foxb1 spielen könnten. Durch diesen veränderten Ansatz konnte gezeigt werden, dass Foxb1 tatsächlich in Säugetierzellen die Expression des Reportergens durch die im *EphA7*-Gen identifizierten Bindungsstellen aktivieren kann.

Die vorliegende Arbeit zeigt, dass das Gen des Tyrosinkinaserezeptors *EphA7* in den Ursprungszellen des mammillothalamischen Traktes exprimiert ist, dass der Transkriptionsfaktor Foxb1 spezifisch an konservierte genomische Sequenzabschnitte von *EphA7* bindet, sowie dass in Abwesenheit von Foxb1 die Expression aller *EphA7*-Isoformen deutlich reduziert ist. Diese Ergebnisse legen nahe, dass *EphA7* die Verbindung zwischen Foxb1-Defizienz und dem resultierenden axonalen Navigationsdefekt darstellt und dass Foxb1 die Ausbildung mammillothalamischer Axone im Diencephalon zumindest teilweise durch eine Modulation der Interaktionen von Ephrin-Liganden und EphA-Rezeptoren beeinflusst.

Schlagwörter: Axonal navigation, Diencephalon, *fkh5*, Transkription, mammillarykörper, *mf3*, *Twh,* Mammillothalamischen Trakt, EphA7, Tyrosinkinaserezeptor, protein-DNA- interaktion, Ephrin ligand.

ABSTRACT

A current question in developmental neuroscience is: how do transcription factors influence the navigational choices of axonal growth cones? Here this question has been addressed by analyzing brain development in a mouse transgenic line carrying a null mutation of transcription factor Foxb1. These mice suffer from axonal navigational failure in a specific axonal bundle, the mammillothalamic tract, which is a distinctive anatomical feature of the diencephalic region of the brain. In the mutants, the mammillothalamic axons are not able to enter their intended target region, the dorsal thalamus. The neurons of origin of this tract express Foxb1. The specific question addressed in this work is: how does Foxb1 control the guidance decisions of the mammillothalamic growth cones?

First, DNA microarrays were used to compare the transcriptome of wild type and mutant brains. This approach yielded a number of candidates to be downstream from Foxb1. The candidates were next validated by *in situ*-hybridization and quantitative real-time PCR. Then the most appropriate candidate was chosen, based on the function of the encoded protein as found in the literature. This candidate was the receptor tyrosine kinase EphA7, reported to be involved in axonal guidance in other parts of the brain.

The biological plausibility of *EphA7* as the gene (or one of the genes) between the regulator protein Foxb1 and the phenomenon of axonal guidance was then investigated. In order to do so, the four isoforms of this gene were cloned and their expression in the appropriate region of wild type and mutant brains was determined. All of the isoforms were decreased in expression level in the diencephalon. The expression of all the potential ligands for this receptor in the region of interest was analyzed. One of them, ephrin A5, was found to be expressed at the right developmental stage in the right place to be the partner for EphA7.

To know if expression of *EphA7* is under the direct control of Foxb1, putative Fox binding sequences were identified in human-mouse conserved regions of the *EphA7* gene. Then sequences actually binding to Foxb1 were determined by means of Yeast One-Hybrid Assay, and validated by Electrophoretic Mobility Shift Assay. Finally, the ability of these binding sites to direct reporter expression in mammalian cells in culture was tested. Since the results obtained were paradoxal (Foxb1 repressed expression through these sites, instead of behaving as an activator, as could be expected from the microarray, *in situ* hybridization and quantitative PCR data), the experiments were repeated by using larger genomic sequence fragments containing not only the EMSA-confirmed binding sites but also the neighboring regions. The rationale was that maybe Foxb1 needs hitherto unknown cofactors in order to exert its normal function. These experiments showed that Foxb1 is indeed able to activate gene expression in mammalian cells through the binding sites found on *EphA7*.

These results show that tyrosine kinase receptor gene *EphA7* is expressed in the cells that originate the mammillothalamic tract; that transcriptional regulator protein Foxb1 binds specific conserved genomic sequences of EphA7; and that, in the absence of Foxb1, expression of *EphA7* and all its isoforms is severely reduced. This work suggests that *EphA7* is the link between Foxb1-deficiency and the resultant axonal navigation phenotype, and that Foxb1 guides the mammillothalamic axons at least in part by modulating the ephrin ligand-EphA receptor interaction in the diencephalon.

Key words: Axonal navigation, Diencephalon, *fkh5*, Transcription, Mammillary body, *mf3*, *Twh,* Mammillothalamic Tract, EphA7, Tyrosine Kinase Receptor, Protein-DNA- interaction, Ephrin ligand.

1 INTRODUCTION

1.1 REGULATION OF GENE EXPRESSION DURING DEVELOPMENT

The genetic information needed for development and metabolism is encoded in the DNA sequences of the chromosomes which, in eukaryotic cells, are located in the nucleus. The information in the DNA determines the structure of proteins and contains thereby the instructions on how to develop from a fertilized egg into pluripotent stem cells and further along particular cell lineages into tissues and organs.

Although every somatic cell contains the same genetic information, not all the genes are transcribed at the same time or at the same level – every cell type expresses a different set of genes which fulfill the specific needs of the cell. Transcriptional regulation of gene expression in eukaryotes is a complex process highly regulated at many levels. It requires the concerted action of several factors to integrate different transcriptional regulatory signals controlling cellular responses such as proliferation, differentiation and apoptosis. Gene expression can be regulated at the transcriptional level (which genes are transcribed into RNA), on RNA processing level (which of transcribed RNAs are transported into the cytoplasm to become messenger RNAs), at the translational level (which of the mRNAs are translated into protein), at the protein modification level (which proteins are allowed to stay functional in the cell) (Gilbert, 1997). Transcription is regulated by a complex assembly of basal transcription initiation factors, sequence-specific DNA-binding transcriptional activators and repressors and associated cofactors on promoters, enhancers and silencers (Tjian and Maniatis, 1994; St-Arnaud, 1998).

1.1.1 Regulatory transcription factors

Where the basal transcription initiation apparatus is needed for initiation of transcription but is unable to regulate the rate of it, this task belongs to regulatory transcription factors. They communicate with the basal factors through coactivator proteins. The number of basal factors is limited, whereas the number of specific transcription factors is high. The expression of regulatory transcription factors may be specific cell types or to a certain stage of development.

Transcription factors bind to *cis*-acting binding sites, located adjacent to the promoter, far upstream of it or even downstream of the gene. Sequence-specific regulators can be subdivided into activators or repressors, but several factors can mediate either activation or repression of the core promoter unitilization in a context-dependent manner. The changes in concentration of a transcription factor may affect whether it acts as an activator or as a repressor, or the response may be dependent upon the ligands present, or the physiological state of the cell (Courey, 2001).

The expression of regulatory transcription factors needs itself to be regulated, in general by other transcription factors (Gilbert, 1997). Often their enhancers and promoters are very complex, allowing them to be expressed only in certain cells (Blackwood and Kadonaga, 1998).

1.1.2 Transcription factor families

Transcription factors can be divided into several families based on the structure utilized for DNA binding or sometimes on the activation domain or oligomerization domain (Mitchell and Tjian, 1989; Tjian and Maniatis, 1994). There are several different DNA-binding domains and motifs that classify transcription families, for example, homeodomain and Myb domain, classical zinc finger motif, MADS domain, basic- region- leucine- zipper domain, forkhead motif and bHLH (basic helix-loop-helix) motif (Pabo and Sauer, 1992; Fairall and Schwabe, 2001).

1.2 FORKHEAD FAMILY OF TRANSCRIPTION FACTORS

1.2.1 General aspects of forkhead proteins

Forkhead proteins are not among the largest transcription factor families, but they are functionally very diverse and are involved in a wide variety of biological processes. The name derives from two-spiked head structures in embryos of the *Drosophila fork head* mutant, which are defective in formation of the anterior and posterior gut (Weigel et al., 1989). With the discovery in 1990 of a 110-amino-acid DNA binding domain that was almost perfectly conserved between FORK HEAD and the mammalian HNF-3 transcription factors, it became clear that this motif defined a

novel transcription factor family (Weigel and Jackle, 1990). Since then, over 100 genes encoding members of the forkhead family have been identified in a variety of eukaryotes ranging from invertebrates to humans (Kaufmann and Knochel, 1996).

1.2.1.1 Nomenclature

The official nomenclature (Kaestner et al., 2000), which uses *Fox* (for "*Forkhead box*") as the root symbol, ensures that the same name is used for orthologous genes in different species and reflects phylogenetic relationships by including a letter that indicates subfamily. Seventeen subfamilies have been delineated for known chordate Fox proteins. The constantly updated phylogenetic tree can be downloaded from the web at http://www.biology.pomona.edu/fox.html (Fig.1.1). Within a subfamily, each gene is identified by a number (e.g., *FoxB1*), the typography follows the conventions used in each species (*FOXB1* in *Homo, Foxb1* in *Mus,* and *FoxB1* in all others), and proteins are distinguished from genes by the use of roman type (e.g., FoxB1).

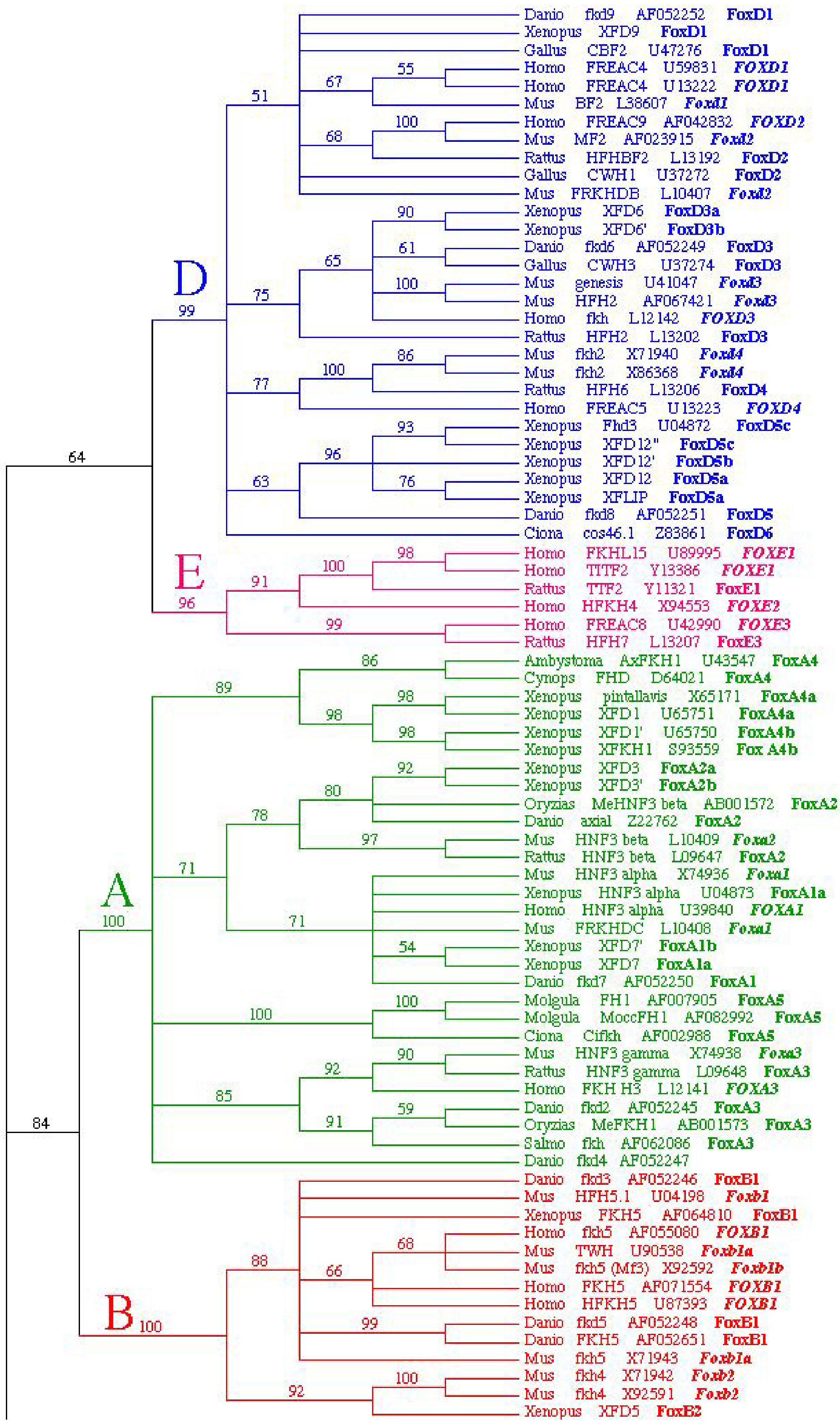
Danio fkd9 AF052252 FoxD1
Xenopus XFD9 FoxD1
Gallus CBF2 U47276 FoxD1
Homo FREAC4 U59831 FOXD1
Homo FREAC4 U13222 FOXD1
Mus BF2 L38607 Foxd1
Homo FREAC9 AF042832 FOXD2
Mus MF2 AF023915 Foxd2
Rattus HFHBF2 L13192 FoxD2
Gallus CWH1 U37272 FoxD2
Mus FRKHDB L10407 Foxd2
Xenopus XFD6 FoxD3a
Xenopus XFD6' FoxD3b
Danio fkd6 AF052249 FoxD3
Gallus CWH3 U37274 FoxD3
Mus genesis U41047 Foxd3
Mus HFH2 AF067421 Foxd3
Homo fkh L12142 FOXD3
Rattus HFH2 L13202 FoxD3
Mus fkh2 X71940 Foxd4
Mus fkh2 X86368 Foxd4
Rattus HFH6 L13206 FoxD4
Homo FREAC5 U13223 FOXD4
Xenopus Fhd3 U04872 FoxD5c
Xenopus XFD12" FoxD5c
Xenopus XFD12' FoxD5b
Xenopus XFD12 FoxD5a
Xenopus XFLIP FoxD5a
Danio fkd8 AF052251 FoxD5
Ciona cos46.1 Z83861 FoxD6
Homo FKHL15 U89995 FOXE1
Homo TITF2 Y13386 FOXE1
Rattus TTF2 Y11321 FoxE1
Homo HFKH4 X94553 FOXE2
Homo FREAC8 U42990 FOXE3
Rattus HFH7 L13207 FoxE3
Ambystoma AxFKH1 U43547 FoxA4
Cynops FHD D64021 FoxA4
Xenopus pintallavis X65171 FoxA4a
Xenopus XFD1 U65751 FoxA4a
Xenopus XFD1' U65750 FoxA4b
Xenopus XFKH1 S93559 Fox A4b
Xenopus XFD3 FoxA2a
Xenopus XFD3' FoxA2b
Oryzias MeHNF3 beta AB001572 FoxA2
Danio axial Z22762 FoxA2
Mus HNF3 beta L10409 Foxa2
Rattus HNF3 beta L09647 FoxA2
Mus HNF3 alpha X74936 Foxa1
Xenopus HNF3 alpha U04873 FoxA1a
Homo HNF3 alpha U39840 FOXA1
Mus FRKHDC L10408 Foxa1
Xenopus XFD7' FoxA1b
Xenopus XFD7 FoxA1a
Danio fkd7 AF052250 FoxA1
Molgula FH1 AF007905 FoxA5
Molgula MoccFH1 AF082992 FoxA5
Ciona Cifkh AF002988 FoxA5
Mus HNF3 gamma X74938 Foxa3
Rattus HNF3 gamma L09648 FoxA3
Homo FKH H3 L12141 FOXA3
Danio fkd2 AF052245 FoxA3
Oryzias MeFKH1 AB001573 FoxA3
Salmo fkh AF062086 FoxA3
Danio fkd4 AF052247
Danio fkd3 AF052246 FoxB1
Mus HFH5.1 U04198 Foxb1
Xenopus FKH5 AF064810 FoxB1
Homo fkh5 AF055080 FOXB1
Mus TWH U90538 Foxb1a
Mus fkh5 (Mf3) X92592 Foxb1b
Homo FKH5 AF071554 FOXB1
Homo HFKH5 U87393 FOXB1
Danio fkd5 AF052248 FoxB1
Danio FKH5 AF052651 FoxB1
Mus fkh5 X71943 Foxb1a
Mus fkh4 X71942 Foxb2
Mus fkh4 X92591 Foxb2
Xenopus XFD5 FoxB2
D
E
A
B

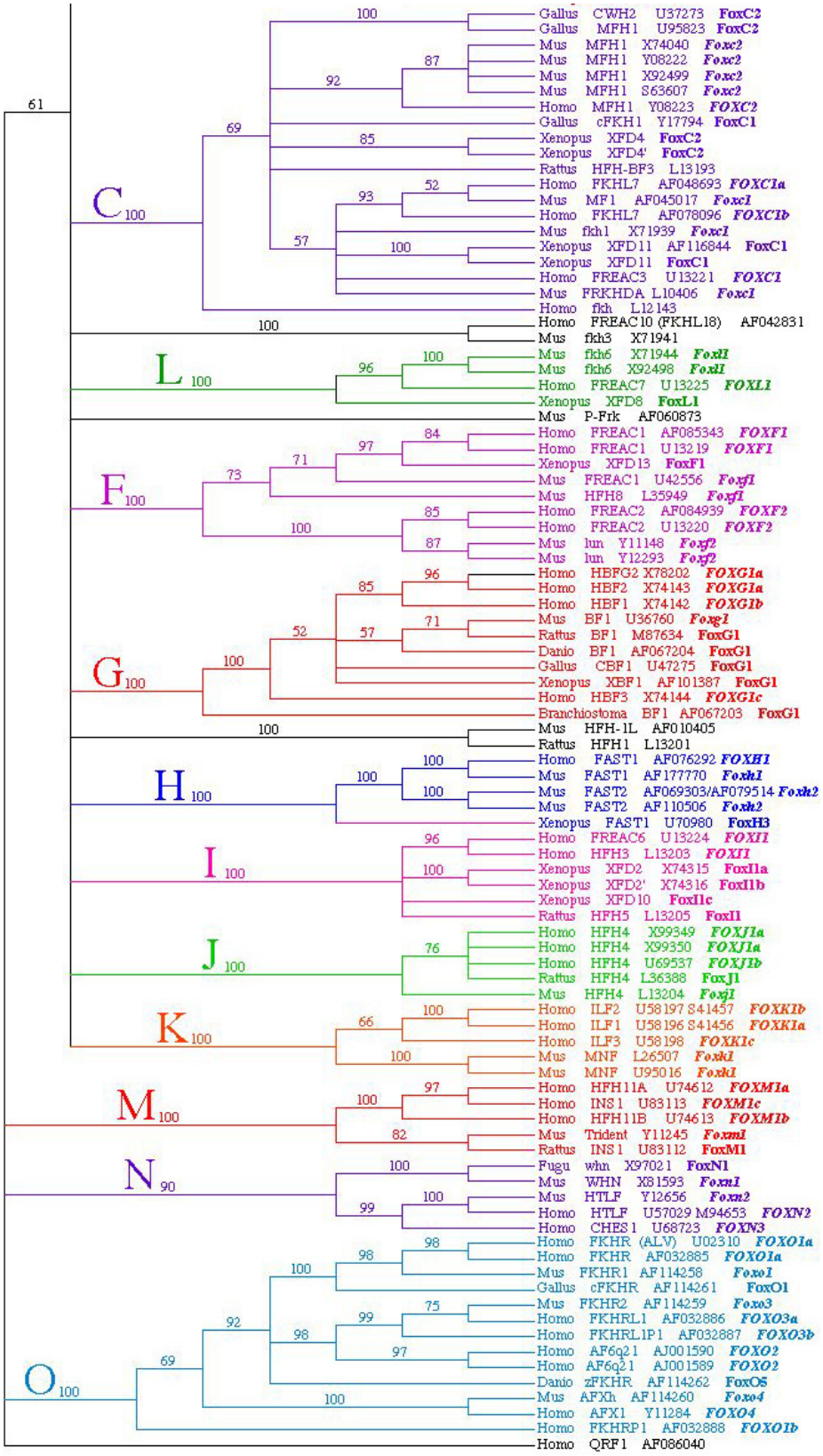

Fig.1.1: phylogenetic tree of chordate Fox proteins.

1.2.1.2 Structure of the forkhead domain (DNA-binding domain)

Clark and co-workers (Clark et al., 1993) worked out the first three-dimentional structure of a forkhead domain of FoxA3 (HNF-3γ) bound to a DNA target by using X-ray crystallography. They compared the fold with the shape of a butterfly and coined the term "winged helix" to describe the structure, which has a helix–turn–helix core of three α helices, flanked by two loops, or "wings" (Fig.1.2). "Winged helix" proteins are often used synonymously with forkhead proteins (Lai et al., 1993). However, several phylogenetically unrelated proteins

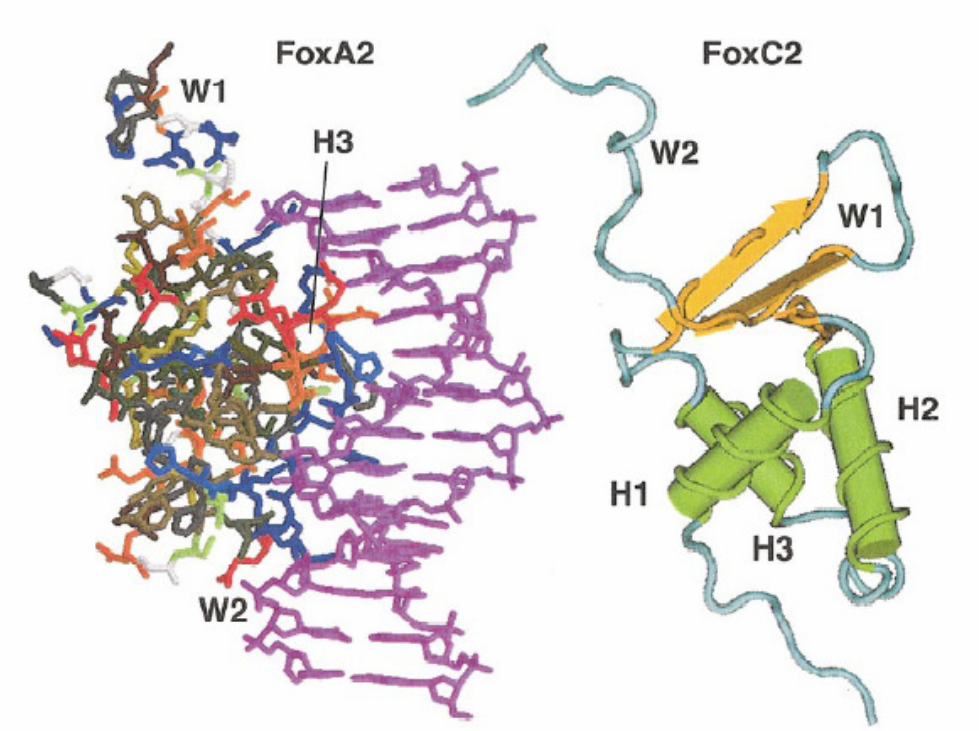

Fig. 1.2: Three-dimensional structure of the DNA-binding domains of FoxA3 bound to DNA (X-ray crystallography; Clark et al., 1993) and FoxC2 (NMR; van Dongen et al., 2000). The FoxA3 structure shows the recognition helix (H3) filling out the major groove of DNA (viewing angle parallel with the H3 helical axis). The first wing (W1) reaches upward, approximately parallel with the DNA helical axis and beyond the (3′) end of the oligonucleotide, whereas the second wing (W2) makes minor groove contacts in the 5′ end of the binding site. The FoxC2 NMR structure shows the helix–turn–helix motif viewed from the side facing away from the DNA with two helices, H1 and H2, stacked on top of the recognition helix (H3). The first wing (W1) consists of two antiparallel ß-strands (yellow) separated by a short loop (Carlsson and Mahlapuu, 2002).

have similar 3D structure and are referred to as winged helix proteins in the literature as well; e.g., MotA from bacteriophage T4, LexA from *Echerichia coli,* E2F, DP, and RFX transcription factors as well as double-stranded RNA adenosine deaminase. Care should be taken to distinguish between these topologically similar proteins of diverse evolutionary origin and forkhead proteins, which form a clearly defined, monophyletic group. A large proportion of the amino acids in the

forkhead domain are invariant or highly conserved, which implies that there is only limited variation in 3D structure and mode of DNA recognition within the forkhead family. This has been confirmed by NMR structural analysis of the DNA binding domains of three additional forkhead proteins: FOXC2, Foxd3, and FOXO4 (Carlsson and Mahlapuu, 2002). While Clark *et al.* (1993) identified three α helices in FoxA3, the NMR structures all show a short fourth helix in the loop between helix 2 and 3. However, Weigelt *et al.* (2001), point out that the backbone fold in this region is nearly identical in all four structures (including FoxA3) and inclusion or omission of a fourth helix mostly reflects differences in interpretation. A 5-amino-acid insertion between helix 2 and 3 found in the FoxO subfamily adds a small extra loop, but has surprisingly little effect on the overall structure (Jin et al., 1999; Weigelt et al., 2001). Binding to a DNA target site appears to cause only minor structural changes in the forkhead domain (Jin et al., 1999), whereas circular permutation data indicate that a substantial bend is induced in the DNA (Pierrou et al., 1994).

1.2.1.3 DNA binding specificity

In contrast to most helix–turn–helix proteins, forkhead proteins bind DNA as monomers (Pierrou et al., 1994). Hence, the binding sites, which typically span 15–17 bp, are asymmetrical. The sequence specificity has been determined for several representatives of this protein family through selection of binding sites from pools of short, random-sequence duplexes. A seven-nucleotide core corresponds to the major groove base contacts made by the recognition helix (helix 3). For the majority of forkhead proteins, the core conforms to the RYMAAYA (R _ A or G; Y _ C or T; M _ A or C) consensus (Pierrou et al., 1995; Kaufmann and Knochel, 1996). An optimal core sequence is essential, but not sufficient for high affinity binding, which also depends on flanking sequences on both sides of the core (Overdier et al., 1994; Pierrou et al., 1994; Kaufmann et al., 1995; Roux et al., 1995).

Pairs or small groups of forkhead proteins have DNA binding domains so similar that the specificities have to be assumed to be identical; for example FOXD1 and FOXD2 have forkhead domains with 100% amino acid identity (Ernstsson et al., 1997), and FOXC1 and FOXC2 are 97% identical (Kume et al., 1998). This exceptional degree of sequence conservation is confined to the forkhead domain--in FOXD-1 and -2, for example, there are no discernable homologies between the rest of the proteins. Since experimental data suggest that a considerable sequence variation within the forkhead domain can be tolerated with no or little effect on sequence specificity, additional interactions and functions are likely to contribute to the selective forces that preserve the forkhead domains.

1.2.1.4 Transcription effector domains

Forkhead proteins have been shown to act mostly as transcriptional activators but not exclusively so. For example, *trans*-repression has been reported for FoxG1 and -p1/2/4 (Bourguignon et al., 1998; Wang et al., 2004). In *C. elegans,* the forkhead protein LIN-31 is thought to act as either repressor or activator, depending on its phosphorylation in response to MAP kinase signaling (Tan et al., 1998). Mammalian FoxG1 represses transcription by forming a complex with transcriptional co-repressors of the Groucho family and histone deacetylases (Yao et al., 2001).

Using deletions and substitutions, the regions that contribute to transcriptional activation have been mapped in detail for several forkhead proteins, such as FoxA2, -F1, -F2, -N1, and others (Pani et al., 1992; Hellqvist et al., 1996; Schuddekopf et al., 1996; Hellqvist et al., 1998). Like many other transcription factors, forkhead proteins often contain several activating regions, and these can be found in any location relative to the DNA binding domain.

Little is known about the mechanisms through which forkhead proteins interact with the transcriptional machinery. *In vitro,* FOXF2 binds the general transcription factors TBP and TFIIB, and in cotransfection experiments, FOXF2 acts synergistically with TFIIB (Hellqvist et al., 1998).

1.2.1.5 Forkhead genes in development

Analysis of gene mutations in mouse is offering insight into the diverse range of biological processes that forkhead genes influence (summarized in Table 1.1). Additionally, members of the Fox family have been shown to be involved in different genetic and tumoral diseases [recently reviewed in (Carlsson and Mahlapuu, 2002)]

TABLE 1.1 The phenotypes of mice resulting from inactivation of *Fox* gene by gene targeting or by spontaneous mutant (Carlsson and Mahlapuu, 2002).

Gene	Mutant phenotype	References
Foxa1 (*HNF-3α*)	Die postnatally with severe growth retardation and hypoglycemia Reduced pancreatic glucagon production	Kaestner *et al.,* 1999; Shih *et a.* 1999.
Foxa2 (*HNF-3ß*)	Absence of node, notochord, and foregut. Embryos do not develop beyond E8.5. Conditional inactivation in pancreas causes hyperinsulinemichypoglycemia	Ang and Rossant, 1994; Sund *et al.,* 2000; Sund *et al.,* 2001; Weinstein *et al.,* 1994
Foxa3 (*HNF-3γ*)	Reduced expression of the hepatic glucose transporter GLUT2 leads to inefficient glucose efflux and fasting hypoglycemia.	Kaestner *et al.,* 1998; Shen *et al.,* 2001
Foxb1 (*Mf3*)	Variable phenotype including perinatal mortality, growth retardation, nursing defects, and defects in the central nervous system.	Alvarez-Bolado *et al.,* 2000; Labosky *et al.,* 1997; Wehr *et al.,* 1997
Foxc1 (*Mf1*)	Die at birth with multiple abnormalities including hydrocephalus,	Hong *et al.,* 1999; Kidson

	skeletal, ocular, renal, and cardiovascular defects. Heterozygotes have ocular defects. Together with Foxc2 required for somitogenesis	*et al.,* 1999;Kume *et al.,* 1998, Smith *et al.,* 2000; Winnier *et al.,*1999
Foxc2 (*Mfh1*)	Die pre- or perinatally with skeletal and cardiovascular defects. Heterozygotes have ocular defects. Together with Foxc1 required for somitogenesis.	Iida *et al.,* 1997; Kume *et al.,* 2000b, 2001; Smith *et al.,* 2000; Winnier *et al.,* 1997; Winnier *et al.,* 1999
Foxd1 (*Bf2*)	Die within 24 h after birth due to renal failure.	Hatini *et al.,* 1996
Foxd2 (*Mf2*)	Viable and fertile, but ca. 40% have renal abnormalities.	Kume *et al.,* 2000b
Foxe1 (*TTF-2*)	Die within 48 h of birth exhibiting cleft palate and either a complete or partial failure of thyroid gland development.	De Felice *et al.,* 1998
Foxe3 (*dysgenetic lens* mutant)	Viable and fertile. Severe cataract and fusion of ornea and iris caused by degeneration of lens epithelium.	Blixt *et al.,* 2000; Brownell *et al.,* 2000
Foxf1 (*FREAC1, HFH-8*)	Die around E9 due to absence of vasculogenesis in yolk sac and allantois as a result of defects in mesodermal differentiation. Heterozygotes have lung and foregut malformations.	Kalinichenko *et al.,* Mahlapuu *et al.,* 2001a,b
Foxg1 (*Bf1*)	Die around birth, with a severe reduction in the size of the cerebral hemispheres.	Xuan *et al.,* 1995
Foxh1 (*Fast*)	Embryonically lethal due to failure to form node, prechordal mesoderm, notochord, and definitive endoderm.	Hoodless *et al.,* 2001; Yamamoto *et al.,* 2001
Foxi1 (*Fkh-10*)	Malformations of the inner ear results in deafness and disturbed balance.	Hulander *et al.,* 1998
Foxj1 (*HFH-4*)	Majority die before weaning and show defective ciliogenesis as well as randomized left-right asymmetry.	Brody *et al.,* 2000; Chen *et al.,* 1998
Foxk1 (*MNF*)	Viable, but growth retarded. Incomplete muscle regeneration after injury due to defect proliferation and differentiation of myogenic stem cells.	Garry *et al.,* 2000
Foxl1 (*Fkh-6*)	The majority die before weaning with intestinal epithelial hyperplasia due to overactivation of the Wnt/ß-catenin pathway.	Kaestner *et al.,* 1997; Perreault *et al.,* 2001
Foxm1 (*Trident, HFH-11*)	Die perinatally with cardiovascular defects and polyploidy in cardiomyocytes and hepatocytes.	Korver *et al.,* 1998
Foxn1 (*Whn*)	Exhibit all features of the original *nude* mutant, such as hairlessness and athymia.	Nehls *et al.,* 1994, 1996
Foxp3	(*scurfy* mutant) Overproliferation of CD4+ CD8-T lymphocytes, extensive multiorgan infiltration and elevation of cytokines.	Jeffery *et al.,* 2001
Foxq1	(*satin* mutant) Have a silky fur coat due to defects in differentiation of the hair shaft.	Hong *et al.,* 2001

1.2.2 Characteristics of forkhead transcription factor Foxb1

Foxb1 was previously known as *Mf3* (Labosky et al., 1996; Labosky et al., 1997), *Fkh5* (Kaestner et al., 1996). *TWH* (Dou et al., 1997), and HFH-E5.1 (Ang et al., 1993). The new WH nomenclature is described by Kaestner *et al.* (Kaestner et al., 2000). *Foxb1* has 324 amino acids, from 13 to 113 is the forkhead domain, a large proportion of amino acids in the forkhead domain are invariant and highly conserved (Fig.1.3). It maps to mouse Chromosome 9 near several well characterized mouse mutations including *prenatal lethal factor 1* (*pnlf1*), and *small thymus* (*sty*) (Kaestner et al., 1996; Labosky et al., 1996).

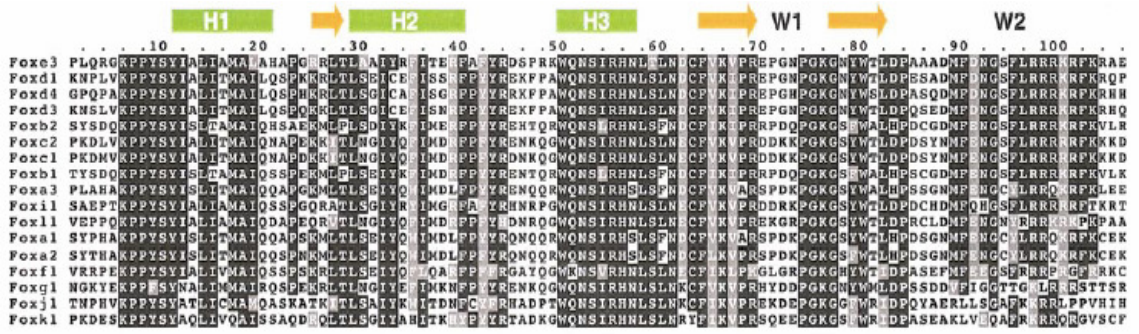

Fig. 1.3: Alignment of 17 mouse forkhead domains illustrates the conserved regions in relation to helices (H1–H3) and ß-strands (yellow).

The expression pattern of Foxb1 has been well characterized (Ang et al., 1993; Kaestner et al., 1996; Wehr et al., 1997; Alvarez-Bolado et al., 1999; Alvarez-Bolado et al., 2000). Transcripts are first localized in the early embryo from day 7.5 p.c onwards in anterior neurectoderm and mesoderm and in the presomitic mesoderm. By E8, the expression was seen in the ventricular layer of the diencephalons, midbrain, hindbrain and spinal cord. From E9 to E10, the expression of this gene is rapidly restricted in the diencephalon and rostral midbrain, the expression in diencephalon is restricted in posterior hypothalamus. while it is constant in the region of the hindbrain and caudal midbrain. By E12 there is a sudden change in pattern- the rostral midbrain acquired a strong expression and the diencephalic restriction of expression stops at the caudal hypothalamus, while the caudal midbrain and hindbrain gradually lose expression intensity. In the adult, only nuclei of the rostral midbrain (the superior colliculus) and caudal hypothalamus (medial mammillary, dorsal premammillary and tuberomedial) show Foxb1 expression. In the mammillary body, the medial and lateral mammillary and dorsal premammillary nuclei express Foxb1 during development; in the adult, the tuberomammillary nucleus expresses Foxb1 transiently during development, and the supramammillary nucleus never expresses Foxb1 (Fig. 1.4). Foxb1 may play a role in the growth and differentiation of a specific segment of the anterior CNS.

Foxb1 is known to participate also in spinal cord differentiation (Dou et al., 1997) as well as in the control of lactation (Labosky et al., 1997).

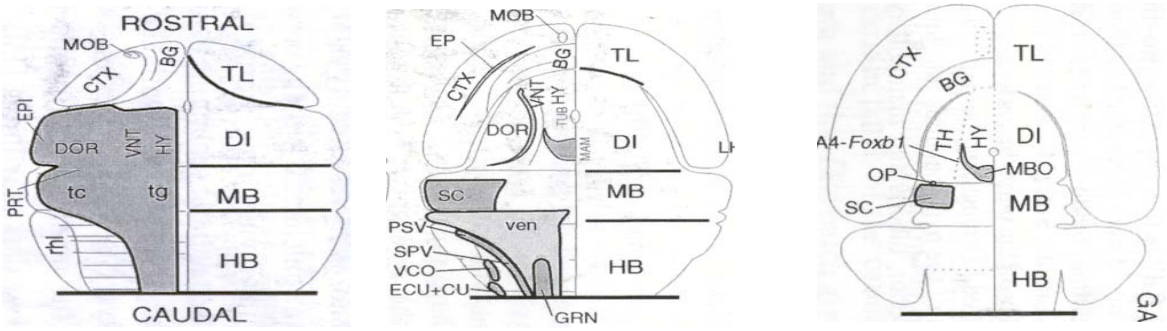

Fig. 1.4: The schematic description of the expression of Foxb1 at E8 (left), E14 (middle) and adult stage (right) (Alvarez-Bolado et al., 1999). DI, diencephalon; MB, midbrain; HB, hindbrain; HY, hypothalamus; MBO, mammillary body.

1.3 HYPOTHALAMUS

1.3.1 General aspects about hypothalamus

The hypothalamus is a morphologically and functionally complex region of the forebrain comprising most of the neural structures governing motivated behavior – the behavior originated by causes or motivators like danger, thirst, hunger or sexual drive.

Many behaviors understood as "emotions" in the human, like anger, fear, love (also maternal love), desire, etc. are also originated in the hypothalamus. Activation of hypothalamic neural systems by motivators leads to basic and highly stereotyped, behaviors, like aggression, escape, foraging (for food, water, salt etc.), sexual display and many others. The same behaviors can be observed in humans, but with a much larger degree of complexity, and having intricate relations with cognitive processes (memory, logical abilities, prospective abilities, etc.).

1.3.2 Mammillary body

The mammillary body is a large neuronal group in the caudal/ventral hypothalamus formed by three nuclei – the lateral and medial mammillary nuclei, and the dorsal premammillary nucleus (Fig.1.5; reviewed by Canteras and Swanson, 1992; Risold and Swanson, 1995).

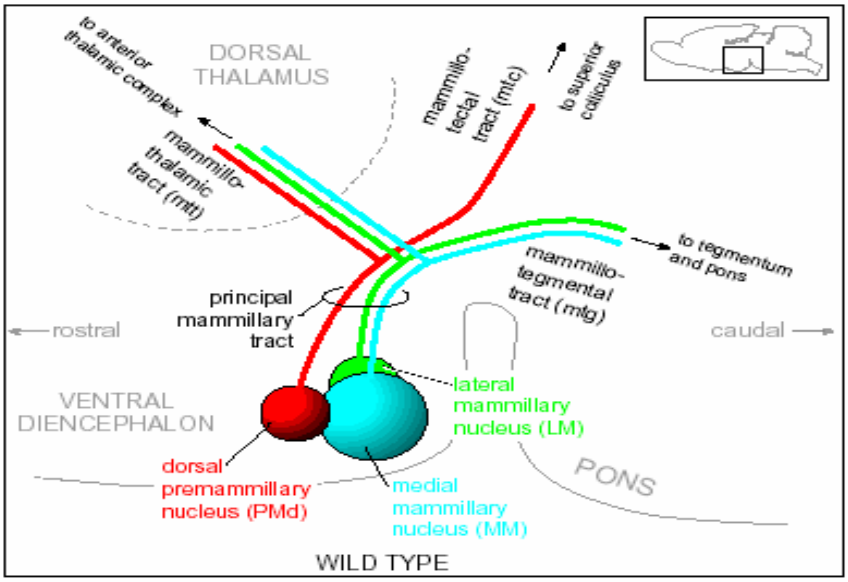

Fig. 1.5: Organization of the three nuclei of the mammillary body and their projections in the adult mouse. The right side of the brain is represented in a sagittal perspective. Rostral is to the left. The three color traits coming out of the nuclei represent each one single axonal stem and its two branches (Alvarez-Bolado et al., 2000).

The mammillary group receives a major input from the postcommissural fornix, which arises in the subicular complex of the hippocampal formation and is a major component of the classical "papez circuit" (1937), which is now thought to play a role in learning and memory.

The mammillary axonal complex (Fig. 1.5) is formed by the axons from these nuclei, which share a branching pattern – every neuron gives off one axonal stem that bifurcates into two branches. One of the branches is directed dorsally to the thalamus and another caudally to the midbrain. This peculiar pattern of connections bridging forebrain and midbrain, also shown by other nuclei in this boundary region, is considered a major feature of diencephalic circuitry with important behavioral implications (Canteras and Swanson, 1992; Risold et al., 1997). In particular, the mammillothalamic tract connects the two major subdivisions of the diencephalons (hypothalamus and thalamus) and closes the circuit originally described by Papez.

Mammillothalamic fibers develop as short, collateral branches of the principal mammillary tract. The mammillothalamic tract forms a compact bundle, reaching the anterior thalamic nuclear group around E18-E19.

There is considerable evidence that damage to MBO and mtt can result in the deficits in the performance of certain spatial memory tasks (Vann and Aggleton, 2003).

1.3.3 Foxb1 function in the hypothalamus

Mice carrying a targeted null mutation in *Foxb1* (Dou et al., 1997; Labosky et al., 1997; Wehr et al., 1997; Alvarez-Bolado et al., 2000) survive to adulthood and are (with limitations) able to reproduce, but lack a large part of the mammillary region of the hypothalamus, the so-called mammillary body, MBO. This defect is accompanied by an axonal navigation defect. In wild type animals, the mammillary axonal tree is formed by a large bundle of axons coming from the neurons of the MBO (Fig.1.5). These axons bifurcate after a short dorsal trajectory. The main bundle (the earliest to appear during development) turns then caudally, towards the midbrain. Some of these axons form the mammillotegmental bundle (mtg) and end in the tegmentum of the midbrain, while other axons form the mammillotectal bundle (mtc) and end in the tectum of the midbrain. However, around embryonic day E18.5 they form a branch, the mtt which is directed towards the dorsal diencephalon and ending in the anterior thalamus.

Examination of axonal development in *Foxb1* mutants has revealed that the MBO is indeed formed during the development of the mutant brain, and it emits the axons of the principal mammillary tract, and in due time these axons branch into the meet and start their growth towards the anterior thalame tract. In the mutant, however, mtt axons are not able to enter their target, the dorsal thalamus, and are instead deflected towards the ventral side. A short time after this navigational failure, which happens around E18.5, the MBO disappears almost completely due to massive apoptosis (Fig.1.6) (Alvarez-Bolade, Gonzalo et al. 2000). The failure of the mtt to connect with its target in the *Foxb1* mutant has major consequences. In wild type, the mtt links the mammillary region of the hypothalamus to the anterior region of the thalamus, and in this way closes the classically described “Papez circuit” (anterior thalamus-cingulate cortex-hippocampus-mammillary-anterior thalamus), which is crucial for some forms of memory (Sgroi et al. 1999). In agreement with this observation, Foxb1-deficient mice suffer from spatial working memory problems (Radyushkin et al., 2005). Therefore, the causal link is established between one transcriptional regulator, Foxb1, one neural circuit, and one specific brain function.

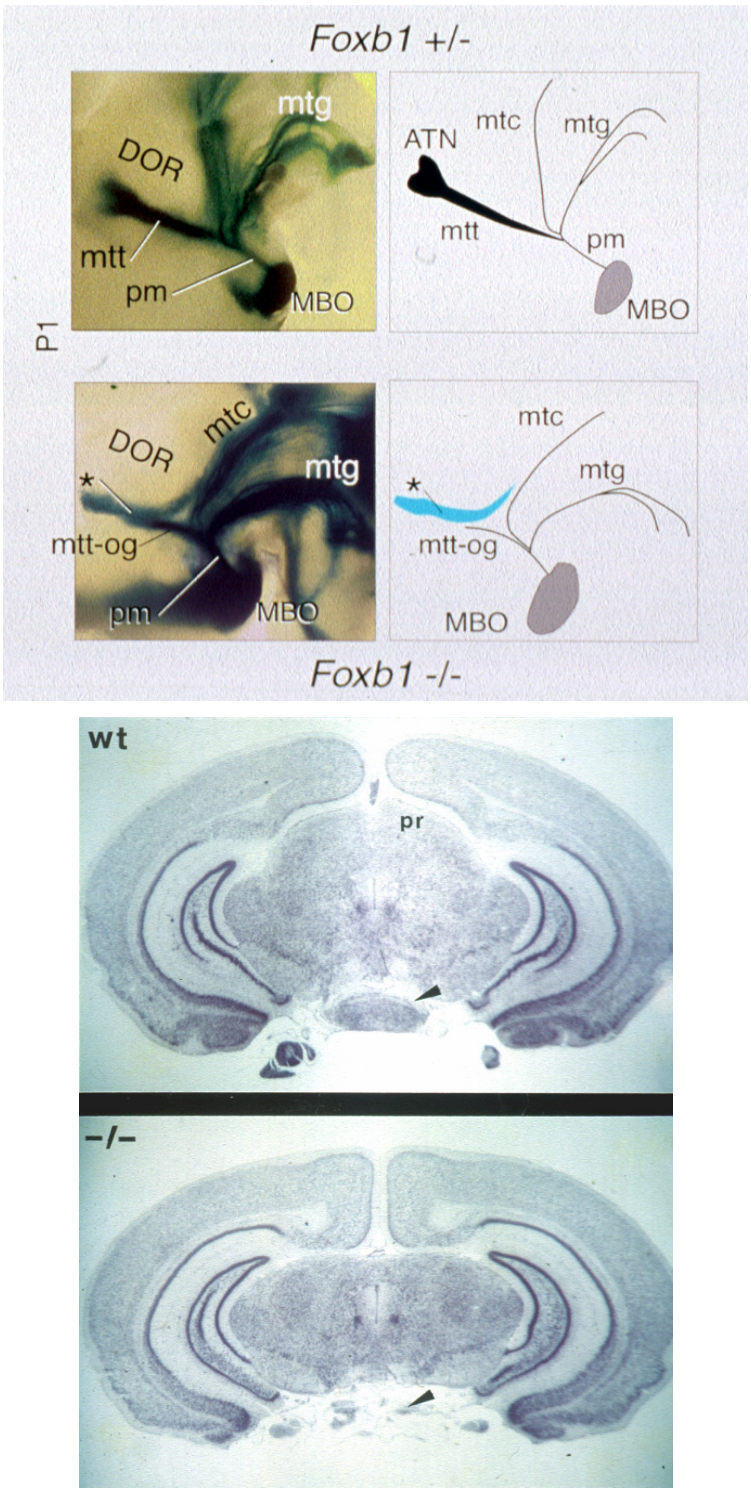

Fig. 1.6: The mammillothalamic tract cannot enter the target in the *Foxb1*-homozygous brain (upper panel, asterisk); *Foxb1*-deficient mice lack one brain nucleus (lower panel, arrowhead) (Alvarez-Bolado et al., 2000).

1.4 AXONAL NAVIGATION

The correct wiring of the nervous system relies on the ability of developing axons and dendrites to locate and recognize their appropriate synaptic partners. To help them find their way in the developing embryo, axons and dendrites are tipped with a highly motile and sensitive structure, the growth cone. Extracellular guidance cues can either attract or repel growth cones, and can operate either at close range or over a distance (Tessier-Lavigne and Goodman, 1996). By responding to the appropriate set of cues, growth cones are able to select the correct path toward their target.

1.4.1 Cellular interactions that guide axons

Embryological, tissue culture, and genetic experiments indicate that axons respond to the coordinate actions of four types of guidance cues: attractive and repulsive cues, which can be either short-range or long-range (Fig.1.7).

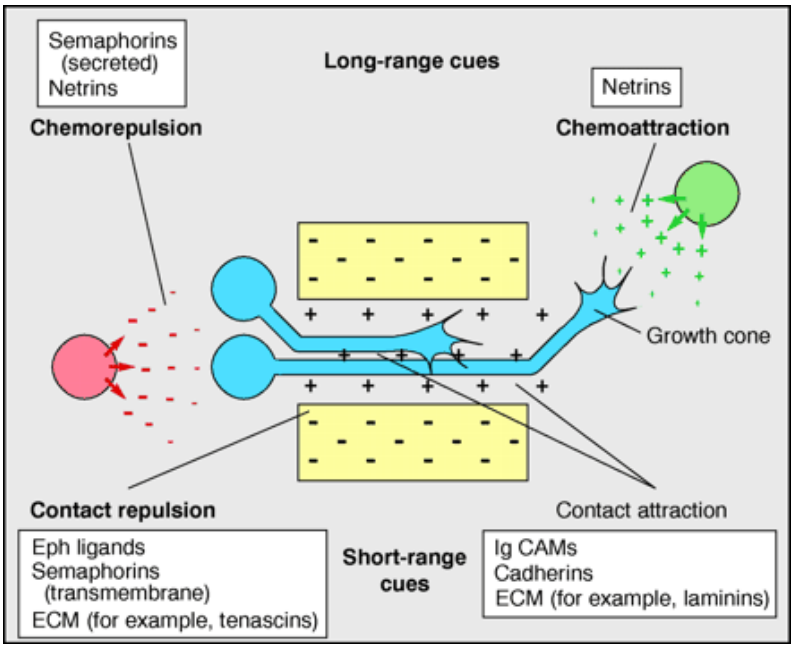

Fig. 1.7: Guidance forces. Four types of mechanisms contribute to guiding growth cones: contact attraction, chemoattraction, contact repulsion, and chemorepulsion. The term attraction is used here to refer to a range of permissive and attractive effects, and the term repulsion to a range of inhibitory and repulsive effects. Examples are provided of ligands implicated in mediating each of these mechanisms. There is not a one-to-one match between molecules and mechanisms because some guidance molecules are not exclusively attractive or repulsive, but rather bifunctional, and some families of guidance cues have both diffusible and nondiffusible members. Individual growth cones might be "pushed" from behind by a chemorepellent (red), "pulled" from afar by a chemoattractant (green), and "hemmed in" by attractive (gray) and repulsive (yellow) local cues. Axons can also be guided by cues provided by other axons (selective fasciculation). Push, pull, and hem: these forces act together to ensure accurate guidance (Tessier-Lavigne and Goodman, 1996).

Many neuronal connections are made by secondary (collateral) branches of axons, which form de novo from secondary growth cones sprouted along the axon shaft. Both the initiation and subsequent guidance of secondary growth cones appear to be directed by the same forces that guide primary growth cones (Roskies and O'Leary, 1994).

The guidance of axons over individual segments of their trajectories appears to involve the simultaneous operation of several, and in some cases possibly all four, of these guidance forces. Thus, an individual axon might be "pushed" from behind by a chemorepellent, "pulled" from afar by a chemoattractant, and "hemmed in" by attractive and repulsive local cues. Push, pull, and hem: these forces appear to act together to ensure accurate guidance. However, this well-engineered redundancy complicates experimental analysis of guidance mechanisms because perturbation of any one mechanism often has a limited effect.

Guidance cues have been classified according to the response they elicit as either attractive or repulsive (Tessier-Lavigne and Goodman, 1996; Mueller, 1999). Prominent among these are the ephrins, netrins, slits, robos and semaphorins (Dickson, 2002). These are not the only known guidance molecules, but they are by far the best understood. I will introduce here in detail only the most relevant to my PhD work, i. e., the ephrins and their receptors, the Eph ("eff") tyrosine kinases.

1.4.2 Ephrins and Eph

The ephrins are membrane-bound ligands for the Eph family of receptor tyrosine kinases (Bartley et al., 1994) (Drescher et al., 1995). They are divided into two subclasses, the A-subclass (ephrinA1–ephrinA5), which are tethered to the cell membrane by a glycosylphosphatidylinositol (GPI) anchor, and the B-subclass (ephrinB1–ephrinB3), members of which have a transmembrane domain that is followed by a short cytoplasmic region.

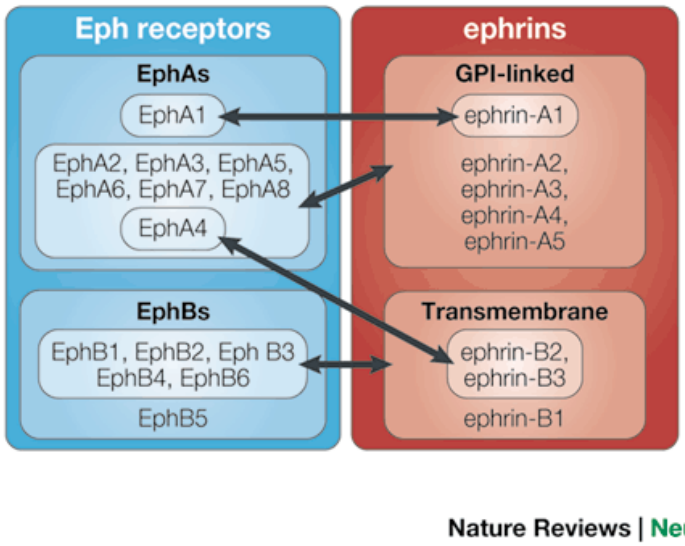

Fig. 1.8: The structural classes of vertebrate Eph receptors and ephrins and their binding specificities are ummarized. Although binding is promiscuous within each of the Eph/ephrin specificity classes, there are differences in affinity that might be functionally important. (GPI, glycosylphosphatidylinositol) (reviewed (Wilkinson, 2001)).

The Eph family, is the largest family of receptor tyrosine kinases (RTKs). It consists of 14 different members subdivided into EphA and EphB receptors on the basis of sequence similarity and ligand affinity. A-subclass, which contains eight members (EphA1–EphA8) and a B-subclass, which in mammals contains five members (EphB1–EphB6). A-type receptors typically bind to most or all A-type ligands, and B-type receptors bind to most or all B-type ligands, with the exception of EphA4, which can bind both A-type and most B-type ligands (Fig. 1.8).

The Eph-receptor extracellular domain is composed of the ligand-binding globular domain, a cysteine-rich region and two fibronectin type III repeats (Fig.1.9). The cytoplasmic part of Eph receptors can be divided into four functional units; the juxtamembrane domain that contains two conserved tyrosine residues, a classical protein tyrosine kinase domain, a sterile a motif (SAM) and a PDZ- binding motif. The solved structure of the SAM domain (~70 amino acids) indicates that it could form dimers and oligomers. The PDZ- binding motif located in the carboxy-terminal 4–5 amino-acid residues — contains a consensus binding sequence that includes a hydrophobic residue (usually valine or isoleucine) at the very carboxyl terminus (Kullander and Klein, 2002).

Functional evidence suggests that Eph receptor - ligands play important roles in the formation of topographic mapping (the mechanism by which axon terminals organize themselves onto a target area) (Drescher et al., 1995; Nakamoto et al., 1996; Frisen et al., 1998; Wilkinson, 2000), in the patterning of forebrain and hindbrain (Xu et al., 1996), and in the formation of certain commissures (Park et al., 1997). At the cellular level, ephrins act as contact-dependent

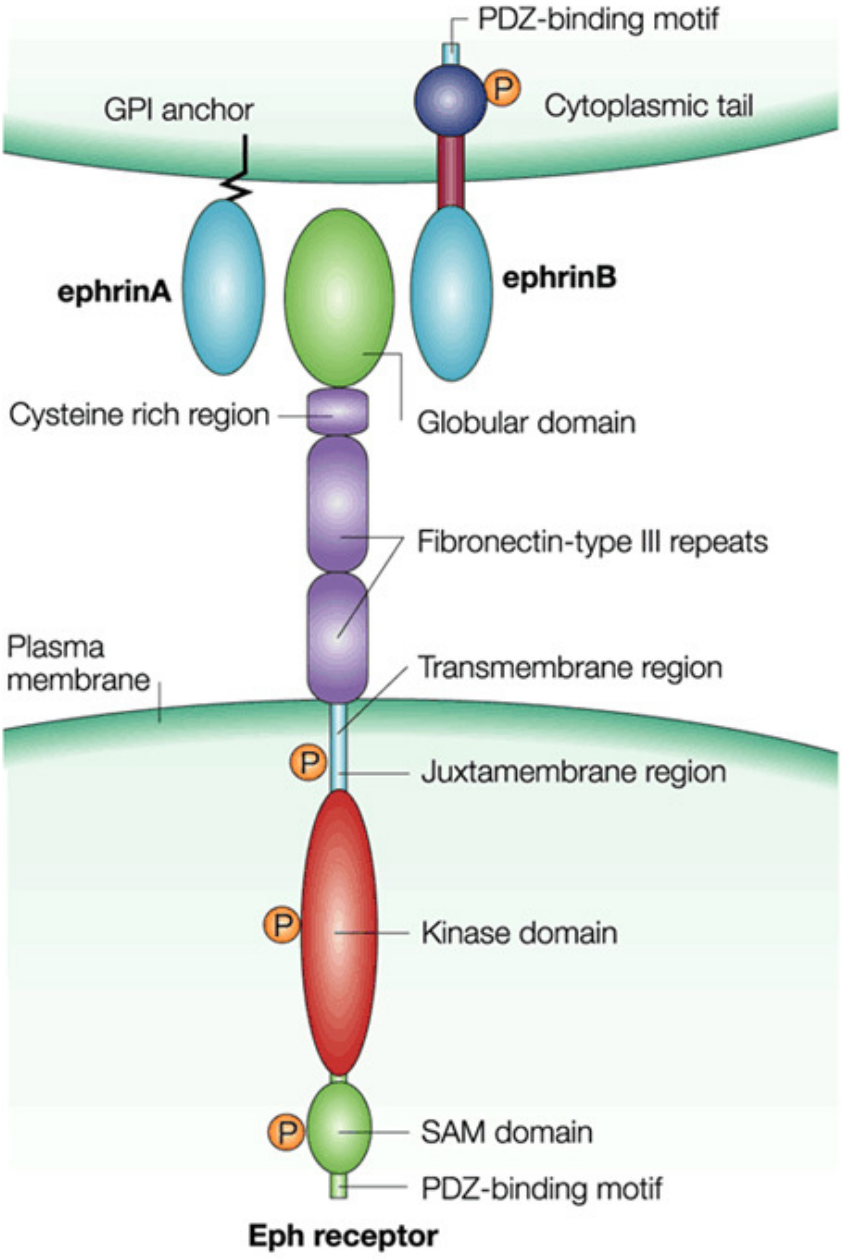

Fig.1.9: General features of Eph receptors and ephrins. A schematic diagram, which shows an ephrin-expressing cell (top) interacting with Eph-expressing cell (bottom). Ligand–receptor interactions (green) have been mapped in detail and have uncovered dimeric and oligomeric Eph–ephrin complexes (not shown). GPI, glycosylphosphatidylinositol; SAM, sterile α-motif (Kullander and Klein, 2002).

repulsive factors for retinal axons, motor axons, cortical neurons, and neural crest cells (Drescher, 1997). A role in axon fasciculation and in formation of axon branches of cortical neurons for one member, ephrin-A5 (AL-1/RAGS), has been shown in vitro experiments (Bolz and Castellani, 1997).

Signal transduction by the Eph receptors has features that are common with growth-factor receptor kinases, and also some unique features. Ephrin induces Eph receptor dimerization and kinase activation. Activation of the Eph receptors results in tyrosine phosphorylation of the receptor itself and downstream substrates, creating binding sites for SH2 domain-containing proteins. In contrast to mitogenic growth factor receptors, which generally activate Ras and MAP kinase signalling, Eph receptors do not activate Ras or extracellular signal-regulated kinase (ERK). Instead, activation of Eph receptors has been reported to result in recruitment of Ras GAP, which then inactivates Ras and suppresses ERK activation. This is consistent with the observation that ephrins do not exhibit mitogenic effects.

Functional analysis of the Eph–ephrin system is challenging for at least two reasons. First, Eph receptors can have overlapping functions in vertebrates, and loss of one receptor can be partially compensated for by another Eph receptor that has a similar expression pattern and ligand-binding specificities. Second, an Eph receptor can also act as a ligand in the same way that an ephrin ligand can act as a receptor (introduced above). The functional consequences of Eph-receptor redundancy are well described by studies in which the functions of EphB2 and EphB3 were examined by targeted deletion of these molecules in mice. Although mice that are singly deficient for EphB2 or EphB3 are viable, most *EphB2–EphB3* double mutants die at birth due to a developmental defect in the upper mouth called cleft palate, which prevents proper food intake. Similarly, during retinal ganglion-cell axon guidance to the optic disc, mouse embryos that lack both EphB2 and EphB3 show increased frequency of axon guidance errors, which could not be detected in the single mutants. Genetic background also has an important role for the discovery and penetrance of phenotypes in mice. By shifting mice with an *EphB2*-targeted deletion from 129 to CD1 genetic background, increased survival rates and a circling behaviour was shown in 61% of the cases. Mice that lack both EphB2 and EphB3 receptors in the CD1 background all showed a circling behaviour, which indicates that these receptors might also be redundant in the CD1 genetic background.

Mammals have 13 Eph receptors and 8 ephrins. Worms and flies both have just a single Eph receptor, with four and one ephrin ligands, respectively. Somewhat surprisingly, the invertebrate ephrin and Eph mutants do not have dramatic axon guidance defects. The *C.elegans* ephrins and the Eph receptor do, however, have critical functions in multiple aspects of epithelial morphogenesis, as do their vertebrate counterparts. It seems that ephrins and Eph receptors are an ancient but versatile system for cell-cell communication that has diversified and acquired its axon guidance functions primarily during vertebrate evolution.

1.5 MICROARRAY TECHNOLOGY

I will briefly introduce here the theory and methods of DNA microarray technology, which has had an important role in my PhD work.

1.5.1 Genomics and DNA arrays

To take full advantage of the large and rapidly increasing body of DNA sequence information, new technologies are required. DNA arrays are powerful and versatile tools for genomics and genetics research. They allow us to make quantitative parallel measurements of gene expression (messenger RNA abundance) for tens of thousands of genes at a time, making possible genome-wide measurements of transcription, and bridging the gap between genotype and phenotype (Lockhart and Winzeler, 2000; Lockhart and Barlow, 2001).

1.5.2 Affymetrix GeneChips

There are different types of microarray in common use (for instance, spotted cDNA arrays and spotted oligonucleotide arrays). All of them have advantages and disadvantages. For my PhD work I have used one particular kind, the commercially available "Affymetrix GeneChips". They are comparatively easy to use, and they have been widely utilized already to address problems in developmental neurobiology.

These microarrays are factory-designed and -synthesized. Design is done using software to choose a series of 11 25-mer probes from the 3′ end of each transcript or predicted transcript in the genome; each of the 11 probes is then paired with a similar mismatch probe that is designed to contain a mutation in the centre. The latter serves as a form of control for hybridization specificity. Synthesis of arrays is done using light-activated chemistry and photolithography methods, and feature size can be reduced to approximately 8 μm^2, with about 1 million probes in a 1.2 cm^2 glass area. Probe-set algorithms interpret the signals from each 22-oligonucleotide probe set, and derive a single value (signal) from the patterns of hybridization to the 22 individual probes. This signal is then normalized to the entire microarray, or to the probe sets across an entire project.

Affymetrix arrays provide multiple measurements — a series of independent or semi-independent oligonucleotides query each RNA in solution (the probe set). Affymetrix probe sets are constructed from a series of perfect-match and paired-mismatch oligonucleotides, allowing some

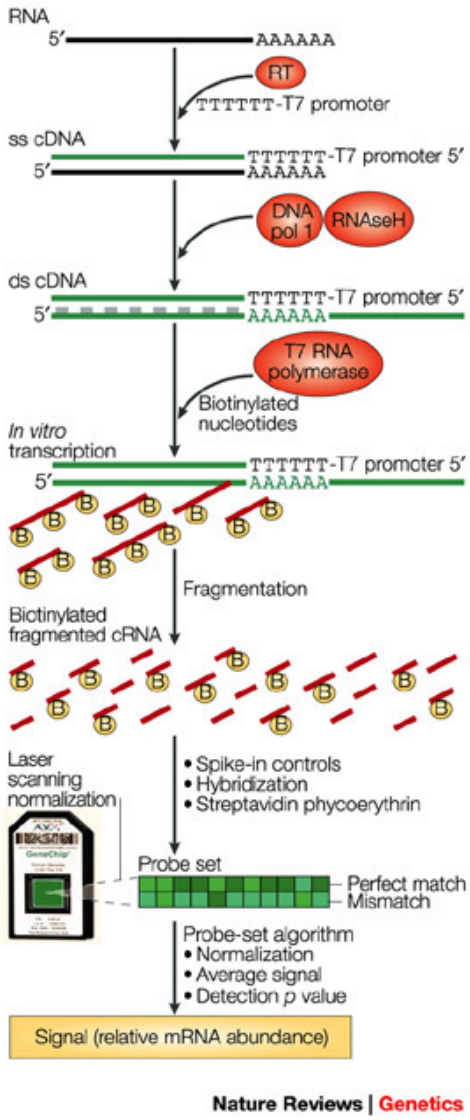

Fig. 1.10: Sample processing and microarray interpretation of Affymetrix GeneChips. Flash-frozen tissue (~50 mg) is homogenized to isolate total RNA. Single-stranded (ss) cDNA and then double-stranded (ds) cDNA is made from ~5 μg of total RNA. Double-stranded cDNA contains a T7 RNA-polymerase promoter adjacent to the 3′ polyA tail of each transcript. It is transcribed *in vitro* to generate more than 400 biotinylated cRNA molecules for each ds cDNA molecule. The biotinylated cRNA is fragmented and hybridized to the microarrays. Each transcript is queried by one or more probe sets of 11 perfect-match and 11 paired-mismatch oligonucleotides (the latter contain a centrally located point mutation as a form of hybridization specificity control). Currently available Affymetrix microarrays have ~54,000 probe sets on each 1.28 cm^2 glass microarray (~1.2 million 25-mer oligonucleotides on the HG-U133Plus 2.0 array). The biotinylated cRNA fragments hybridize to the appropriate oligonucleotide features. A laser scanner determines the amount of bound biotinylated cRNA indirectly through the streptavidin-conjugated phycoerythrin fluorescence at each feature within a probe set. The component probe pairs are interpreted and averaged to arrive at a single signal that reflects the relative abundance of the original mRNA. Probe sets are interpreted by any one of a number of probe-set algorithms, each providing a signal that reflects the relative hybridization intensity across the probe set. RT, reverse transcriptase (Collective, 2004).

assessment of non-specific binding and performance of the probes. Overall, the Affymetrix probe sets provide a variety of measurements that allow robust measures of gene expression. The use of multiple perfect-match and mismatch probes for each gene enables the development of different methods of interpreting the hybridization patterns across the probe set and calculating a single ′expression level′ or ′signal′ that reflect the gene′s relative expression level. A number of probe-set interpretation algorithms for Affymetrix arrays are available (Mills et al., 2001; Collective, 2004).

The standard laboratory protocol for generating RNA profiles using Affymetrix microarrays involves a series of steps (Fig.1.10).

Currently available Affymetrix microarrays have 54,000 probe sets on each 1.28 cm^2 glass microarray (1.2 million 25-mer oligonucleotides on the HG-U133Plus 2.0 array). The biotinylated cRNA fragments hybridize to the appropriate oligonucleotide features. A laser scanner determines the amount of bound biotinylated cRNA indirectly through the streptavidin-conjugated phycoerythrin fluorescence at each feature within a probe set. The component probe pairs are interpreted and averaged to arrive at a single signal that reflects the relative abundance of the original mRNA. Probe sets are interpreted by any one of a number of probe-set algorithms, each providing a signal that reflects the relative hybridization intensity across the probe set. RT, reverse transcriptase.

1.5.3 Application of Affymetrix GeneChips to brain development questions, and attending technical challenges

One of the best illustrations of the future challenges for microarray analysis is provided by several recent applications of this technology to studies of neurobiology. At the cellular level, there are questions concerning the genetic programs responsible for specification of neural cell fates and the differentiation of the myriad neuronal and glial types (Geschwind et al., 2001); (Ramalho-Santos et al., 2002). At the circuit level, the processes of axon guidance, target selection, synapse formation and refinement of synaptic connections each rely on a combination of intrinsic gene-expression patterns and environmental influences (Diaz et al., 2002). In addition, at the systems level, there is a drive to fully map the spatial and temporal expression patterns of each gene. The utilization of microarrays to probe gene expression patterns at each of these levels has resulted in the identification of a considerable number of candidate genes, of which a few have been confirmed with *in vivo* studies (Sandberg et al., 2000; Zhao et al., 2001; Zirlinger et al., 2001).

However, it is important to recognize the technical challenges of these studies. One challenge is that many brain regions of interest are tiny, making it difficult to obtain sufficient RNA for conventional microarray studies. Another technical challenge for microarray studies of the brain arises from the need to dissect different subregions of the brain with functional properties of interest. The exquisite sensitivity of microarray analysis and the distinct transcript profiles of different brain subregions make analyses of dissected tissues susceptible to false positive detections from inclusion of variable amounts of adjacent tissue in a given sample of a desired subregion (Mirnics and Pevsner, 2004); (Shoemaker and Linsley, 2002). In almost all cases, experiments should be conducted at least in duplicate, with replicates done as independently as possible (for example, different mice or independent dissections of a region, independent sample preparations and independent hybridizations to physically different arrays). It is not sufficient to merely remake samples from the same extracted RNA from the same mouse or tissue sample, or to simply rehybridize samples to other arrays, as has been done in some studies. If genetically identical, inbred mice are not used, then it is necessary to do more experiments or to pool mice to effectively average out differences due to genetic inhomogeneity (Lockhart and Barlow, 2001).

1.5.4 Validation of microarray data

Once the appropriate mathematical tools have been used to identify genes likely to be regulated in the manner of interest, the next step is biological characterization of these genes. The first stage of this process is validation, which requires measuring the expression of specific genes of interest using independent methods and independent RNA samples. There are important reasons why a gene identified on an array should be validated by another method. For oligonucleotide arrays, the labeled RNA used for hybridization to the chip is not the original RNA population but an amplified copy whose production requires multiple enzymatic steps, each of which may bias array results. Cross-hybridization due to sequence homology may lead to erroneous results, especially when using cDNA arrays to examine genes that have many closely related family members. Data normalization errors and sample amplification errors are also the obstacle to discover the differential expression (Griffin et al., 2003; Collective, 2004; Mirnics and Pevsner, 2004).

Quantitative RT-PCR is extremely valuable for high-throughput validation of microarray findings whereas in situ hybridization identifies the cellular localization of expression changes (Mimmack et al., 2004),. Quantitative RT-PCR is the most sensitive and accurate of the quantification methods (Wang and Brown, 1999; Giulietti et al., 2001). Visualizing changes in mRNA expression using in *situ* hybridization allows the cellular localization of regulated genes to be

identified. This is critical for the nervous system, where it is the specific pattern of circuitry that is the vital information (Blackshaw et al., 2001).

2 MATERIALS AND METHODS

2.1 Routine for animal work

All work with animals was accomplished according to the regulations of the federal animal law for the protection (BGB1 S.1105, ber. S. 181, Abschnitt 2 (§2+3), 5 (§7-9) und 8 (§119)) (Germany). *Foxb1* deficient mice in a 129/sv background were made available by Dr. Gonzalo Alvarez-Bolado (Alvarez-Bolado et al., 2000). *EphA7* receptor deficient mice were made by T. Ciossek (unpublished) and kindly available from P. Vanderhaeghen (Belgium).

2.2 General molecular biological methods

Bibliographical Note: All the techniques used in the present PhD work are well-known and commonly used by molecular biologists and histologists all over the world. I have not considered it necessary to cite the original methodological literature (first ever description of the concept, first ever usage of the method in a practical context, etc.) In carrying these methods out, however, I have relied on some specific reference works which have been very useful. For the general laboratory work, the classical manual universally known as "the Maniatis" (after the senior author of the first edition) (Sambrook and Russell, 2001) has been invaluable. The books of Docherty (Docherty, 1996) and Latchman (Latchman, 1999) were very useful for me to understand the principles behind DNA-protein interaction, particularly the chapters about EMSA protocols (Read, 1996; Dent et al., 1999).

2.2.1 Isolation of nucleic acids

2.2.1.1 Isolation of genomic DNA from tissue samples

About 0,5cm of the tail from a mouse or leg tissue from a mouse embryo was incubated in 500ul of lysis buffer (100mM Tris-Cl, pH8.0; 5mM EDTA, pH8.0; 0,2% SDS; 200mM NaCl) containing 25ul proteinase K (10mg/ml, Merck) in thermometer mixture at 56°C with 500rpm overnight. An equal volume of phenol/chloroform/isoamylalcohol (PCI) (25:24:1) was added, mixed by inverting, and centrifuged at full speed at room temperature for 10min. 250ul of the aqueous phase was transfer to a new tube, the DNA was precipitated with the same volume of isopropanol. Air dry the pellet 10min at room temperature. Resuspend and dissolve DNA in about 500ul of TE buffer (pH7.5) (10mM Tris-Cl, pH7.5; 1mM EDTA, pH8.0) in thermometer mixture at 37°C with 500rpm. Use 1ul of DNA (about 100ng) for PCR genotyping.

2.2.1.2 Small-scale isolation of plasmid DNA

I used the "MACHEREY-NAGEL NucleoSpin® Plasmid" kit (Germany), according to the instructions of the manufacturer. Briefly: 5ml of LB medium with the appropriate amount of antibiotic was inoculated with a single *E. coli* colony and incubated overnight at 37°C with shaking. Using 1-5ml of this culture, pellet cells in a microcentrifuge for 30s at full speed. Add 250ul A1, resuspend the cell pellet by vigorous vortexing. Add 250ul A2, mix gently by inverting the tube 6-8 times, incubate at room temperature for a maximum of 5min. Add 300ul A3. Mix gently by inverting the tube 6-8 times, centrifuge for 10min at full speed at room temperature or at 4°C. Place a NucleoSpin plasmid column in a 2ml collecting tube and load the supernatant on the column. Centrifuge for 1min at full speed. Discard the flowthrough. Place the NucleoSpin plasmid column back into the 2ml collecting tube and add 600ul A4, centrifuge for 1min at full speed. To dry the silica membrane completely, reinsert the NucleoSpin plasmid column into the 2ml collecting tube. Centrifuge for 2min at full speed. Place the NucleoSpin plasmid column in a 1,5ml microcentrifuge tube and add 50ul AE. Incubate 1min at room temperature. Centrifuge for 1min at full speed.

2.2.1.3 Midi preparation of plasmid DNA

I used the "Qiagen Plasmid Midi Kit" (QIAGEN, USA) according to the instructions of the manufacturer. Briefly: In order to isolate a larger amount of plasmid DNA, the midi preparation DNA isolation method was carried out. 50ml of miniprep culture was used. Inoculate 50ml LB medium containing the appropriate antibiotics and incubated overnight in the shaker (300rpm) for

16-18 hours at 37°C. The bacterial suspension was centrifuged at 1300g for 15min at 4°C, and the pellet was then resuspended in 4ml of Buffer P1. For the cell lysis, 4ml of Buffer P2 was added, then mixed gently but thoroughly by inverting 4-6 times, the suspension was incubated at room temperature for 5min. 4ml of Buffer P3 was added to neutralize the suspension and mixed by inverting the tube. The suspension was centrifuged at 13000g for 30min and the supernatant applied to a previously equilibrated Qiagen-tip100 column (by applying 10ml of Buffer QBT for column equilibration) and left to run through the column resin by gravity flow. The column was washed twice with 10mL of Buffer QC. The DNA was eluted with 5ml of Buffer QF, and precipitated by adding 3,5ml (0,7 volumes) of isopropanol. Which was then centrifuged immediately at 13000rpm for 30min at 4°C. The pellet was washed with 70% ethanol, air dried for 10 minutes at room temperature and dissolved in 50ul buffer TE.

2.2.1.4 EndoFree plasmid Maxi protocol

I used the "QIAGEN Endofree Plasmid Midi Kit" (QIAGEN, USA) according to the instructions of the manufacturer, since it yields endotoxin-free DNA, which improves transfection into sensitive eukaryotic cells. The protocol is as follows:

Pick a single colony from a freshly streaked selective plate and inoculate a starter culture of 2-5ml LB medium containing the appropriate selective antibiotic. Incubate for about 8h at 37°C with rigorous shaking. Dilute the starter culture 1/500 to 1/1000 into selective LB medium. For high-copy plasmids inoculate 100ml medium, and for low-copy plasmids, inoculate 250ml medium. Grow at 37°C for 12-16h with rigorous shaking. Harvest the bacterial cells by centrifugation at 6000 x g for 15min at 4°C. Resuspend the bacterial pellet in 10ml Buffer P1. Add 10ml Buffer P2, mix gently but thoroughly by inverting 4-6 times, and incubate at room temperature for 5min. During this incubation prepare the QIAfilter Cartridge, screw the cap onto the outlet nozzle of the QIAfilter Maxi Cartridge. Place the QIAfilter Cartridge into a convenient tube. Add 10ml chilled Buffer P3 to the lysate, and mix immediately but gently by inverting 4-6 times, immediately pour the lysate into the barely of the QIAfilter Cartridge. Incubate at room temperature for 10min. Do no insert the plunger. Remove the cap from the QIAfilter outlet nozzle, gently insert the plunger into the QIAfilter Maxi Cartridge and filter the cell lysate into a 50-ml tube. Add 2,5ml Buffer ER to the filtered lysate, mix by inverting the tube approximately 10 times, and incubate on ice for 30min. Equilibrate a QIAGEN-tip 50 by applying 10ml Buffer QBT, and allow the column to empty by gravity flow. Apply the filtered lysate to the QIAGEN-tip and allow it to enter the resin by gravity flow. Wash the QIAGEN-tip with 2 x 30ml Buffer QC. Elute DNA with 15ml Buffer QN. Precipitate DNA by adding 10,5ml (0.7 volumes) room

temperature isopropanol to the eluted DNA. Mix and centrifuge immediately at 9500 x g for 1h at 4°C. Carefully decant the supernatant. Wash DNA pellet with 5ml of endotoxin-free, room-temperature 70% ethanol (add 40ml of 96-100% ethanol to the endotoxin-free water supplied with the kit) and centrifuge at 9500 x g for 30min, carefully decant the supernatant without disturbing the pellet. Air-dry the pellet for 5-10min, and redissolve the DNA in a suitable volume of endotoxin-free Buffer TE.

2.2.1.5 Isolation of DNA fragments from agarose gel

For the isolation of DNA fragments from agarose gel, I used the excellent MACHEREY-NAGEL, NucleoSpin® Extract 2-in-1 kit. The protocol is as follows:
Take a clean scalpel to excise the gel containing the DNA fragment to minimize the gel volume. Determine the weight of the gel slice and transfer it to a clean tube. For each 100mg agarose gel add 300ul NT1, incubate sample at 50°C until the gel pieces have been dissolved (5-10min). Vortex the sample every 2-3min briefly. Place a NucleoSpin Extract column into a 2ml collecting tube and load the sample. Centrifuge 1min at 8000 x g (10000rpm). Discard flowthrough and place the NucleoSpin Extract column back into the collecting tube. Add 600ul NT3, centrifuge for 1min at full speed (13000rpm). Discard flowthrough and place the NucleoSpin Extract column back into the collecting tube. Add 200ul buffer NT3, centrifuge for 2min at full speed (13000rpm) to remove NT3 quantitatively. Place the NucleoSpin Extract column into a clean 1,5ml microcentrifuge tube, add 50ul elution buffer NE, leave at room temperature for 1min. Centrifuge for 1min at full speed (13,000 rpm).

2.2.1.6 Direct purification of PCR products

For this procedure, I used again the MACHEREY-NAGEL, NucleoSpin® Extract 2-in-1 kit, according to the instructions of the manufacturer. This is a brief description of the procedure:
Mix 4 volumes of NT2 with 1 volume of sample, insert the NucleoSpin Extract column into a 2ml collecting tube. Load sample onto the column. Centrifuge 1min at full speed (11000 x g, ~13000rpm) at room temperature. Discard flowthrough and place the NucleoSin Extract column back into the 2ml collecting tube. Add 600ul of buffer NT3 to the NucleoSpin Extract column. Centrifuge at 11000 x g (~13000rpm) for 1min. Discard flowthrough and place the NucleoSpin Extract column back into the 2ml collecting tube. Add 200ul buffer NT3. Centrifuge for 2min at full speed (11000 x g, ~13000rpm) to remove NT3 quantitatively. Place the NucleoSpin Extract column into a clean 1,5ml microcentrifuge tube and add 50ul elution buffer NE. Leave at room

temperature for 1min to increase the yield of eluted DNA. Centrifuge for 1min at 11000 x g (~13000rpm).

2.2.1.7 Isolation of total RNA from cells

I used a very simple protocol based on RNAzol B:

Cells grown in monolayer are lysed directly in the culture dish by addition of RNAzol B (WAK Chemie). Use at least 1ml of the reagent for a 3,5cm Petri dish. Pass the lysate through a pipette several times to ensure lysis. Add 0,2ml chloroform per 1ml of RNAzol B, cap the tube and shake vigorously for 15-30 seconds. Store the sample on ice (or at least 4°C) for 5 minutes. Centrifuge the homogenate at 12000g for 15 minutes at 4°C. Following centrifugation, the sample forms the lower blue phenol-chloroform phase, interphase, and the upper colorless aqueous phase. RNA remains exclusively in the aqueous phase whereas DNA and proteins are in the interphase and organic phase. The volume of the aqueous phase is about 50% of the initial volume of RNAzol B plus sample volume. Transfer the aqueous phase to a clean tube, add 0,5ml of isopropanol, and store the sample for 5-10 minutes at room temperature. Centrifuge at 12000g for 5 minutes at 4-25°C. RNA precipitate forms a white pellet at the bottom of the tube. Remove the supernatant and wash the RNA pellet once with 75% ethanol, shaking or votexing to dislodge the pellet from the side of the tube. Centrifuge for 5 minutes at 7500g at 4-25°C. Use 1ml of ethanol solution per 1ml of RNAzol B used for the initial homogenization. Briefly air-dry the RNA pellet (5-10 minutes). It is important not to let the RNA pellet dry completely, as this greatly decreases its solubility. Do not dry RNA by centrifugation under vacuum. Dissolve the RNA in water with DEPC treatment. The final preparation of RNA has an OD260/280 ratio 1,6-1,9.

2.2.1.8 Isolation of poly(A)-enriched RNA

To isolate polyadenylated mRNA, I used the Dynabeads Oligo $(dT)_{25}$ kit (Dynal #610.02 or #610.05, DYNAL BIOTECH), following the invaluable protocol developed in our Department by Dr. Axel Visel:

First, set a water bath or heat block to 65°C and prepare and label three 1,5ml tubes:

(1) PCI extraction, *(2)* quantitation tube (containing 90ul DEPC-H_2O), *(3)* mRNA storage tube (containing 600ul 100% ethanol).

On ice, mix 4ml of Lys-bind (0,1M Tris, pH7.5; 500mM LiCl; 10mM EDTA; 1%SDS) with 40ul DTT (30mg/ml in DEPC-H_2O) and take the 1,5ml tubes containing tissues out of the freezer (e.g., 5 tubes, each containing tissue from wild type mouse). Immediately distribute the cold Lys-bind + DTT mix evenly into the tubes containing the tissue (e.g., 808ul per tube); keep on ice. Use a

clean micropestle that fits into a 1,5ml tube to homogenize the tissue. Use a clean 2ml syringe with a 0,9mm (20G) needle to transfer the homogenate into the two 2ml tubes. Shear DNA by pipetting up and down through the needle 7-9 times. Spin down at full speed for 2min in a microcentrifuge. Distribute the supernatant evenly (~1ml each) into the four 2ml tubes containing the resuspended Dynabeads (in 400ul Lys-bind each), vortex. Leave at room temperature for 5min, (annealing), vortex occasionally. Place tubes in magnet rack, after separation remove supernatant into bead recycling bottle. Add 400ul Wash-SDS (20mM Tris pH7.5; 1M LiCl; 2mM EDTA, 1%SDS) to each tube, vortex, separate in magnet rack, remove supernatant (recycling bottle), repeat this step with 400ul Wash-SDS per tube, repeat again with 400ul Wash-high (20mM Tris, pH7.5; 1M LiCl; 2mM EDTA) per tube, repeat once more with 400ul Wash-conc (10mM Tris, pH 7.5; 150mM LiCl; 1mM EDTA) per tube. Add 55ul DEPC-H_2O per tube (220ul total), resuspend and incubate 3min at 65°C, resuspend. Separate in magnet rack, transfer supernatant into tube *(1)*, put on ice, transfer a 10ul aliquot from tube *(1)* to tube *(2)*, use contents of tube *(2)* to determine mRNA concentration on a spectrophotometer: $1OD_{260}$ = 40ng (= 0,04ug) RNA/ul; 1:10 dilution is used and about 200ul of mRNA is left, so OD_{260} x 80 = total amount of mRNA in ug. Add 200ul PCI to tube *(1)* and vortex rigorously, spin at full speed for 2min in a microcentrifuge. Transfer top phase into tube *(3)*, mix and store at -80°C.

2.2.1.9 Removal of contaminating genomic DNA from RNA samples

The reaction was:

18ul RNA

1ul 10x DNase I reaction buffer

1ul DNase I (RNase-Free) (2U/ul) (NEB)

Incubate at 37°C for 10min. Inactive DNase I by incubating at 75°C for 10min. Add EDTA to a final concentration of 5mM to protect RNA from being degraded during enzyme inactivation.

2.2.1.10 Determination of nucleic acid concentration

The concentration of DNA or RNA was determined photometrically (8452A photometer, Hewlett Packard, Hamburg) by measuring absorption of the diluted sample, at 260nm, 280nm and 320nm (control). The concentration was calculated according to the following formula:

C = E260 x f x c

C = concentration of the sample (ug/ul)

E260 = absorption at 260nm

E320 = absorption at 320nm, normally, E320 is nearly zero.

f = dilution factor

c = concentration (standard)/absorption(standard)

For double stranded DNA, c = 0,05ug/ul; for RNA, c = 0,04ug/ul and for single stranded DNA, c = 0,03ug/ul.

2.2.2 Enzymatic modifications of DNA

(Restriction enzymes and DNA markers were from NEB unless indicated otherwise).

2.2.2.1 Restriction of DNA

Restriction cutting was performed by incubating double-stranded DNA molecules with an appropriate amount of restriction enzyme in its respective buffer as recommended by the supplier at optimal reaction temperature. Typical digestions included 1-5U of enzyme/ug DNA. The reactions were usually incubated for 1-3h to ensure complete digestion. The following is the general reaction I used:

1ug DNA

2ul 10x reaction buffer

0,5ul enzyme (10U/ul)

add distilled H_2O to a total volume of 20ul

2.2.2.2 Dephosphorylation of plasmid DNA

To prevent the recircularization of vector plasmid without insertion of foreign DNA, alkaline phosphatase treatment was peformed. Alkaline phosphatase catalyzes the hydrolysis of 3′-phosphate residues from DNA. The followings were mixed,

1-5ug linearized vector DNA

5ul 10 x reaction buffer

0,5-2,5ul alkaline phosphatase (0,5-2,5U), Calf Intestinal (CIP)

add distilled H_2O to a total volume of 50ul

Incubate at 37°C for 60 min and stop the reaction by heating reaction at 85°C for 15min, purify DNA by gel purification, spin-column purification or phenol extraction.

2.2.2.3 Ligation of DNA fragments

The ligation of an insert into a vector was carried out in the following reaction mix:

30ng vector DNA

100ng insert DNA

1ul 10 x ligation buffer

1ul T4 DNA ligase (5U/ul)

add distilled H_2O to a total volume of 10ul

Blunt-end and cohesive-end ligations were carried out at 16°C overnight.

2.2.2.4 Quick ligation of DNA fragment

The Quick Ligation ™ Kit (NEW ENGLAND, $BioLabs_{Inc}$) enables ligation of cohesive end or blunt end DNA fragments in 5 minutes at room temperature(25°C). It is a very efficient and time-saving method to clone DNA fragment into a vector.

Combine 50ng of vector with a 3-fold molar excess of insert.

Add 10ul of 2 x Quick Ligation Buffer and mix.

Add 1ul of Quick T4 DNA ligase and mix thoroughly.

Adjust volume to 20ul with distilled H_2O.

Centrifuge briefly and incubate at room temperature (25°C) for 5min. Chill on ice, then transform or store at - 20°C.

2.2.2.5 Preparation of competent E. coli

A straightforward procedure common in every molecular laboratory: Pick a single colony of *DH5a* and inoculate 10ml of LB-ampicilium, grow overnight at 37°C; add 1ml overnight culture to 100ml prewarmed LB media containing 80ug/ml ampicillin in a 500-ml flask, and shake at 37°C until an OD600 of 0,5 is reached; cool the culture on ice for 5 minutes, and transfer the culture to a sterile, round-bottom centrifuge tube; collect the cells by centrifugation at low speed (5min, 4000 x g, 4°C); discard the supernatant carefully, always keep the cells on ice; resuspend the cells gently in cold (4°C) 30ml TFB1 buffer (100mM RbCl, 50mM $MnCl_2$, 30mM potassium acetate, 10mM $CaCl_2$, 15% glycerol, pH5.8; sterile-filter) and keep the suspend on ice for an additional 90min; collect the cells by centrifugation (5min, 4000 x g, 4°C); discard the supernatant carefully in 4ml ice-cold TFB2 buffer (10mM MOPS, 10mM RbCl, 75mM $CaCl_2$, 15% glycerol, adjust to pH6.8 with KOH, sterile-filter); prepare aliquots of 100-200ul in sterile microcentrifuge tubes and freeze in liquid nitrogen or a dry-ice-ethanol mix. Store the competent cells at -70°C.

2.2.2.6 Transformation of bacteria

Thaw competent cells on ice. Chill approximately 5ng (2ul) of ligation mixture in a 1,5ml microcentrifuge tube. Add 50ul of competent cells to the DNA and mix gently by pipetting up and down. Incubate on ice for 30min. Heat shock for 90s at 42°C, chill on ice for 5min. Add

950ul of room temperature media and incubate at 37°C for 60min. Spread 200ul onto the appropriate solid medium. Incubate overnight at 37°C.

2.2.2.7 Blunting ends reaction

Blunting ends 3′overhang removal and 3′recessed end fill-in: 0,1-4ug of digested DNA was mixed with 33uM each dNTP and 1-5U of DNA Polymerase I Large Fragment (Klenow) in 1 x EcoPol buffer or any restriction buffer. The reaction was incubated at 25°C for 15min. Stop reaction by adding EDTA to a final concentration of 10mM and heating at 75°C for 20min.

2.2.3 Gel electrophoresis

Gel electrophoresis is the technique by which mixtures of charged macromolecules, especially nucleic acids and proteins, are rapidly resolved in an electrical field.

2.2.3.1 Agarose gel electrophoresis of DNA

Agarose gels are used to electrophorese nucleic acid molecules from as small as 50bp to more than 50kb, depending on the concentration of the agarose and the precise nature of the applied electrical field (constant or pulse). 1g agarose was dissolved in 100ml of 0,5 x TAE buffer (50 x: 242g Tris base, 57,1ml glacial acetic acid, 100ml 0,5M EDTA) by boiling in the microwave, then cooled down to about 50°C before adding 3ul ethidium bromide (10mg/ml). The gel was poured into a horizontal gel chamber. Before loading samples, 0,1volume of stop mix (10 x loading buffer, 0,4% bromophenol blue, 0,4% xylene cyanol FF, 50% glycerol, store at 4°C) was added and mixed. The samples were then loaded into the wells of the gel and electrophoresis was carried out at a steady voltage. The 0,5 x TAE buffer was also used as electrophoresis buffer.

2.2.3.2 Agarose gel electrophoresis of RNA

Non-denaturing gel electrophoresis was employed here. The difference from DNA electrophoresis is the way of preparing agarose gel. Dissolve agarose in 0,5 x TAE, treat with DEPC and incubate at 37°C overnight before heating up in microwave. 0,5 x TAE for running the gel and loading buffer were treated with DEPC.

2.2.3.3 DNA length standards

In order to be able to determine the size of the DNA fragments with gel electrophoresis, parallel to the DNA samples, 0,5ug of the “1kb DNA Ladder” or “100bp DNA ladder” length standard was loaded on the electrophoresis gel. The DNA ladder was diluted in sample buffer.

2.2.4 Non-radioactive dye terminator cycle sequencing

The non-radioactive sequencing was achieved with a Dye Terminator Cycle Sequencing Kit (Applied Biosystems) and the reaction products were analyzed with automatic sequencing equipment, namely a 377 ABI Prism DNA Sequencer (Applied Biosystems). For the sequencing reaction, four different dye labeled dideoxy nucleotides were used. These, when exposed to an argon laser, emit fluorescence which could be detected and interpreted. The reaction progressed in a total volume of 10ul containing 500ng plasmid DNA or 50ng purified PCR products, 1ul of 5uM primer, and 2ul reaction mix (contains dNTPs, dideoxy dye terminators and Taq DNA polymerase), add distilled H_2O to a final volume of 10ul. Elongation and chain termination took place during the following program in a thermocycler: 96°C 1min denaturing followed by 25 cycles of 96°C 5s, denaturing; 50°C 5s, annealing; 60°C 4min, elongation. After the sequencing reaction, add 190ul of dH_2O into reaction tube, transfer to a 1,5ml tube, add 500ul of 100% ethanol and 20ul of 3M NaAc pH4.8, mix. Centrifuge at 13000rpm for 20 minutes at room temperature, carefully decant the supernatant. Wash pellet by adding 400ul of 70% ethanol, mix, centrifuge at 13000rpm for 10 minutes at room temperature. Decant the supernatant as before, dry for 5 minutes in the concentration at room temperature, dissolve the pellet in 2ul of 5:1 fromamide:dextranblue-EDTA and denatured at 90°C for 2 minutes. Samples can be stored at -20°C and finally samples were loaded on the sequencing gel.

2.2.5 Methods of the "polymerase chain reaction" (PCR)

2.2.5.1 PCR of plasmid-DNA

A general PCR reaction was conducted as follows with QIAGEN Taq DNA polymerase. The reaction was placed in a 50ul reaction tube in a total volume of 20ul.

2ul 10 x PCR buffer
4ul Q
0,2ul 10mM dNTPs
1ul upstream primer (5uM)
1ul downstream primer (5uM)
50ng DNA
0,15ul Taq DNA polymerase (5U/ul)
add distilled H_2O to a final volume of 20ul.

Standard program:

segment 1 (1x), 4min 94°C (denaturation)

segment 2 (35x), 40sec 94°C (denaturation)

40sec 55-60°C (annealing)

1min 72°C (extension) (1min per 1kb for most polymerases)

segment 3 (1x), 7min 72°C (final extension)

segment 4, 4°C for ever

After finishing the PCR, 5ul of the reaction was mixed with loading buffer and run on an agarose gel.

2.2.5.2 Gradient PCR

The difference between gradient PCR and general PCR is the annealing temperature designation. The gradient PCR is to determine the best annealing temperature. The reactions are the same as *1.2.5.1*. Run an analytical (gradient) PCR with 6-7 tubes in a range of 20°C (PCR efficiencies may change according to various thermocyclers). The typical gradient program used in the Biometra thermocycler:

Step	Temp(°C)	Time (min)	Cycles	Gradient
1	94	2.00	1	
2	94	0.20	34	20
3	50	0.20		
4	70	1.10		
5	72	9.00	1	
6	4	pause		

2.2.5.3 Single-colony PCR

To screen large amounts of bacterial colonies for desired inserts, single colony was picked from a transformation plate with a sterile toothpick and dotted on a new LB selecting plate. The rest of the colony on the toothpick was subjected to a standard 30ul PCR reaction with appropriate primers to test for the presence of the insert. For plasmid preparation, the colony that contained desired insert vector was inoculated into LB medium with the colony dotted on the LB selecting plate.

2.2.5.4 High fidelity long fragment pull from single BAC clone by PCR

Pick up a single BAC clone from the transformation plate and subject to the following 50ul PCR reaction with *PfuTurbo*® DNA Polymerase (STRATAGENE).

distilled water 41,6ul
10 x cloned *Pfu* DNA polymerase reaction buffer 5,0ul
dNTPs (20mM) 0,4ul
upstream primer (5uM) 1,0ul
downstream primer (5uM) 1,0ul
Pfu turbo polymerase 1,0ul (2,5U)
total reaction volume 50ul

Perform PCR using cycling conditions listed below:
95°C 1min; (30 x) 95°C 30Sec, 65°C 30Sec, 72°C 4min; 72°C 10min.

2.2.5.5 Foxb1 mice and EphA7 mice colony genotyping assay by PCR

2.2.5.5.1 Foxb1 mice colony

Primers for wild type (WT) band
GAB20. 5′ CACTGGGATGGCGGGCAACGTCTG3′
GAB22. 5′ CATCGCTAGGGAGTACAAGATGCC3′
Primers for knock out (KO) band
GAB20. 5′ CACTGGGATGGCGGGCAACGTCTG3′
GAB24. 5′ CGATGCCTGCTTGCCGAATATCATGG3′
Each reaction:

1ul DNA
1ul 10 x PCR buffer
2ul Q
1ul primer GAB20 (5uM)
1ul primer GAB22 (5uM)
1ul primer GAB24 (5uM)
0,2ul dNTPs (10mM)
0,15ul Taq polymerase (5U/ul) (Qiagen)
Add dH_2O to a final volume of 20ul

PCR conditions:

94ºC, 4min+ 30 x (94ºC, 40sec + 65ºC, 40sec + 72ºC, 40sec) + 72ºC, 7min.

The size of fragments are 500bp (KO) and 300bp (WT).

2.2.5.5.2 EphA7 mice colony

Primers for WT band

1. 5′TTCTAAGGTCCTATTTTGCCTGAG3′

2. 5′GAGTCCAGGATTCCCTCCCAGATC3′

Primers for KO band

3. 5′CGAAGTTATTAGGTCCCTCGAAG3′

4. Idem 1

Each reaction:

1ul DNA

1ul 10 x PCR buffer

2ul Q

1ul primer 1 (5uM)

1ul primer 2 (5uM)

1ul primer 3 (5uM)

0,2ul dNTPs (10mM)

0,15ul Taq polymerase (5U/ul) (Qiagen)

Add H_2O to a final volume of 20ul

PCR conditions:

95ºC, 4min+ 35 x (95ºC, 30sec + 52ºC, 40sec + 72ºC, 40sec) + 72ºC, 7min

The size of fragments are 270bp (KO) and 620bp (WT).

2.2.5.6 Reverse transcriptase PCR (RT-PCR)

ThermoScript™ RT, an avian RNase H-minus reverse transcriptase (ThermoScript™ RT-PCR System, Invitrogen) was used to synthesize cDNA from RNA template as follows.

1-5ug total RNA was mixed with 1ul of Random Hexamers (50ng/ul) or oligo $(dT)_{20}$ primer (50uM), and adjust volume to a 10ul with DEPC-treated water in a 0,2 or 0,5ml tube. Denature RNA and primer by incubating the reaction tube at 65°C for 5min, then place on ice. Vortex the 5 x cDNA Synthesis Buffer for 5s just prior to use. Prepare a master reaction mix on ice and vortex gently.

5 x cDNA Synthesis Buffer 4ul

0,1M DTT 1ul

RNaseOut™ (40U/ul) 1ul

DEPC-treated water 1ul

10mM dNTP-Mix 2ul

ThermoScript™RT (15U/ul)

Pipet 10ul of master reaction mix into the reaction tube on ice and incubate at 50°C for 60min in a water bath. Stop the reaction by incubating at 85°C for 5min. Add 1ul RNase H (2U/ul) and incubate at 37°C for 20min. cDNA synthesis reactions can be stored at - 20°C or used for PCR immediately. 10% of the cDNA synthesis reaction (2ul) was used for subsequent PCR.

2.2.5.7 Quantitative real-time PCR (Q-PCR) and relative gene expression comparisons between wild type and knock-out

An iCycler real-time PCR system (BIO-RAD) was used, which provides a simple 96-well plate format for the detection of DNA samples. iQ SYBR Green Supermix (BIO-RAD) (SYBR Green I is a double-strained DNA intercalating dye that fluoresces upon laser light excitation) was used in the PCR reaction.

An inherent property of PCR that is exploited in real-time PCR is that the more copies of nuclei acid one starts with, the fewer cycles of template amplification it takes to make a specific number of products. Therefore, the number of cycles needed for the amplification-associated fluorescence to reach a specific threshold level of detection (the C_T value) is inversely correlated to the amount of nucleic acid that was in the original sample. Because the progress of amplification is monitored throughout the PCR process in real-time PCR, a C_T value can be determined during the exponential phase of a PCR reaction, when amplification is most efficient and least affected by reaction-limiting conditions. The quantity of DNA in the sample can then be obtained by interpolation of its C_T value versus a linear standard curve of C_T values obtained from a serially diluted standard solution.

The housekeeping gene e*longation factor 1 alpha* (*EF1α*) is used to normalize different cDNA samples amounts.

Primers:

EF1α-forward: 5′GTCCCCAGGACACAGAGACTTCA3′

EF1α-reverse: 5′AATTCACCAACACCAGCAGCAA3′

EphA7 full length (FL) - forward: 5′TTCCAAAGAAAATTGGGCTG3′

EphA7 full length (FL) - reverse: 5′CCACATGACCAAACAACACC3′

EphA7 truncated 1 (Tr1) –forward: 5′ATGTGTTACCTGCATGCTTCTG3′

EphA7 truncated 1 (Tr1) -reverse: 5′TAGGAGGAGGTAGCCAGTATGC3′

EphA7 truncated 2 (Tr2) –forward: 5′TAAGAAGTGGATGATTGCATCG3′

EphA7 truncated 2 (Tr2) - reverse: 5′TTTCCGGAAGAGAGGATTACAG3′

EphA7 truncated 3 (Tr3) – forward: 5′AAGTCAGTTGGAGAAGCCAGAC3′

EphA7 truncated 3 (Tr3) - reverse: 5′AGTGTCAGTTGAGAAAAGCTCC3′

Mammillary body tissue was dissected and mRNA was prepared from wild type and Foxb1 mutant as described in Microarray methods *1.3***.** cDNA was prepared as described in section *1.2.5.6*. Experimental samples were diluted 1:50 with double distilled H_2O. A control cDNA sample was serially diluted to produce a set of cDNA samples 1:10, 1:100, 1:1000, 1:10000. In theory, a perfect primer set should generate a straight line using the C_T values of the diluted cDNA samples plotted against the logarithm of the cDNA concentration. Gene-specific forward and reverse primers were mixed and used at a concentration of 1,4uM each. PCR reactions were set up in optical tubes at 15ul reaction volume per tube. To minimize pipetting deviations the reaction set-up was combined by preparing a master-mix containing the primer-mix and the SYBR-Mix for all of the samples which was added to the cDNA. Each sample was tested as triplicate or hexaplicate.

Each reaction contained:

3,75ul cDNA (1: 50 dilution of the cDNA stock solution)

3,75ul Primer-mix (1,4uM each)

7,5ul 2 x SYBR Green Mix

PCR program:

Cycle 1: (50x, amplification phase)

Step 1: 94,0ºC for 00:15

Step 2: 59,0ºC for 00:25

Step 3: 72,0ºC for 00:20

Data collection and real-time analysis enabled.

Cycle 2: (90x, melt curve determination)

Step 1: 50,0ºC for 00:10

Increase setpoint temperature after cycle 2 by 0,5ºC

Melt curve data collection and analysis enabled.

Cycle 3: (1x)

Step 1: 4,0ºC HOLD

After PCR, amplicon size and reaction specificity were confirmed by melting curve analysis and agarose gel electrophoresis using 5ul from each reaction.

The quantity of each transcript (SQ = starting quantity) in relation to the sample cDNA could be determined from the standard curve generated by the serial dilution control cDNA samples. The relative expression level of each gene in each sample (e.g. EphA7-FL in knock out) was computed as follows:

$$\text{Relative expression (EphA7-FL in KO)} = \frac{\text{SQ(KOcDNA) EphA7-FL}}{\text{SQ(KOcDNA) EF1a}}$$

2.3 DNA arrays

2.3.1 Mammillary body dissection and tissue collection

Before start, prepare dry ice, "normal" ice, large Petri dish, small Petri dishes, RNA-grade 1 x PBS, dissection tools, RNA-grade eppis (Labeled 1, 2, 3…..and "tissue") 70% ethanol, paper tissue, and logbook to put down the data about the tissue collection.

Microdissect the anterior and posterior portion of the hypothalamus of E18.5 mouse embryos from Foxb1 mutant and wild type littermates. To this effect, the brains were removed whole, inverted to make the ventral side of the hypothalamus visible in order to dissect it from the telencephalic hemispheres. The resulting medial piece of brain will then be sectioned sagittally, and the hypothalami will be separated from the mass of the dorsal thalamus through a horizontal cut. A vertical cut at the level of the pituitary will give an anterior (containing among others the suprachiasmatic nucleus) and a posterior (containing the mammillary body) portion of the hypothalamus. These pieces of tissue will be immediately frozen in dry ice, separately, in previously labeled containers. Two types of tissue are of interest for our purpose: Foxb1-/- posterior hypothalamus(HO-P), wild type posterior hypothalamus (WT-P). Leg tissue of each embryo will be collected at the same time, washed to remove contaminating blood and prepared to obtain genomic DNA for the genotyping assay.

2.3.2 mRNA isolation

After genotyping by PCR, the tissue was pooled according to genotype, then mRNA was isolated by means of Dynabeads® technology (Dynal Biotech, Oslo, Norway). See *1.2.1.8*. mRNA quality was checked by complementary methods: UV 260/280 ratio, agarose gel electrophoresis and an Agilent Bioanalyzer to visualize clear 18S and 28S ribosomal RNA bands.

2.3.3 Hybridization

Hybridization to the Affymetrix Chips, as well as the informatic analysis of the resulting data, was done by the Deutsches Ressourcenzentrum für Genomforschung(RZPD, Berlin). We used the GeneChip® DNA microarrys made by Affymetrix, specifically, the Murine Genome U74 Set, consisting of three Chips Av2, Bv2, Cv2), containing sequences representing approximately 36000 genes (6000 functionally characterized plus 30000 Expressed Sequence Tags). The transcriptome of the tissues was compared (also at RZPD) by means of Affmetrix proprietary analytical software. The comparisons were as follows: HO-P vs. WT-P.

2.4 *In situ* hybridization on sections

Note about High-Throughput In Situ Hybridization: The mRNA "in situ" detection necessary to carry out this PhD work was performed with the help of a team of technicians of our Department, using automated protocols implemented by a Tecan Genesis 2000 Fluid Handling Platform (the "In Situ Robot"). This High-Throughput In Situ Hybridization method has been set up by Prof. Gregor Eichele in our Department, and has been documented elsewhere (Herzig et al., 2001; Visel et al., 2004).

2.4.1 RNA probe preparation

2.4.1.1 Primer design

Design a gene specific primers either by using a primer selection program or own experience/strategy (GC content in the range of 40 to 60%, the end at which the polymerase will extend should have a GC or CG, avoid repeats, no homology to other genes in the genome, no long hairpin structures, no dimer formation). Normally 20-24bp long primers are picked up that border the desired sequence. The sequence of the T7 or SP6 universal recognition primer, with 3 extra bases (GCG) to the 5′ end of the forward primer and the 3′ end of the reverse primer are attached to allow the polymerase to bind better. The sequence of the T7 promoter is GCGTAATACGACTCACTATAGGG and for the SP6 the sequence is GCGATTTAGGTGACACTATAG. The annealing temperature depends on the sequence of the gene specific part of the primer because the T7 (GCG-TAATACGACTCACTATAGGG) or Sp6 (GCG-ATTTAGGTGACACTATAG) promoter sequences play no role in binding to cDNA.

2.4.1.2 Template preparation

Here the template is got from PCR product. RT-PCR methods see above *1.2.5.6*. Using gradient PCR (see *1.2.5.2*) to decide the best annealing temperature, those PCRs that show only the desired band are pooled and purified. If multiple bands present, all left samples are pooled, re-run on an agarose gel, cut out and extract the desired band. Basically 50ng are used for sequencing to verify the PCR product (see 1.2.4) and the T7 and SP6 primers could be used for the sequencing reaction. In order to prepare template for the RNA probe, a new 100ul PCR is carried out using the purified 1st PCR product as template (described above). Analyzed 5ul PCR product on an agarose gel and purify the rest with a Qiagens PCR purification kit and finally eluted with 25ul of buffer (10mM Tris-Cl, pH8.5). 3ul are used to measure the concentration and determine DNA purity. Typically yields are in the range of 200-400ng/ul.

2.4.1.3 In vitro RNA transcription

Stratagene RNA transcription kit is used. The RNA polymerase T7 and SP6 are from NEB. The following are added to a reaction tube on the ice.

	conc	vol.
H_2O (DEPC)		add to 20ul
5 x transcription buffer		4ul
rATP	10mM	2ul
rCTP	10mM	2ul
rGTP	10mM	2ul
rUTP	10mM	1,3ul
DIG-UTP	250nmol	0,7ul
DTT	0,75M	2ul
RNasin	40U/ul	1ul
RNA Polymerase (T7 or SP6)	50U/ul	0,5ul
Template		1ug

Incubated the reaction tube is at 37°C for 150min and then 1ul of the following mix is added to stop the reaction and remove the template DNA.

H_2O (DEPC)	16,4ul
$MgCl_2$ (0,3M)	1,6ul
DNaseI (10U/ul)	2,0ul

Incubate the reaction at 37°C for 30 minutes, precipitate the mix with 72ul NH_4Ac (4M, autoclaved) and 470ul EtOH (100%). RNase free solutions are used. Store at –80°C for 30min after adding the solutions, and centrifuge with 13000 rpm for 20min at 4°C. Wash the pellet with ice-cold 70% EtOH. Use 25ul DEPC H_2O to dissolve the precipitated RNA, 2ul of the RNA are analyzed on a 1% agorse gel to check the quality of the RNA probe, eventually adjust the concentration with DEPC water to 50ng/ul for the RNA probe and make 50ul aliquots that are stored at –80°C. Before using it, dilute the probe with hybridization mix to a concentration of 100 to 200ng/ml and keep it at –20°C for a maximum of 2 months.

2.4.2 Preparation and fixation of sections

Take the embryos of the appropriate stage out of the mother and put into ice-cold phosphate buffered saline (PBS) (0.137M NaCl, 0.0027M KCl, 0.01M Na2HPO4, 0.002M KH2PO4, pH 7.4). Isolate each embryo from placenta, cut the head and put it into ice cold OCT and kept there for 5 minutes. The head was transferred to an OCT embedding chamber, where it was frozen slowly. The head was sectioned (20um thick) with a Leica CM3050S cryostat (Germany). Sections were placed in appropriate positions on a Super Frost Plus microscopy slide (Germany). The sections on the slides were fixed for 20 minutes with 4% paraformaldehyde (PFA) (EMS, USA) in 1 x PBS solution. Then the slides were washed in PBS twice to remove the fixative, and acetylated for 5 minutes (2x) with acetylation solution (0,25% acetic anhydride, 0,1M triethanolamine, pH8.0, Sigma, Fluka respectively). The sections on the slides were refixed with 4% Para formaldehyde (EMS, USA) PBS solution for 20 minutes, then washed for 5 minutes in PBS to remove the fixative, and transferred to 0,9% NaCl for 5 minutes and dehydrated the cells in a graded series of ethanol (30%, 50%, 70%, 80%, 95% and 2 x 100%) for 2 minutes each step at room temperature (Automatic done). The slides were air dried. Slides are storable for up to 3 months at –80°C in air tight dessicated chambers.

2.4.3 RNA detection by automated *in situ* hybridization

2.4.3.1 Prehybridization

1. Treat the slides mounted into slide chamber, 6 times for 5 minutes with 300ul of MeOH solution (ROTH) containing 0.6% hydrogen peroxide (Fluka, Germany). The slides are then washed 6 times with 300µl of PBS with 0.05% Tween-20.

2. Then the slides are treated 2 times for 4 minutes with 300ul of 0,2N HCl with 0,05% Tween-20. Wash the slides with 300µl of PBS with 0,05% Tween-20 8 times.

3. Next they are treated 2 times for 7 minutes with 300ul of Proteinase K in buffer (with appropriate concentration corresponding to the stage of tissue to be treated) (50mM Tris, 5mM EDTA, pH 8.0) with 0,05% Tween-20. The slides are then washed 8 times with 300ul of PBS with 0,05% Tween-20.

4. The slides are treated 2 times for 10 minutes with 300ul of 4% PFA in PBS solution with 0,05% Tween-20, followed by 8 washing steps with 300ul of 0,05% Tween-20 in PBS.

5. Finally the probes are pre-hybridized with In Situ Hybridization Buffer (Ambion, Cat. # B8807G, USA) for 30 minutes at 60°C.

2.4.3.2 Hybridization

Incubate the slides with In Situ Hybridization Buffer containing the riboprobe (300µl per slide, final concentration of 100ng/ml) overnight at 60°C.

2.4.3.3 Post hybridization and detection of the hapten-labeled probe (Automated)

1. Wash 5 times for 6 minutes with 300µl wash solution 1 (5 x SSC) at 65°C.

2. Wash 5 times for 6 minutes with 300ul of wash solution 2 (1 x SSC, 50% Formamide) at 65°C.

3. Wash 5 times for 6 minutes with 300ul of wash solution 3 (0,5 x SSC, 50% Formamide) at 65°C.

4. Wash 5 times for 6 minutes with 300ul of wash solution 4 (0,1 x SSC) at 65°C.

5. Wash 3 times with 250ul of NTE (0.05% Tween 20, 5mM EDTA, 10mM Tris, 500mM NaCl, pH 7.6).

6. Incubate 2 times at room temperature, for 5 minutes each, by applying 250µl of 20mM Iodoacetamide diluted in NTE.

7. Wash 3 times with 250ul of NTE.

8. Incubate 2 times at room temperature, for 45 minutes each, by applying 250µl of heat-inactivated 4% Sheep-serum (Chemicon International) in TNT solution (0,05% Tween 20 in 100mM Tris/150mM NaCl, pH 7.6) (filter before use, 0,45um).

9. Wash 8 times with 250ul of TNT solution.

10. Incubate 2 times at room temperature, for 30 minutes each, by applying 250ul of TNB blocking buffer (0,05% Tween 20 in 100mM Tris/150mM NaCl, 0,5% blocking reagent (PerkinElmer Lifesciences) pH 7,6) (filter before use, 0,45um).

11. Incubate 2 times at room temperature, for 45 minutes each, by applying 250ul of Roche′s Anti-Dig-POD diluted in TNB blocking buffer (1:500 diluted in TNB).
12. Incubate 8 times at room temperature, for 5 minutes each, by applying 250ul of TNT.
13. Incubate 2 times at room temperature, for 15 minutes each, by applying 250ul of Tyramide-Biotin (T/B) diluted with NEN amplification diluent buffer for use with tyramide signal amplification (TSA) (PerkinElmer Lifesciences)**.**
14. Wash 8 times with 250ul of maleate wash buffer (MWB) (100mM Maleate, 150mM NaCl, 0,05% Tween 20, pH7.5).
15. Incubate 2 times at room temperature, for 30 minutes each, by applying 250ul of Neutravidin-alkaline phosphatase conjugate (Pierce) diluted in 1% blocking reagent (Roche) containing MWB (1:600 dilution in 1% blocking reagent containing MWB, filter 0,45um before adding antibody).
16. Wash 8 times with 250ul of maleate wash buffer (MWB) (100mM Maleate, 150mM NaCl, 0,05% Tween 20, pH7.5).
17. Wash 2 times with 250ul of TNT solution.
18. Incubate 3 times at room temperature, for 20 minutes each, by applying 250ul of TMN solution (0,1M Tris, 0,05M MgCl2, 0,1M NaCl, 0.05% Tween, pH9.5) containing BCIP (1:250) NBT (1:200) (Roche, Germany) containing Levamisol (0,5mg/ml) (Sigma, Germany). This step maybe extended depending on signal strength.
19. Wash 4 times with 250ul water (0,05% Tween).
20. Wash with 250ul TNT twice.
21. Fix for 20 minutes with 4% PFA, 0,5% Glutaradehyde (Sigma) containing PBS (with 0,05% Tween) by applying 250ul twice.
22. Wash 4 times with 250ul PBS (with 0,05% Tween).
23. Wash 4 times with 250ul water (with 0,05% Tween).
24. Let the slides air dry overnight and coverslip them the next day with aqueous coverslipping medium (Hydromatrix).

2.5 Yeast one hybrid assay

2.5.1 Introduction

A one-hybrid system is an in vivo genetic assay used for isolating novel genes encoding proteins that bind to a target, *cis*-acting regulatory element (or any other short, DNA-binding site; Fig.2.1). The system can also be used to map the DNA-binding domain of previously known, or newly identified, DNA-binding proteins (DNA-BP).

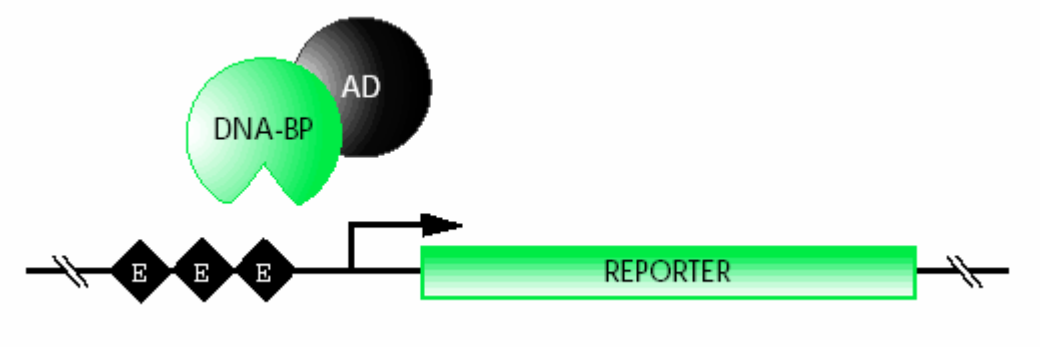

Fig.2.1. Detection of DNA-binding proteins using the MATCHMAKER One-Hybrid System. A sequence consisting of at least three tandem copies of a known target element (E) is inserted upstream of a reporter gene and integrated into the yeast genome to make a new reporter strain. This yeast strain is transformed with an activation domain cDNA library that includes a fusion of a target-specific, DNA-binding protein (DNA-BP) of interest and the target-independent GAL4 activation domain (AD). Binding of an AD/DNA-BP hybrid protein to one of these target elements allows activation of reporter gene transcription.

2.5.2 Prepare target-reporter constructs

2.5.2.1 Synthesizing tandem copies of target elements

Each element sense strain has 5′AATT overhang, it is easy to clone the annealed elements into the vector of pHISi, pHISi-1 and pLacZi with the digestion of EcoRI and SmaI.

E1 sense strain:

AATT.AATAAATAAATAAATAAATAAATAAATAAATAAATAAATAAATAAATA
AATAAATA

E1 anti-sense stain:

TATTTATTTATTTATTTATTTATTTATTTATTTATTTATTTATTTATTTATTT

E2 sense strain:

AATT ATAAATACAAACATGC AATAAATACAAACATGCAATAAATACAAACATGC

E2 anti-sense strain:

GCATGTTTGTATTTATTGCATGTTTGTATT TATTGCATGTTTGTATTTATT

E3 sense strain:

AATT.CACAAACAAAACAAACACACCACAAACAAAACAAACACACCACAAACAAAA
CAAACACAC

E3 anti-sense strain:

GTGTGTTTGTTTTGTTTGTGGTGTGTTTGTTTTGTTTGTGGTGTGTTTGTTTTGTTTGTG

E4 sense strain:

AATT.CAATAAATACAAATAATCCACAATAAATACAAATAATCCACAATAAATACAA
ATAATCCA

E4 anti-sense strain:

TGGATTATTTGTATTTATTGTGGATTATTTGTATTTATTGTGGATTATTTGTATTTATT
G

E5 sense strain:

AATT.ACCAATAAATAAACAAATAACCAATAAATAAACAAATAACCAATAAATAAAC
AAATA

E5 anti-sense strain:

TATTTGTTTATTTATTGGTTATTTGTTTAT TTATTGGTTATTTGTTTATTTATTGGT

E6 sense strain:

AATTCAAACAAACAAACAAACAAACAAACAAACAAACAAACAAACAAACAAACAA
ACAAACAAA

E6 anti-sense strain:

TTTGTTTGTTTGTTTGTTTGTTTGTTTGTTTGTTTGTTTGTTTGTTTGTTTGTTTG

2.5.2.2 Insert tandem copies of target upstream of reporter genes

For each construct planned, mix 0,1mg of sense-strand and 0,1mg of antisense-strand oligonucleotide in 10ml of 50mM NaCl. Anneal the oligonucleotides by heating at 70°C for 5min and then slowly cooling to room temperature (~30min). Use a standard method to do ligation and transformation reaction.

2.5.3 Small-scale LiAC yeast transformation procedure

Inoculate 1ml of YEPD (Yeast extract 2g/liter, Pepton 4g/liter, Glucose 4g/liter) or SD (Yeast Nitrogen Base (W/O AA) 6.7g/liter, Glucose 20g/liter, 10% the appropriate sterile 10 x Dropout Solution) with several colonies of Yeast YM4271, 2-3mm in diameter. Vortex vigorously for 5min to disperse any clumps. Incubate at 30^{o}C for 16-18h with shaking at 250rpm to stationary phase (OD_{600} > 1,5). Transfer 30ml of overnight culture to a flask containing 300ml of YEPD. Check the OD_{600} up to 0,2-0,3. Incubate at 30^{o}C for 3h with shaking (230rpm). At this point, the OD_{600} should be 0,4-0,6. Place cells in 50-ml tubes and centrifuge at 1000 x g for 5min at room temperature (20-21^{o}C). Discard the supernatants and thoroughly resuspend the cell pellets in sterile TE (1 x TE: 10mM Tris, 1mM EDTA, pH7.5). Centrifuge at 1000 x g for 5min at room temperature. Decant the supernatant. Resuspend the cell pellet in 1,5ml of freshly prepared, sterile 1 x TE/1 x LiAc (0,1M LiOAC, 1 x TE). Add 0,1ug of plasmid DNA (linearized or supercoil) and 0,1mg of herring testes carrier DNA to a fresh 1,5ml tube and mix. Add 0,1ml of yeast competent cells to each tube and mix well by vortexing. Add 0,6ml of sterile PEG/LiAC

solution (0,1M LiOAC, 40% PEG3350, TE, pH7.5) to each tube and vortex at full speed for 10sec to mix. Incubate at 30°C for 30min with shaking at 200rpm. Add 70ul of DMSO. Mix well by gentle inversion. Do not vortex. Heat shock for 15min in a 42°C water bath. Chill cells on ice for 1-2min. Centrifuge cells for5 sec at 14000 rpm at room temperature. Remove the supernatant. Resuspend cells in 0,5ml of sterile 1 x TE buffer. Plate 100ul on each SD agar plate (Yeast Nitrogen Base (W/O AA) 6.7g/liter, Glucose 20g/liter, 20g/liter agar, 10% the appropriate sterile 10 x Dropout Solution) that will select for the desired transformants. Incubate the plates, up-side-down, at 30°C until colonies appear (generally, 2-4 days).

2.5.4 Test yeast colonies for background expression

2.5.4.1 Yeast colonies with integrated target pHISi or target pHISi-1

Pick a single colony and suspend it in 1ml of TE buffer. Plate 5ul of the suspension on SD/- His+ 15mM, 30mM, 45mM, 60mM 3-AT (Yeast Nitrogen Base (W/O AA) 6.7g/liter, Glucose 20g/liter, Agar 20g/liter, Lys 30mg/liter, Ade 20mg/liter, Trp 20mg/liter, Tyr 30mg/liter, Leu 30mg/liter, Ura 20mg/liter).

If yeast grows on SD/- His, +>45 mM 3-AT, then background HIS3 expression is high (very leaky).

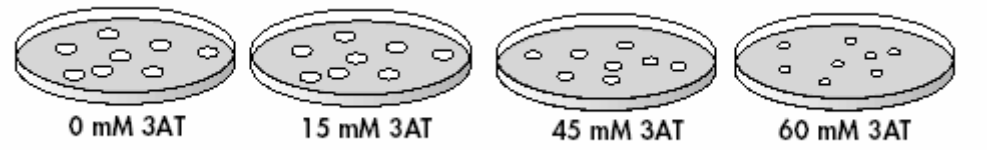

If yeast only grows on SD/-His and < 45mM 3-AT, then background HIS3 expression is low.

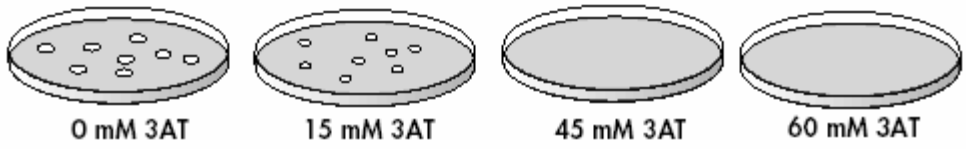

Compare results for yeast colonies with integrated target-pHISi or target-pHISi-1. Identify the HIS3 reporter strain with lower background level of HIS3 expression for use in the one-hybrid screening.

2.5.4.2 Yeast colonies with integrated target pLacZi construct in a ß-gal filter assay

Reagents and Materials: Whatmann #5 paper filter, sterile; Forceps for handling the filters; Z buffer ($Na_2HPO_4 \cdot 7H_2O$ 16,1g/L, NaH_2Po_4 7H2O 5,5 g/L, KCl 0,75 g/L, $MgSO4 \cdot 7H_2O$ 0,246 g/L,

adjust to pH 7.4 and autoclave); X-gal stock solution (Dissolve 5-bromo-4-chloro-3-indolyl-ß-D-galactopyranoside (X-GAL; #8060-1) in N,N-dimethylformamide (DMF) at a concentration of 20mg/ml, store in the dark at -20°C); Z buffer/X-gal solution (100ml Z buffer, 0,27ml ß-mercaptoethanol (ß-ME; sigma #M-6250), 1,67 ml X-gal stock solution); Liquid nitrogen

Use fresh colonies, 1-3mm in diameter. For each plate of transformants to be assayed, presoak a sterile Whatmann #5 paper by placing it in 2,5-5ml of Z buffer/X-gal solution in a clean 100 or 150mm plate. Using forceps, place a clean, dry filter over the surface of the plate of colonies to be assayed. Gently rub the filter with the side of the forceps to help colonies cling to the filter. Poke holes through the filter into the agar in three or more asymmetric locations to orient the filter to the agar. When the filter has been evenly wetted, carefully lift it off the agar plate with forceps and transfer it (colonies facing up) to a pool of liquid nitrogen. Using the forceps, completely submerge the filters for 10sec. After the filter has frozen completely (~10sec), remove it from the liquid nitrogen and allow it to thaw at room temperature. Carefully place the filter, colony side up, on the presoaked filter. Avoiding trapping air bubbles under or between the filters. Incubate the filters at 30°C and check periodically for the appearance of blue colonies.

If the colony life turns blue in < 15 min, then background *LacZ* expression is high. Do not use pLacZi reporter strain.

If colony lift turns blue in > 15 min, then background LacZ expression is low. Use pLacZi reporter strain to construct a dual reporter.

2.5.5 Screening Foxb1 protein binding elements

Foxb1 coding region including 21 nucleotides upstream of the start ATG was PCR-amplified from plasmid GAB2 (from Gonzalo), EcoRI restriction site and BamHI restriction site with two protection bases were added to the forward primer and the reverse primer respectively. The PCR product was cloned into pGAD424 plasmid. After the sequence verification, transform pGAD424-Foxb1 (supercoil) into pHISi-pLacZi and pHISi-1pLacZi dual reporter strain respectively, and plate the transformation mixture on each agar plate containing SD/-His, -Ura3, -Leu (Yeast Nitrogen Base (W/O AA) 6.7g/liter, Glucose 20g/liter, Agar 20g/liter, Lys 30mg/liter, Ade 20mg/liter, Trp 20mg/liter, Tyr 30mg/liter); +15mM 3-AT. Incubate at 30°C for 4-6 days. Pick the largest colonies and resuspend in 1ml of TE buffer. Plate 5ul of the suspension in SD/-His, -Ura3, -Leu, + optimal 3-AT. Colonies resulting from HIS3 activation should grow and colonies resulting from leaky HIS3 expression should not grow. Streak the colonies onto duplicate SD/-His, -Ura3, -Leu, + optimal 3-AT plates, and use one set of plates for a ß-galactosidase filter Assay.

2.6 Transient cotransfections and reporter assays

2.6.1 Cell culture

P19 cells (ECACC) were cultured in Alpha MEM (SIGMA)+ 2mM Glutamine (GIBCO BRL) + 1% Non Essential Amino Acids (NEAA) (SIGMA) +2,5% Fetal Calf Serum (FCS) (GIBCO BRL) +7,5% Calf Serum(CS) (GIBCO BRL). Transfer cells with the transport medium into a 25cm^2 flask and add 15ml of fresh medium. Re-gas with 5%CO_2 where appropriate and incubate overnight at 37^{o}C. At confluence trypsinise by decanting culture medium and washing the cell sheet twice with PBS and adding 2ml of trypsin/EDTA solution to a 25cm^2 flask ensuring that all cells are covered. Incubate at 37^{0}C until cell sheet detached, usually 5 minutes. Resuspend cells in fresh media at the recommended seeding density. Prepare freeze medium by allowing 1ml for each ampoule. 90% FCS +10%DMSO was used for P19 cells.

2.6.2 Plasmids

Foxb1 coding region was under the CMV promoter in GAB2 plasmid (+Foxb1). GAB3 has a reverse orientated promoter, as a control plasmid of GAB2 (-Foxb1). Regulation element was cloned at the MCS upstream of the promoter of reporter plasmid pGL3-C (Promega). TKß is a ß-galactosidase expression plasmid. ß-galactosidase expression level is the internal control of the transfection efficiency. All plasmids were prepared with "QIAGEN Endofree Plasmid Midi Kit", see *1.2.1.4.*

2.6.3 Transfection

The day before transfection, seed 1,5~5 x 10^4 cells per well of a 24-well plate in 0,7 ml of the complete growth medium. Incubate the cells at 37^{o}C in a CO_2 incubator until the cells are 50-80% confluent (usually about 18 hours). For each well in a transfection, dilute 600ng DNA into 25ul medium without serum, add 4ul Plus™ Reagent (Cat. No. 11514-015, Invitrogen), mix again, and incubate at room temperature for 15min. Dilute 1,5ul Lipofactamine™ Reagent (Invitrogen) into 25ul dilution medium without serum in a second tube and mix. Combine pre-complexed DNA and diluted Lipofectamine™ reagent, mix and incubate for 15min at room temperature. While complexes are forming, replace the medium on the cells with 0,2ml of cell growth medium without serum. Add the DNA-Plus™-Lipofactamine™ Reagent complexes to each well of cells contaning fresh medium. Mix complexes into the medium gently; incubate at 37^{o}C at 5% CO_2 for 4 hours. After incubation, add medium and serum to bring the final composition and volume to

that of normal growth medium. Assay cell extracts for transient gene expression 48 hours after the start of transfection. To minimize pipetting deviations the complex set-up was combined by preparing a pre master-mix containing GAB2 or GAB3 and TKß. Each combination sample was tested as triplicate or hexaplicate, which was prepared as a master mix for 3 or 6 wells.

2.6.4 Harvesting of transfected cells and luciferase activity assay

Take out the cells from the incubator and place them at room temperature about 15 minutes before lysis. Also put the MEM-a medium (Gibco) at room temperature. Aspirate the medium from the wells. Wash cells in each well once with 500ul MEM-a medium. To each well add 100ul of 1 x reporter lysis buffer (Promega). Shake for 15 minutes at room temperature with 150-200rpm, meanwhile put the tube containing the Steady-Glo (Promega) in water bath at room temperature. From each well save 50ul cell lysate for ß-Galactosidase assay. Mix well the Steady-Glo reagent in the tube and add 50ul into each well, shake for 15 minutes at room temperature with 150-200rpm. Transfer 70ul from each well in a costar-3610 96 wells plate. Measure the luciferase activity in LUMIstar (BMG-Lab Technologies, in IPF lab) or Fluoroskan AscentFL (Thermo, in MHH lab).

2.6.5 ß-Galactosidase activity measurement

ß-Galactosidase Enzyme Assay System with Reporter Lysis Buffer (Cat.# E2000, Promega) was used. Add 30ul of Assay 2 x Buffer to 30ul of cell lysate, incubate at 37°C for about 30min. When the reaction color turns yellow, the reaction was stopped by addition of 100ul of 1M Na_2CO_3, and the relative galactosidase activity was measured with a spectrophotometer at 420nm, Assay 2 x Buffer took the place of cell lysate and was used in blank.

2.7 FoxB1 protein expression and purification in *E.coli*

2.7.1 FoxB1 coding region enframing construct

Digest pGAD424-Foxb1 (from yeast one hybrid assay, see *1.5.5*) with EcoRI, treat with Klenow, then was digested with PstI, the fragment of Foxb1 coding region including 21 nucleotides upstream of the start ATG ($EcoRI^k$ - PstI fragment) was cloned into the MCS sites of SmaI-PstI site of pQE-31 plasmid. After the sequence verification, transform pQE-31-Foxb1 into XL1-blue competent cells according to the standard procedure.

2.7.2 FoxB1 expression in *E.coli*

2.7.2.1 IPTG-induction of E. coli, small scale induction

Prepare an over-night culture (each culture from a picked colony) of at least 2ml in LB selective medium (amp, 80mg/l). Inoculate 4ml of selective LB medium (amp, 80mg/l) with 0,4ml of your fresh over-night culture (it should be dense/stationary); Store over-night culture at -4°C for further use and/or make glycerol stocks. Let the cultures grow for 1,5h to 3h (~ 2 generations, to give the cells time for "physiologically adjusting" to the fresh medium). Measure the OD_{600} (a 1:10 dilution is recommendable). Prepare 4,4ml culture (amp, 80mg/l) with OD_{600} = 0,7 for each sample using above cultures and fresh amp (calculation: 0,7 x 4,4 ml/ OD_{600} measured = ml of culture you have to take, 4,4ml – ml of culture to take = ml of fresh medium to add. Cells should be in log-phase before inducing them). Measure OD_{600} again (a 1:5 dilution is recommendable; vortex the freshly prepared cultures before taking samples for the measuring). Induce the cultures with 44ul 100 mM IPTG (to a final concentration of 1mM) for 4 hours.

2.7.2.2 SDS-PAGE electrophoresis and western Blotting

2.7.2.2.1 Sample preparation

Harvest cells from above culture in an eppendorf tube by centrifugation (1min, 14000rpm), remove supernatant thoroughly, resuspend the cells in 100ul sterile water, add 1 volume 2 x SDS-PAGE sample buffer (20% glycerol; 0.1M DTT; 2% SDS; 0.09M Tris-Cl, pH6.8; 0,02 % bromo-phenol blue), mix by vortexing, and boil at 100°C (90°C is also ok) for 5 minutes. Go forward or store extract at -20°C.

2.7.2.2.2 Detection by Tris –Glycine SDS-PAGE electrophoresis

Assemble the glass plates according to the manufacture′s instructions and prepare two gel mold (Bio-RAD system, 10cm x 8cm x 0.1cm). Prepare 10ml 12% acrylamide solution for the resolving gel (H_2O, 3,3ml; 30% acrylamide mix, 4,0ml; 1.5M Tris, pH8.8, 2,5ml; 10% SDS, 0,1ml; 10% ammonium persulfate, 0,1ml; TEMED, 0,004ml), without delay, swirl the mixture rapidly and pour the acrylamide solution into the two gaps between the glass plates respectively, and leave enough space for the stacking gel, overlay the acrylamide solution with 70% isopropanol. After polymerization is complete (30min), pour off the overlay and wash the top of the gel several times with deionized water to remove any unpolymerized acrylamide. Prepare the stacking gel 3ml (H_2O, 2,1ml; 30% acrylamide mix, 0,5ml; 1,0M Tris, pH6.8, 0,38ml; 10% SDS,

0,03ml; 10% ammonium persulfate, 0,03ml; TEMED, 0,003ml), without delay, swirl the mixture rapidly and pour directly onto the surface of polymerized resolving gel. Immediately insert a clean comb (from Bio-RAD system) into the stacking gel solution. After polymerization is complete (30min), remove the comb carefully and wash the wells immediately with deionized water to remove any unpolymerized acrylamide. Mount the gel in the electrophoresis apparatus (Bio-RAD system). Add Tris-glycine electropheresis buffer (25mM Tris; 250mM glycine, pH8.3; 0.1% SDS) to the top and bottom reservoirs.

Load 20ul of each of the samples in a predetermined order into the bottom of the wells. By using protein markers of known molecular weight (NEB, #P7708S), estimate the molecular weight of target protein.

Attach the electrophoresis apparatus to an electric power supply and apply a voltage of 120V and run the gel until the bromophenol blue reaches the bottom of the resolving gel. And turn off the power supply. Remove the glass plates from the electrophoresis apparatus and separate the gels out, one can be fixed and stained with Coomassie Brilliant Blue. Another one gel was used for western blotting.

2.7.2.2.3 Detection with Ni-NTA AP Conjugate, western blotting procedure

To verify Foxb1 expression, find out which strain has high expression level, and find out the differences between not induced and induced cultures, apply 10ul of above samples on the gel for western blotting. See above.

Incubate the gel for 40 minutes in transfer solution (190mM glycin, 25mM Tris, 20% methanol, 0,05% SDS), softly shaking at room temperature; prepare 4 filter papers (3MM whatman) the size of the gel (measure size of the gel), prepare an Immobilon TM -P Transfer Membrane (Millipore) the size of the gel, dip it in methanol, and equilibrate in transfer buffer for 30 minutes, softly shaking at room temperature, then submerse in transfer solution to avoid air bubbles (remove any air bubbles with an test tube), build on BLACK part of the blotting apparatus (to the top): BLACK => wet sponge => 2 filter paper => gel => membrane => 2 filter paper => wet sponge => WHITE, transfer at 1 hour at 50V and 4°C, mark marker bands by pinching little holes with a needle. Wash membrane twice for 10min each time with TBS buffer (10mM Tris-Cl, pH7.5; 150mM NaCl). Incubate for 1h in 3% BSA in TBS at room temperature. Wash 3 times for 10 min with TBS-Tween buffer (20mM Tris-Cl, pH7.5; 500mM NaCl; 0,05% Tween 20). Incubate the membrane for 1h at room temperature in TBS-Tween buffer containing a 1/1000 dilution of Ni-NTA AP (alkaline phosphatase) Conjugate stock solution (QIAGEN). Wash 3 times for 10min in TBS-Tween buffer at room temperature. Stain with AP staining solution (66 µl NBT stock

solution and 33 µl BCIP stock solution to 10ml buffer of 100mM Tris-Cl, pH 9.5, 100mM NaCl, 5mM $MgCl_2$) until the signal is clearly visible (approximately 5–15 min for AP). Do not shake blots during color development. Stop the reaction by rinsing the membrane twice in water. Dry the membrane and photograph as soon as possible.

2.7.2.3 Large scale induction and purification on Ni-NTA beads

Inoculate 200 ml LB (amp, 80mg/l) with 4 ml (= 1/50 volume) of fresh over-night culture and measure OD_{600} every hour. As soon as the cells reach an OD_{600} = 0.7 – 0.9, add 2.004ml 100mM IPTG to a final concentration of 1mM. After 4 hours induction, divide the culture into 4 tubes and 50ml culture per tube, harvest the cells by centrifugation at 4000 x g for 20 minutes at 4°C. Remove the supernatant and use one tube of cells to go forward, and store the rest cell pellets at -20°C for further use. Resuspend the cell pellet in 5ml of lysis buffer (50mM NaH_2PO_4, 300mM NaCl, 10mM imidazole, adjust pH to 8.0 using 1N NaOH) with 200ul of 100mM PEFABLOC (Roche) and 200ul 100mM Complete Mini, EDTA-Free (Roche) proteinase inhibitor. Add Lysozyme to 1mg/ml and incubate on ice for 30 min. Centrifuge lysate at 10000 x g for 20-30min at 4°C to pellet the cellular debris. Save supernatant. Add 200ul of the 50% Ni-NTA matrix (QIAGEN), tumbling for 1h at 4°C. Centrifuge for min at 13000rpm, take out the supernatant away carefully. Wash the protein-Ni-NTA mixture twice with 4ml wash buffer(50mM NaH_2PO_4, 300mM NaCl, 20mM imidazole, adjust pH to 8.0 using 1N NaOH) by tumbling at 4°C for 10min. Centrifuge and take the supernatant away. Elute the protein 3 times with 100ul elution buffer (50mM NaH_2PO_4, 300mM NaCl, 250mM imidazole, adjust pH to 8.0 using 1N NaOH) with 4ul of proteinase inhibitor 100mM PEFABLOC and 100mM Complete Mini, EDTA-Free. Collect the eluate in three tubes and analyze by SDS-PAGE.

2.8 DIG Gel Shift Assay

DIG Gel Shift Kit, 2nd Generation (Cat. No.3353591, Roche) was used.

2.8.1 Annealing and labeling of oligonucleotides

Oligonucleotides were synthesized and HPSF purification in MWG. Mix ss oligonucleotide into a molar ratio of 1:1 in TEN-buffer (10mMTris, 1mMEDTA, 0,1MNaCl, pH8.0, incubate 10min at 95°C and cool slowly to 15-25°C. Dilute with sterile TEN-buffer to 4pmol/ul. Add 4pmol ds oligonucleotide and sterile double distilled water to a final volume of 10ul to a reaction vial. Add the following on ice.

Reagent	Volume	Final conc.
5 x labeling buffer	4ul	1x
$CoCl_2$-solution	4ul	5mM
DIG-ddUTP solution	1ul	0,05mM
Terminal transferase	1ul	20U/ul

Stop the reaction by adding 2ul 0,2M EDTA (pH8.0). Add 3ul double distilled water to a final volume of 25ul, to obtain a final concentration of 4 ng/ul of the labeled oligonucleotide.

2.8.2 Determination of labeling efficiency

Prepare a dilution series of labeled control oligonucleotide from the kit and experimental labeled oligonucleotides as described in the table.

Tube	Oligo(ul)	From tube #	TEN-buffer	Dilution	Final concentration fmol/ul	ng/ul
1		Original	0	-	155	4
2	2	1	18	1:10	15,5	0,4
3	2	2	18	1:100	1,55	0,04
4	2	3	18	1:1000	0,15	0,004
5	-	-	20	-	0	0

Apply a 1ul spot of tubes 1-5 from the labeled oligonleotides and the labeled control to the nylon membrane (positively charged, Roche). Fix the nucleic acid to the membrane by cross linking with UV-light. Transfer the membrane into a plastic container with 20 ml washing buffer (0.1M Maleic acid, 0.15M NaCl; pH7.5; 0.3% Tween 20) and incubate under shaking for 2min at 25°C. Incubate for 30min in 10ml blocking solution (Dissolve blocking reagent 1% (w/v) in maleic acid buffer under constantly stirring on a heating block (65°C), the solution remains opaque). Incubate for 30min in 10ml antibody solution (centrifuge Anti-Digoxigenin-Ap for 5min at 10000rpm in the original vial prior to each use and pipet the necessary amount carefully from the surface. Dilute anti-digxigenin-AP 1:100000 in blocking solution). Wash with 10ml washing buffer, 2 x 15min. Equilibrate 2-5min in 10ml detection buffer (0,1M Tris-Cl, 0,1M NaCl, pH9.5). Place membrane with DNA side facing up on a fresh plastic membrane and apply 0,1ml CSPD working solution (dilute 0,1mg/ml stock solution 1:100 in detection buffer). Immediately cover the membrane with the rest part and spread the substrate evenly and without airbubbles over the membrane, incubate for 5min at 25°C. Squeeze out excess liquid. Drying of the membrane during

exposure will result in dark background. Incubate the damp membrane for 10min at 37°C to enhance the CSPD chemiluminescent reaction. Expose to X-ray film. Multiple exposures can be taken to achieve the desired signal strength. X-ray film was developed in KODAK X-OMAT M43 Processor.

2.8.3 DIG Gel shift reaction

2.8.3.1 Prepare reaction

Each reaction prepared three samples: Sample 1, labeled oligonucleotide without Foxb1 protein; sample 2, labeled oligonucleotide with Foxb1 protein; sample 3, labeled oligonucleotide with Foxb1 protein and with an 125-fold excess of unlabeled oligonucleotide for specific competition. 5 x binding buffer is: 100mM Hepes, adjust to pH7.9 with 1N NaOH; 5mM DTT; 1% Tween 20 (w/v); 150mM KCl; 5mM $MgCl_2$.

	sample 1	**sample 2**	**sample 3**
5 x Binding buffer	4ul	4ul	4ul
poly [d(I-C)] [1ug/ul]	1ul	1ul	1ul
poly L-lysine, [0.1ug/ul]	1ul	1ul	1ul
DIG-labeled oligo-nucleotide[0.4 ng/ul]	2ul	2ul	2ul
double dist. water	12ul	10ul	8ul
unlabeled oligo-nucleotide[10uM]	-	-	2ul
FoxB1 protein [100ng/ul]	-	2ul	2ul

Mix carefully and incubate for 30min at 4°C, place tube on ice. Add to each sample 5µl of loading buffer with bromophenol blue, apply sample immediately to a pre-electrophoresed polyacrylamide gel.

2.8.3.2 Polyacrylamide gel electrophoresis

One day before, prepare a native polyacrylamide gel 8% acrylamide in 0,5 x TBE buffer (15cm x 15cm x 0,1cm PAGE). The gel must be pre-run (45min). Before loading samples, clean sample wells to remove APS, residual polyacrylamide to ensure sample application without diffusion. Load the samples to the gel. Run PAGE in 0,5 x TBE buffer at 120 V and run dye 2/3 of the way to the bottom of the plates (2,5h).

2.8.3.3 Blotting and crosslinking

After electrophoresis, remove one glass plate carefully from the gel. Equilibrate a sheet of nylon membrane trimmed to the size of the gel for 5min in transfer buffer (0,5 x TBE buffer). Place equilibrated nylon membrane carefully onto the gel. Place 4 layers of gel-sized Whatman 3MM papers, presoaked in transfer buffer on the filter. Roll with a glass rod or a pipette over the 4 layers Whatman 3MM paper to remove air bubbles. Remove pad of Whatman 3MM paper/nylon membrane/gel from the other glass plate. Add 4 layers of pre-soaked Whatman 3MM papers on the other side of the gel. Place resulting sandwich between the electrodes of the electroblotting device. Transfer is performed for 30min at 100V (Bio-RAD System). Place the membrane on a Whatman 3MM paper presoaked with 2 x SSC (NaCl 87,65g/liter, sodium citrate 44,1g/liter, adjust to pH7.0 with NaOH), cross-link at 120 mJ in a Stratalinker twice.

2.8.3.4 Chemiluminescent detection

Rinse membrane briefly (1-5) min in Washing buffer. Incubate for 30min in 100ml Blocking solution. Incubate for 30min in 20ml Antibody solution. Wash 2 x 15min in 100ml Washing buffer. Equilibrate 2-5min in 20ml Detection buffer. Place membrane with DNA side facing up on a fresh plastic membrane and apply 1ml CSPD® working solution. Immediately cover the membrane with the rest part of the fresh plastic membrane, spread the substrate evenly and without airbubbles over the membrane. Incubate for 5min at 15 to 25°C. Squeeze out excess liquid. Drying of the membrane during exposure will result in dark background. Incubate the damp membrane for 10min at 37° C to enhance the luminescent reaction. Expose to X-ray film for 15-25min at 25°C. Multiple exposures can be taken to achieve the desired signal strength.

2.9 Histological staining

2.9.1 Immunohistochemical staining

In these techniques an antibody is used to link a cellular antigen specifically to a stain that can be more readily seen with a microscope. Detection of antigens in tissues is known as immunohistochemistry.

Detection of ß-galactosidase in *Foxb1* mutant tissue with Polyclonal Rabbit Antibody was done as follow. Paraffin section was used because it provides for excellent morphological detail and resolution.

Fresh embryo head or adult brain taken out of the mouse after perfusion was fixed in 4% formaldehyde in 1x PBS for 4 days. Then transfer to 50% ethanol (one day), 75% ethanol for one

day, 2 x 100% ethanol (one day each), 2 x Tuluol (one day each), 3 x fresh liquid paraffin (one day each). Then process for embedding in paraffin wax. And paraffin blocks were sectioned at 20um. For the section deparaffinization and hydration, incubate sections in 2 x Xylene, 10 minutes each; 100% absolute ethanol, 10 minutes; 100% absolute ethanol, 5 minutes; 90% 5 minutes; 75% ethanol, 5 minutes; 50% ethanol, 5 minutes. Dip slides shortly in water, then amount slides containing sections into the immuno-rack in 1 x PBS. Gently wash slides with 1 x PBS 3 times. Incubate sections in 1 x PBS with 3% H_2O_2 for 15 minutes. Wash slides with 1 x PBS 3 times, Preincubate sections in PBSTF (1 x PBS, 0.1% Tx-100, 10% FCS) for one hour. Apply 200ul anti-ß- galactosidase (1:500 dilution in PBSTF, Eugene, Oregon, USA) per slide, incubate overnight at 4°C in the dark. The next day morning, rinse slides gently with 1 x PBS 3 times. Apply 200ul anti-rabbit biotin-conjugated antibody directed against rabbit immunoglobulins (1:300 dilution in PBSTF), incubate one hour. Rinse slides gently with 1 x PBS 3 times.), apply 200ul Extravidine peroxidase conjugate (1:100 dilution in PBSTF, SIGMA) and incubate one hour. Rinse slides with 1 x PBS 3 times and add substrate diaminobenzidine (DAB) (1ml 10 x DAB; 9ml 1 x PBS, 30ul H_2O_2) until desired color intensity has developed (3-5min). Wash slides with 1 x PBS and dissemble slides in 1 x PBS, for the dehydration, transfer slides to distilled water for a few seconds, incubate slides in 50% ethanol 5 minutes, 75% ethanol 5 minutes, 90% ethanol 5 minutes, 100% ethanol 5 minutes, 100% ethanol 10 minutes, xylene twice 10 minutes each, coverslip slides with Pertex medium.

2.9.2 Nissl staining

Principle: Neurons contain Nissl substance, which is primarily composed of rough endoplasmic reticulum, with the amount, form, and distribution varying in different types of neurons. Because of the RNA content, Nissl substance is very basophilic and will be very sharply stained with basic aniline dyes. By varying the pH and the degree of differentiation, both Nissl substance and nuclei or only Nissl substance may be demonstrated.

Procedure: the whole work was done in a series of manual staining racks. First for the deparaffinization and hydration, the sections were incubated in 2x for 10min in xylene, then transfer to the following ethanol grade (100%, 95%, 70%, in each case 2 x 5min). After 5min in water, incubate slides for 10-30min (10min embryo, 30min P56 brain) into 1% Cresyl violet (Chroma 1A396) staining solution (2,721% sodium acetatic, 100ml, 1,2% glacial acetic acid 400ml, pH3.8-4 adjusted by using 1,2% glacial acetic acid; 0,1% Cresyl violet). Put slides in 70% isopropanol/0.1% CH3COOH for approximately 15 seconds, then into water for a few seconds.

Incubate slides in 70% ethanol for 5 minutes, 95% ethanol for 5 minutes, 100% ethanol for 5 minutes, in xylene twice, 5 minutes each. coverslip slides with Pertex medium.

3 RESULTS

3.1 FINDING A DOWNSTREAM CANDIDATE FOR *Foxb1* IN THE CAUDAL HYPOTHALAMUS

For our genomic analysis of the regulatory chain starting with Foxb1, we needed relatively large amounts of tissue. Since the mouse strain 129Sv, of choice in the preparation of targeted mutant lines (Nagy et al., 2002), gives small litters, we decided to backcross this mutant line into an outbred one, NMRI, of current use in our institute, which normally yields litters of around 12 to 14 pups. The 129Sv line is highly inbred, that is, has a very high degree of homozygosis. This means the mice are as homogeneous genetically as possible. It also means this line is "weaker", in the sense that mutant phenotypes can be more obvious than in outbred lines, which have a high degree of heterozygosis. The outcome is that a primary concern at this point was the maintenance of the mammillary axonal phenotype in this outbred line. A "robust" phenotype is largely independent on the alleles whose products interact with the protein produced by the mutated gene, while a "weak" phenotype will be more or less obvious (more or less abnormal) depending on the genotype of the genes whose products interact physiologically with the product of the mutated gene.

3.1.1 The mammillary axonal phenotype of the Foxb1 mutant is conserved in the NMRI genetic background.

The original 129Sv mutant mice were crossed into wild type NMRI strain for 7 generations, then the analysis of the phenotype was started. First paraffin blocks were prepared which contained formaldehyde-fixed heterozygous or homozygous brains of different embryonic ages, and cut along the sagittal plane of section and treated them with anti-ß-galactosidase antibody. The

rationale was that the reporter gene for this targeted mutation is tau-LacZ, which generates a fusion protein containing a tau moiety (tau is an intermediary filament protein typical but not exclusive of neuronal axons) and a ß-galactosidase moiety (this is a bacterial enzyme which can be easily detected by specific, commercially available antibodies and whose expression in heterozygous or homozygous tissues "reports" on the transcriptional activity of *Foxb1*). In this way, I was able to detect the axons coming from the mammillary body (MBO) in the heterozygous (which shows a completely normal phenotype (Alvarez-Bolado et al., 2000) and homozygous brain. To identify structures in the embryonic brain, my main reference was the "Developing Brain Maps" Atlas (Alvarez-Bolado and Swanson, 1996). At embryonic day 14.5 (E14.5), the profile of the MBO was easily distinguishable in both heterozygotes and homozygotes (Fig.3.1A, B). The principal mammillary (pm) tract emerged from the dorsal surface, and first spread out more dorsally, then extended parallel to the ventral part, caudally reaching ventral and dorsal midbrain tegmental nuclei. It showed a well developed mammillotegmental bundle (mtg). At this age, no difference was observed between heterozygotes and homozygotes. By E17.5 differences between heterozygotes and homozygotes started to be evident: the axons of the heterozygous principal mammillary tract extended a new outgrowth. This was the mammillothalamic tract (mtt) (Fig.3.1C, D). In the mutants, however, only a few growing axonal tips were present at the collateral bifurcation (Fig.3.1D). Within 24 hours, another axonal tract, the mammillotectal tract (mtc), started to be visible (Fig.3.1E). This tract coursed first dorsally, then turned caudally in the direction of the midbrain tectum, and was well established by E18.5 (Fig.3.1E,F).The mtc is probably formed by principal axons from the dorsal premammillary nucleus, and not by collateral branches of the principal mammillary tract (Canteras and Swanson, 1992; Alvarez-Bolado et al., 2000). In heterozygotes, the mtt tract was clearly visible at E18.5 (Fig.1E), formed by pioneer fibers provided with growing tips advancing dorsalward into the dorsal thalamus. However, in homozygotes, only a few short outgrowths could be seen to hang towards their target, dorsal thalamus.

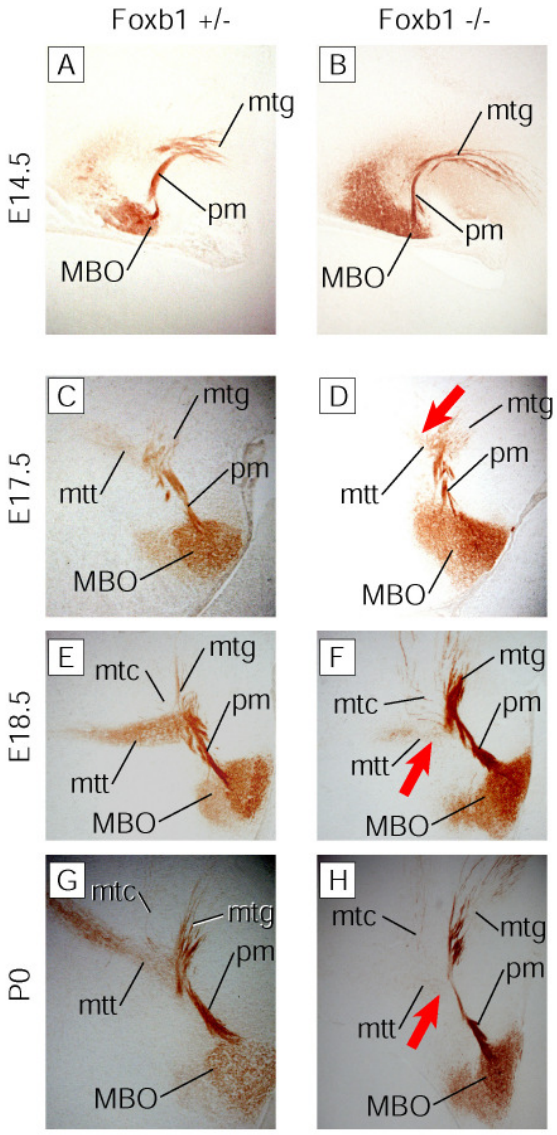

Fig.3.1: The *Foxb1* mutant (NMRI, F7) mammillothalamic tract fails to enter the target region and most of the mammillary body cells die immediately afterwards. (A, B) Sagittal paraffin sections through heterozygous (A) and homozygous (B) E14.5 mouse brains reacted for the detection of ß-galactosidase. In A and B, principal mammillary tract (pm) can be seen and mammillotegmental tract developed very well at this stage, but there is no difference between A and B. (C, D) Sagittal paraffin sections through heterozygous (C) and homozygous (D) E17.5 mouse brains reacted for the detection of ß-galactosidase. In D, a few outgrowth of principal mammillary axons can be seen forming a second bifurcation towards the thalamus (arrow). (E, F) Sagittal paraffin sections through heterozygous (E) and homozygous (F) E18.5 mouse brains reacted for the detection of ß-galactosidase. In E and F, the third bifurcation mammillotectal tract can be seen and is well developed at this stage. In F, a small outgrowth of mammillothalamic tract starts towards the thalamus (arrow). (G, H) Sagittal paraffin sections through heterozygous (G) and homozygous (H) new born mouse brains reacted for the detection of ß-galactosidase. In H, mammillothalamic tract is almost absent at this stage. (I, J) Sagittal paraffin sections through heterozygous (I) and homozygous (J) P15 mouse brains reacted for the detection of ß-galactosidase. In J, one or two axons from mammillothalamic tract extended, but did not enter the target of dosal thalamus, and the mammillary body (MBO) is much smaller compared to the mammillary body in I. MBO, mammillary body; mtt, mammillothalamic tract; mtc, mammillotectal tract; mtg, mammillotegmental tract, pm, principal mammillary tract.

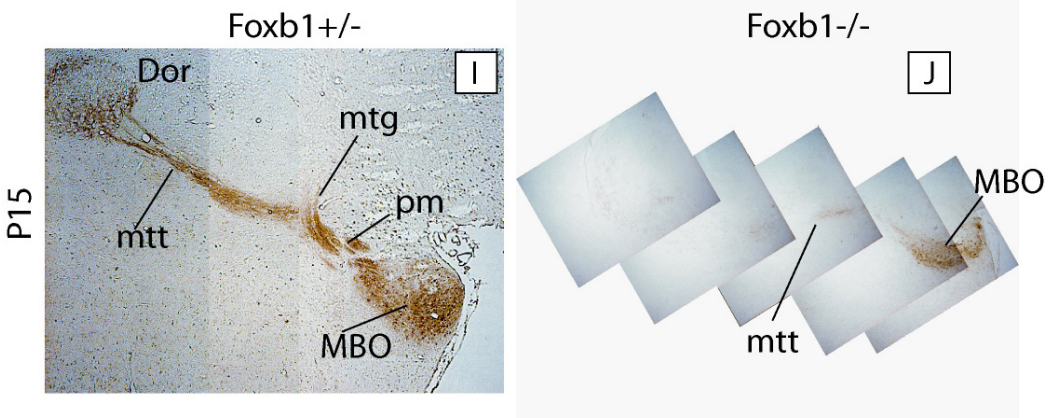

At P0 (day of birth), the heterozygous mtt tract was a compact fiber bundle spanning the distance between MBO and anterior thalamic complex and expanding terminal fiber arbors into it (Fig.3.1G). In the mutant, the mtg, mtc bundles followed an apparent normal trajectory, but the mtt tract was almost completely absent, except for a few short axons, at E18.5, or later (Fig.3.1F, H). We concluded that, as in the 129Sv background, the NMRI *Foxb1* mutant develops a medial mammillary nucleus (MM), but fails to develop or maintain a mtt. The size of the MBO was normal in homozygotes at P0 (Fig.3.1H). By P15, the size of MBO was abnormally decreased.

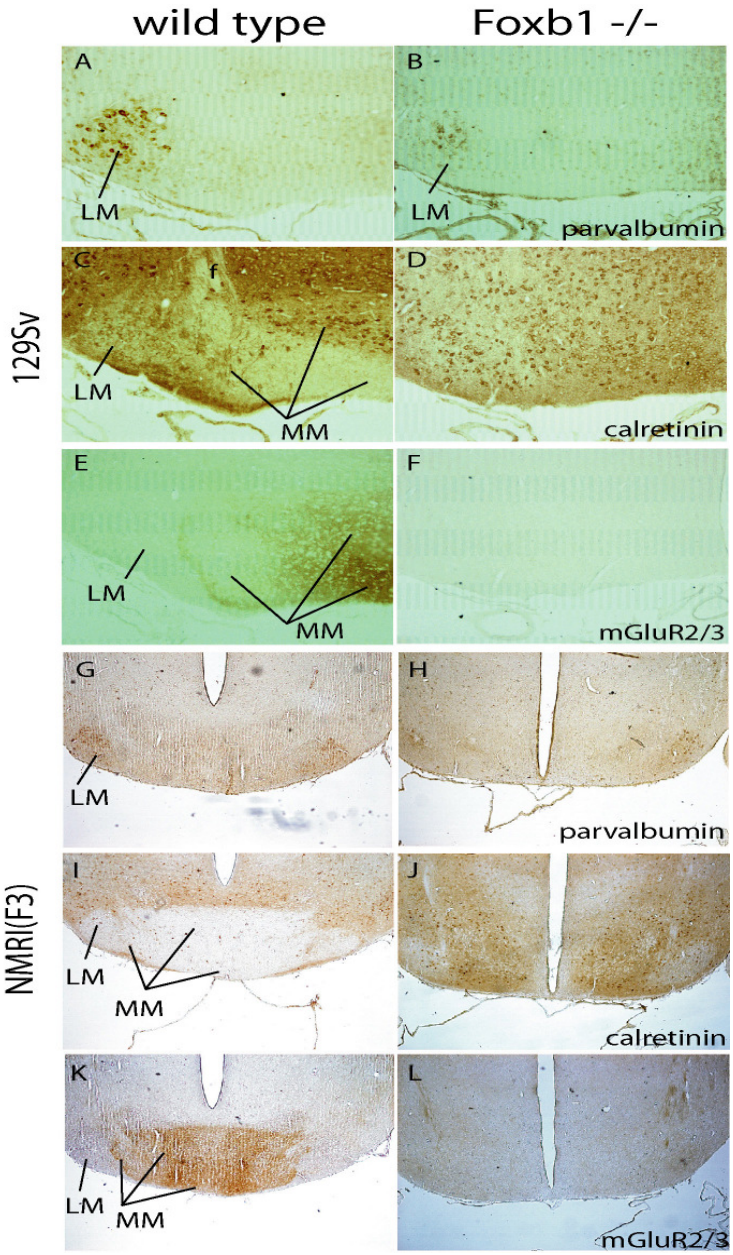

Fig.3.2: The Foxb1 mutant (129Sv, NMRI) lacks one brain nucleus, the medial mammillary nucleus, and the size of the lateral mammillary nucleus is much smaller by the detection of several hypothalamic maker antibodies. (A, B, G, H) Transverse paraffin sections through wild type 129Sv (A), NMRI (G) and homozygous 129Sv (B), NMRI (H) adult mouse brains reacted for the detection of lateral mammillary nucleus marker: parvalbumin. In B and H, much less cells were in the lateral mammillary nucleus. (C, D, I, J) Transverse paraffin sections through wild type 129Sv (C), NMRI (I) and homozygous 129Sv (D), NMRI (J) adult mouse brains reacted for the detection of calretinin. In D and J, medial mammillary nuclei that were surrounded by the calretinin-expressing cells could not be detected. (E, F, K, L) Transverse paraffin sections through wild type 129Sv (E) and homozygous (F) 129Sv adult mouse brains reacted for the detection of medial mammillary nuclei marker: mGluR 2/3. In F and L, medial mammillary nuclei cells completely disappeared. LM, lateral mammillary nucleus; MM, medial mammillary nuclei; f, fasciculus retroflexus.

Most MBO cells died (Fig.3.1J), probably due to apoptosis, as has been established for the 129Sv strain mutant (Alvarez-Bolado et al., 2000).

Transverse paraffin sections were prepared from *Foxb1* mutant adult brains and treated with different hypothalamic marker antibodies respectively to detect the size of MBO in *Foxb1* mutants (Fig. 3.2) (A, B, C, D, E, F were from Alvarez-Bolado, Gonzalo). A group of cells in the lateral nucleus of wild type were detected by anti-parvalbumin (Fig. 3.2 A, G), but, there were only a few cells in the lateral mammillary nucleus in the homozygotes were detected and the size of lateral mammillary nucleus in homozygotes was obviously smaller than that in wild type (Fig.3.2B, H). In wild type, the lateral nucleus and the medial mammillary nuclei were dorsally surrounded by calretinin-expressing cells (Fig.3.2C, I). The morphology was completely different in the homozygotes by the detection of anti-calretinin and the medial mammillary nuclei disappeared (Fig.3.2 D, J). mGluR2/3 is a medial mammillary nuclei marker (Fig.3.2E, K), anti-mGluR2/3 did not detect even one single cell in the MBO region in homozygotes (Fig.3.2F, L). The third ventricle that was very low and near the border (Fig.3.2 H, J, L) also showed that medial mammillary nuclei disappeared.

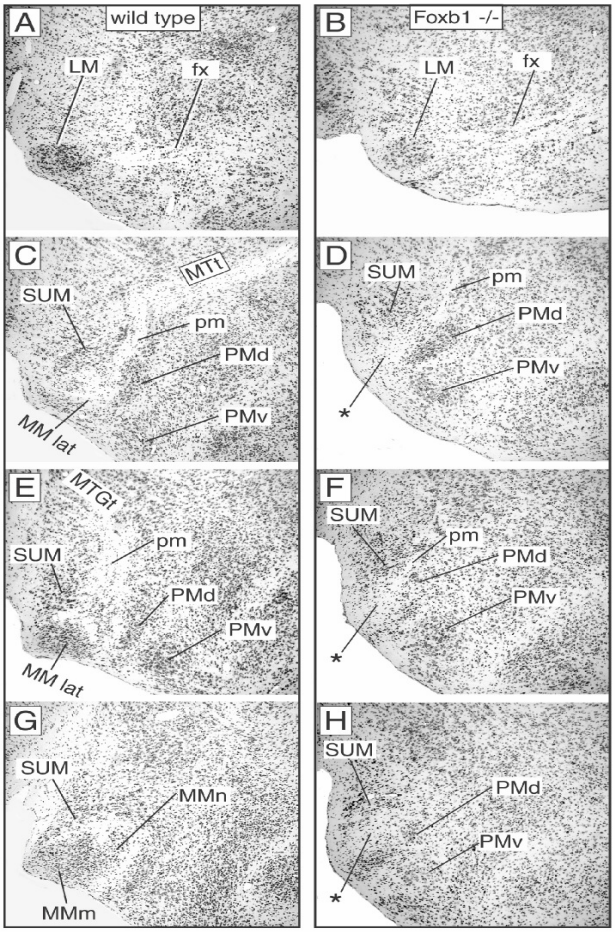

Fig.3.3: Confirmation that *Foxb1* mutant (NMRI) lacked a medial mammillary nuclei and had smaller size of lateral mammillary nucleus by Nissl staining. Sagittal paraffin sections of the posterior hapothalamus of wild type (A, C, E, G) and homozygous (B, D, F, H) adult brains stained with Cresyl violet. By which the subdivisions of mammillary body were shown (A, C, E, G). In B, Lateral mammillary nucleus is smaller; in D, there was no lateral subdivision of medial mammillary nuclei; in F, there was no medial subdivision of medial mammillary nuclei; in H, there was no median subdivision of medial mammillary nuclei. LM, lateral mammillary nucleus; MM lat, lateral subdivision; MMm, medial subdivision; MMn, median subdivision; SUM, supramammillary nucleus; pm, principal mammillary tract; fx, fasciculus retroflexus; PMd, dorsal premammillary nucleus; PMv, ventral premammillary nucleus.

Different nuclei of the mammillary body: lateral mammillary nucleus (LM), lateral subdivision (MM lat) of medial mammillary nuclei (MM), medial subdivision (MMm) and median subdivision (MMn,) were shown by the staining with Cresyl violet on paraffin sagittal sections from wild type adult mouse brains (Fig.3.3A, C, E, G). The lateral mammillary nucleus (LM) was less compact and very much reduced in the *Foxb1* NMRI mutant (Fig. 3.3B). The mutant were absent of all MM lat, MMm, and MMn subdivisions of MM.

It was concluded that the mammillary axonal phenotype in the Foxb1 mutant on the NMRI genetic background was very similar or identical to that of the Foxb1 mutant on the 129Sv strain. The Foxb1 mutants on both genetic backgrounds lacked MM, and had very reduced lateral mammillary nucleus. This robust phenotype could then be analyzed in the more productive NMRI strain.

3.1.2 The transcriptome of the caudal hypothalamic region in the *Foxb1* mutant is different from that of the wild type

Once the mutant phenotype in the NMRI background had been established, this mutant line was used in order to compare the mutant and wild type transcriptomes of caudal hypothalamus. The rationale behind this experiment was that this comparison would show which genes are downstream of *Foxb1* (i. e., those whose expression was altered in the mutant). Although mRNA is not the end product of a gene, the transcription of a gene is both critical and highly regulated, thereby providing an ideal point of investigation (Brazma and Vilo, 2000).

3.1.2.1 Tissue collection and mRNA extraction

First, the posterior portion of the hypothalamus of E18.5 mouse embryos from heterozygous Foxb1-NMRI crossings was microdissected. A piece of embryonic tissue outside the brain (leg tissue) for each piece of hypothalamus collected was taken carefully, so that genomic DNA can be isolated and used for PCR to find the genotype of each piece of brain tissue collected. Then the tissue was pooled according to genotype. The Dyna Beads method was used (see Materials and Methods) to isolate mRNA from wild type and homozygous tissue pools. The mRNA used to make samples for Affymetrix genechips has to be of the highest quality. The quality integrity of the mRNA was assessed by optical density (OD) measurements, and made sure that OD260/280 was always above 1.9 (indicating no contamination from protein or solvent) (Fig.3.4A). And agarose gel electrophoresis was used to observe the sharp ribosomal RNA (18S, 28S) bands on the gel to control for possible degradation of the mRNA samples. Other bands on the gel were because of the secondary structure of RNA, which disappeared after the denaturation of sample

(Fig.3.4B). Finally, the Agilent 2100 Bioanalyzer system was used to confirm the quality of the samples as an independent method, with very satisfactory results: no degradation and no ribosomal RNA (18S and 28S) peaks (Fig.3.4C).

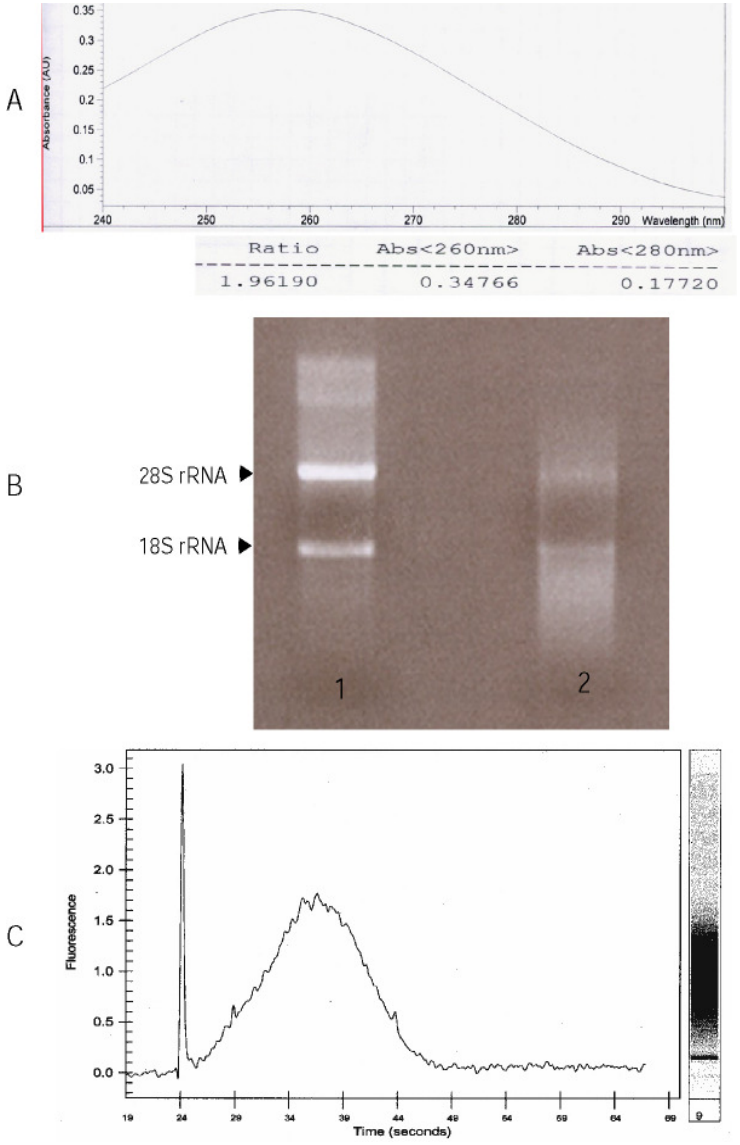

Fig.3.4: mRNA quality assessment. (A) Optical density measument of mRNA. At 260nm, there is a nucleic acid absorption peak and the ratio (260nm/280nm) is equal to 1.96. 1OD at 260nm = 40µg/ml pure RNA. (B) Agarose gel electrophoresis analysis of mRNA. In 1, the sharp 28S and 18S ribosomal RNA bands were seen. In 2, sample was incubated at 70°C for 10 minutes and RNA secondary structure disappeared. (C) Agilent 2100 Bioanalyzer plots depicting highly pure mRNA. RNA size distribution did not shift to the smaller fragments and there was no degradation. There was no presence of ribosomal RNA peaks, and the mRNA was highly pure.

Two series of microdissections were preformed. For the first one, the dissected pieces of hypothalamus were large, including not only the caudal hypothalamus, but also other hypothalamic parts dorsal to the mammillary region. Fifteen brains of each genotype were pooled. This mRNA was used for the first (1st large) and second (2nd large) microarray hybridizations. The second series of microdissections used small dissections, containing probably only the mammillary subdivision of the hypothalamus; 10 brains of each genotype were pooled. This mRNA was used for the third microarray hybridization (1st small) (Fig.3.5B).

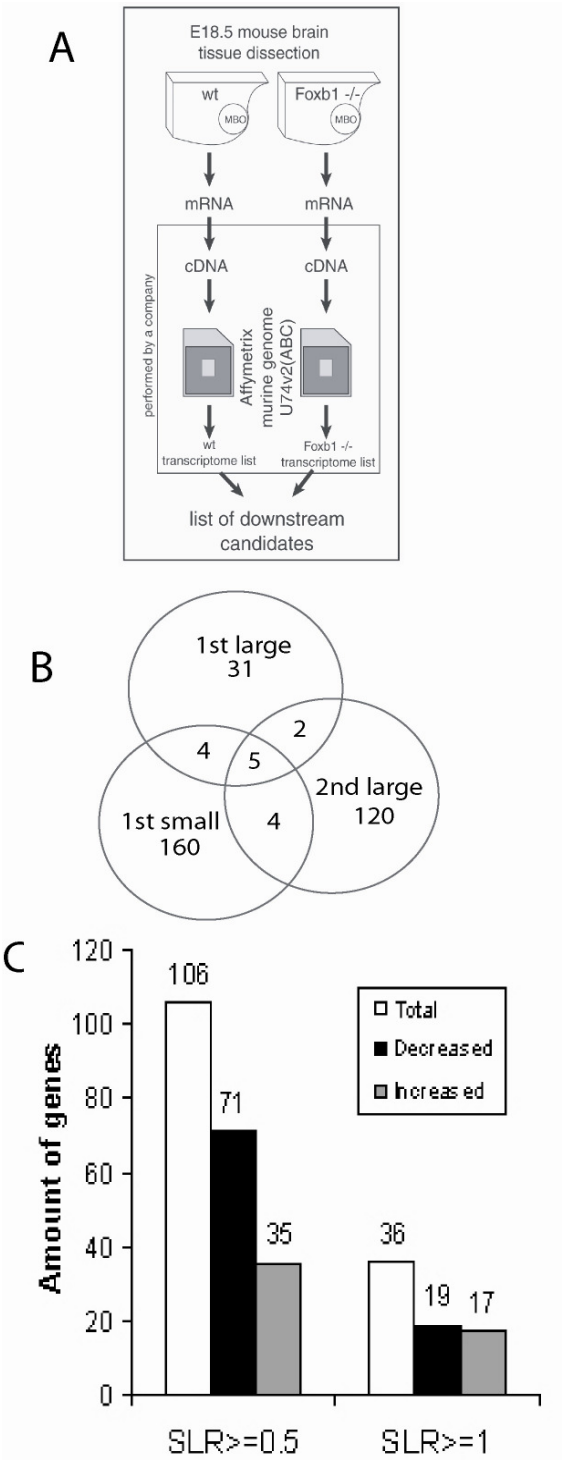

3.1.2.2 *Microarray analysis*

Preparation of the probe and hybridization to the Affymetrix Microarrays (Murine Genome U74 A, B and C), as well as the informatic analysis of the resulting data, was done by the Deutsches Ressource Zentrum für Genomforschung (RZPD, Berlin) for a fee. We used the GeneChip® DNA microarrys made by Affymetrix, specifically, the Murine Genome U74 Set, consisting of three Chips (Av2, Bv2, Cv2), containing sequences representing approximately 36,000 genes (6000 functionally characterized plus 30000 Expressed Sequence Tags.). The transcriptome of the tissues was compared (also at RZPD) by means of Affymetrix proprietary analytical software. The comparison was as follows: HO-P vs. WT-P (HO: homozygotes; p: posterior hypothalamus) (Fig.3.5A). 31 genes altered from the first hybridization, 120 genes altered from the second hybridization, and 160 genes altered from the third hybridization (Fig.3.5B). Real signals were distinguished from noise by imposing an arbitrary threshold of signal difference between experiments and baseline. This is done in terms of the so-called Signal Log Ratio (SLR). The SLR is related to the fold change by the following formulas:

Fig.3.5. Sample process, microarray hybridization and data summary. (A) mRNA was isolated from wild type and homozygous tissues and sent to RZPD for the synthesis probes and hybridization with Affymetrix Murine Genome U74 Set Genechips. (B) The third hybridization (1st small) was done with tissue from new, more precise dissections. Thirty-one genes were obtained from the first hybridization, 120 genes from the second, 160 genes from the third. (C) In total we found 36 genes with SLR>=1 (19 decreased, 17 increased), and 106 genes with SLR>=0.5 (71 decreased, 35 increased).

$$Fold\ change = 2^{SLR}\ for\ SLR \geq 0$$

$$Fold\ change = (-1) \times 2^{-SLR}\ for\ SLR < 0$$

So, for instance, an SLR of +2 means a fourfold increase in expression in experimental (homozygote) as compared to control (wild type). An SLR of -2 would mean a fourfold decrease. We ranked the genes by fold change, from high to low. There were 36 genes with the SLR >=1 (That is, at least twofold increase or decrease). I selected for further analysis the SLR changes (an increase or decrease of SLR >=0.5) plus all the genes detected in the three hybridizations, to a total of 106 genes (Fig.3.5C).

For the following validation, we used an automated, high-throughput in situ procedure developed in this department under the direction of Prof. Eichele (Herzig et al., 2001; Visel et al., 2004). This procedure routinely provides high-quality, very reproducible data. The second technique, quantitative real-time PCR (Q-PCR), was used to detect small differences in the level of expression, and as such helps to eluminate "false positive" given by microarray. This combination of DNA microarrays and Q-PCR is rapidly becoming a standard approach to expression analysis (Sgroi et al., 1999; Mills et al., 2001); (Mutch et al., 2001); (Mayanil et al., 2001); (Jiang et al., 2002). Of note, Q-PCR will add a numerical value to the magnitude of change and thus complement the data obtained by in situ hybridization.

3.1.2.3 Validation of microarray data by In situ hybridization (GenePaint) and quantitative PCR

Among the list of 106 genes that had been compiled and annotated, on the basis of the information found in the literature, we selected the 76 potentially more interesting genes to be validated. To carry out this selection, an "educated guess" was made on which kind of genes can be affected in the Foxb1 mutant, given the phenotype: genes with specific expression in brain, involved in development or in processes like axonal pathfinding, cell differentiation, etc. were preferred over ubiquitously expressed genes, house-keeping genes, mesoderm-specific genes, etc. These 76 downstream candidates were then submitted to a first round of validation through in situ hybridization. Any true downstream genes to Foxb1 involved in the mammillary phenotype have to be expressed in the mammillary body. With the help of technicians, in situ probes were prepared against 57 of the 76 candidates by means of RT-PCR[1]. *In situ* hybridization was made

[1] Probes for the remnant 19 genes proved to be difficult to clone. The time-consuming task of solving the specific cloning problems for each of them has been taken up by the team of technicians of GenePaint in our Department.

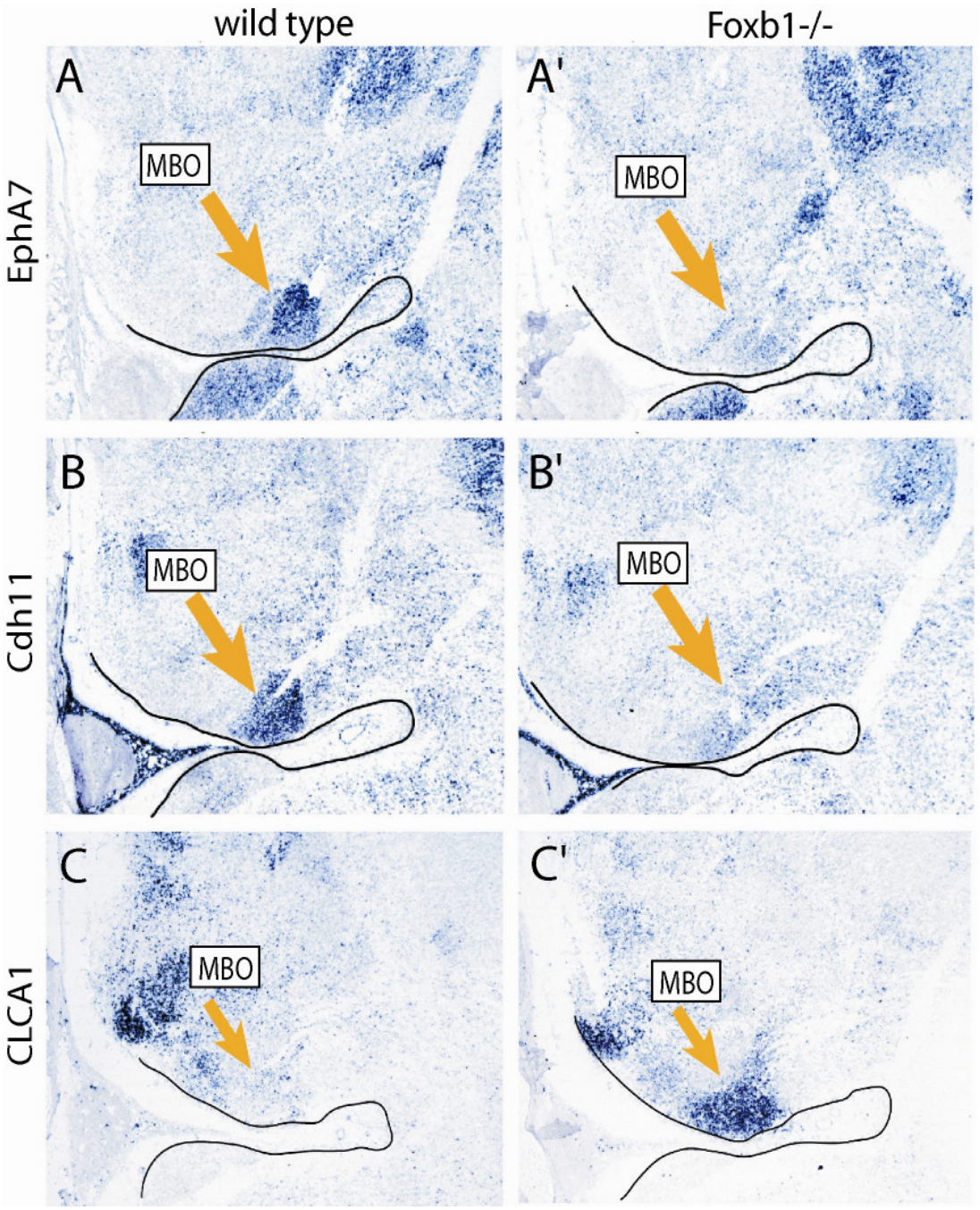

Fig.3.6: Candidate genes differentially expressed in wild type and *Foxb1* homozygotes. *In situ* hybridization was performed on cryostat sections of wild type (A, B, C) and homozygous (A′, B′, C′). **(A, A′)** E18.5 mice with riboprobe against *EphA7* mRNA. In A, *EphA7* is very specifically expressed in the mammillary body (arrow), while in A′, expression was much decreased in the mutant mammillary body (arrow). **(B, B′)** E18.5 mice with riboprobe against *cadherin 11 (Cdh 11). Cdh 11* is expressed specifically in the mammillary body (B, arrow), however, in B′, the expression of *cadherin 11* was almost absent in mammillary body (Arrow). **(C, C′)** E18.5 mice with the riboprobe of *CLCA1*gene. In C, *CLCA1* did not express in the mammillary body (arrow), however, it was present in C′ (arrow). MBO, mammillary body.

on cryostat sections of wild type E14.5 and E18.5 mice. The expression data so obtained revealed that 32 of the candidates were not interesting: they were either not expressed on the mammillary body, or ubiquitously expressed. Specific expression patterns in the hypothalamus, including the mammillary body, were found for 25 of the candidates.

The next validation step consisted of proving that expression of the 25 MBO-specific candidates was actually altered in mutant tissue. Probes for the 25 MBO-specific downstream candidates were hybridized to cryostat sections of E18.5 *Foxb1* homozygous brains. The patterns of 4 of the candidates were actually altered in the mutant. Three of them were reduced (*EphA7*, *Cdh11* and *Foxb1*) and one was increased in the mutant as compared to the wild type: *CLCA1* (Fig.3.6).

Although the purpose of my thesis work was not to evaluate microarray technology, it is maybe worth to summarize here some conclusions about the method which can be gathered from my data. As evidenced by validation results, the fold change (SLR) can not be used alone to ascertain expression changes between wild type and mutant tissues. ISH data showed 14.3% concordance with microarray data, and Q-PCR analysis demonstrated 27% ISH and Q-PCR agreed on 73% of the cases.

3.1.2.4 Identity and function of the downstream candidates to Foxb1

First of all, finding that *Foxb1* transcripts are very much reduced in the *Foxb1* mutant did not come as a surprise, and it is mentioned as a further validation of the method.

EphA7 encodes a membrane receptor tyrosine kinase (Ciossek et al., 1999; Rogers et al., 1999) whose ligands are the ephrins A. The Eph receptor-ephrin interaction has a major involvement in axonal guidance (Gale et al., 1996b; Ciossek and Ullrich, 1997; Zhou, 1998; Holmberg et al., 2000).

Cdh11 (cadherin 11) encodes a transmembrane protein acting as a homophylic cell-cell adhesion molecule, and has been involved also in axonal guidance and in selective aggregation of neurons to form brain nuclei (Marthiens et al., 2002).

CLCA1 (calcium-sensitive chloride conductance protein) encodes a transmembrane protein forming a activated during apoptotic processes (Gandhi et al., 1998; Elble and Pauli, 2001).

3.2 BIOLOGICAL VALIDATION OF *EphA7* AS A DOWNSTREAM CANDIDATE TO *Foxb1* IN THE HYPOTHALAMUS

3.2.1 *EphA7* is a biologically relevant downstream candidate for Foxb1 in the diencephalon.

All further work focuses on EphA7 as the most interesting candidate. Since EphA7 is a receptor molecule, the finding that its expression is altered in the *Foxb1* mutant would reach biological significance only in the case that expression of appropriate ligands in the caudal hypothalamus could be demonstrated. From the literature the EphA7 receptor binds the family of cell-attached ephrin-A ligands (Gale et al., 1996a; Ciossek and Ullrich, 1997; Drescher et al., 1997; Flanagan and Vanderhaeghen, 1998; Wilkinson, 2001). Consequently, and with the assistance of technical personnel of the department, GenePaint technology was used to demonstrate the pattern of expression of the five known genes of the ephrin A family on E18.5 wild type and *Foxb1* mutant mouse hypothalamus (Fig.3.7). *Foxb1* mutant hypothalamus was also used. The results showed that the expression pattern of each ligand in ephrin A family did not alter in *Foxb1* mutant, and that ephrin-A1, ephrin-A2 and ephrin-A3 have ubiquitous expression in the brain at E18.5. Ephrin-A4 is apparently not expressed in the brain at that age (data not shown). Finally, ephrin-A5 showed a specific expression pattern in diencephalon, specifically in the dorsal thalamus(Fig.3.7E,F), which is the target region of the mtt axons whose failure to enter this region is the hallmark of the *Foxb1* diencephalic phenotype (Alvarez-Bolado et al., 2000). This finding shows that EphA7 is a biologically relevant downstream candidate for *Foxb1*.

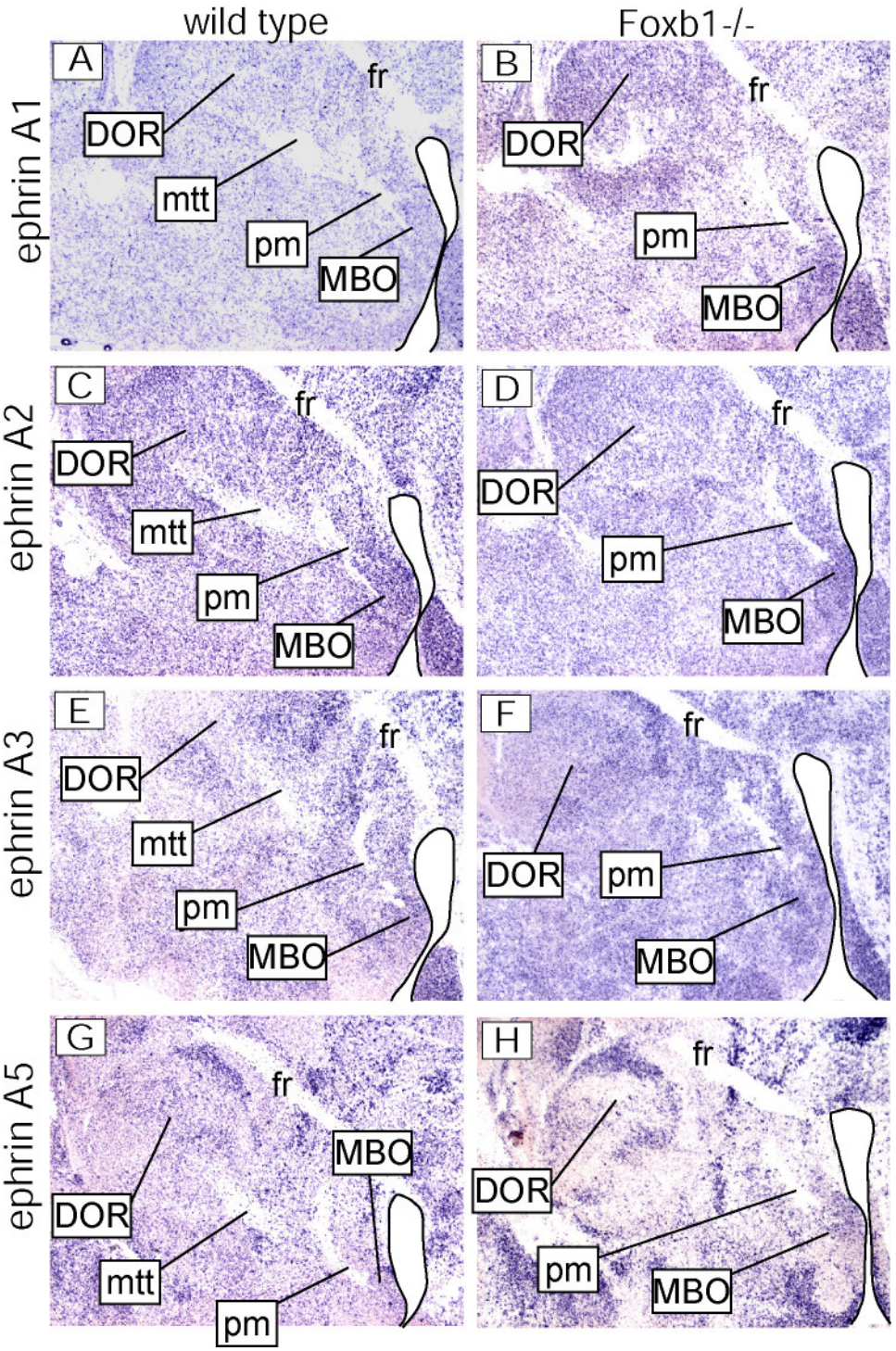

Fig.3.7: Expression analysis of ephrin A ligand family at E18.5 stage on wildtype (A, C, E, G) and *Foxb1* (B, D, F, H) homozygous hypothalamus. **(A, B)** ephrin A1 had ubiquitous expression in the brain. The same expression pattern for ephrin A2 ligand **(C, D)** and ephrin A3 ligand **(E, F)**. **(G, H)** ephrin A5 showed no expression difference between wildtype and mutant (After checking the whole series of sections of the brain). Ephrin A5 showed however very specific expression pattern in hypothalamus.
Abbreviations: pm, principal mammillary tract; mtt, mammillothalamic tract; MBO, mammillary body; DOR, dosal thalamus; fr, fasciculus retroflexus.

3.2.2 Expression of known and novel isoforms of receptor tyrosine kinase gene *EphA7* is very much reduced in the caudal hypothalamus of the *Foxb1* mutant.

The receptor EphA7, originally called EBK or MDK1 or EHK3 (Ciossek et al., 1995a; Ellis et al., 1995; Valenzuela et al., 1995). The EphA7 locus encodes not only a typical receptor tyrosine kinase (TK+), but also isoforms lacking the tyrosine kinase domain (TK-), produced by alterative RNA splicing (Ciossek et al., 1995b; Mori et al., 1995; Talukder et al., 1997).

By searching Genebank, at mRNA level, two different EphA7 full length (EphA7-FL) transcripts were found, both of them consisting of 18 exons. The Genebank accession number of EphA7 full length is XM_131334. One of them is 5336bp, the other is 12bp shorter. The first truncated variant, EphA7-Tr1 (Genebank Accession No.: X79083), has 10 exons and is 2901bp long. The second truncated variant, EphA7-Tr2 (Genebank Accession No.: X79084), also has10 exons and is 2323bp long. By BLAST sequence comparison against the NCBI nucleotide database (Altschul et al., 1990), I found a yet un-described truncated variant (Genebank Accession No.: AK032973) which is 3189bp long (Fig. 3.8C). In total, there are five variants, in coincidence with the "expected transcripts" for the EphA7 locus in the Celera sequence database (Fig. 3.8A). All of them are different at 3′ UTR region.

At protein level, one of the full length transcripts was 4 amino acids shorter than the other (994 amino acids vs. 998 amino acids). The missing amino acids correspond to the intracellular domain. Since both full length forms have the ephrin binding domain and two fibronectin III domains in the extracellular part, as well as the tyrosine kinase domain and SAM domain in the intracellular part (Fig.3.8B), they are probably equivalent functionally.

As for the truncated transcripts, EphA7-Tr1 and EphA7-Tr2 encode the same protein, 662 amino acids. They have ephrin binding domain and two fibronectin III domains in the extracellular part, and can dock on the cell membrane. They are missing the tyrosine kinase domain (Fig.3.8B), and consequently can bind the ligand and probably serve an adhesive function (Holmberg et al., 2000) but do not signal to the interior of the cell.

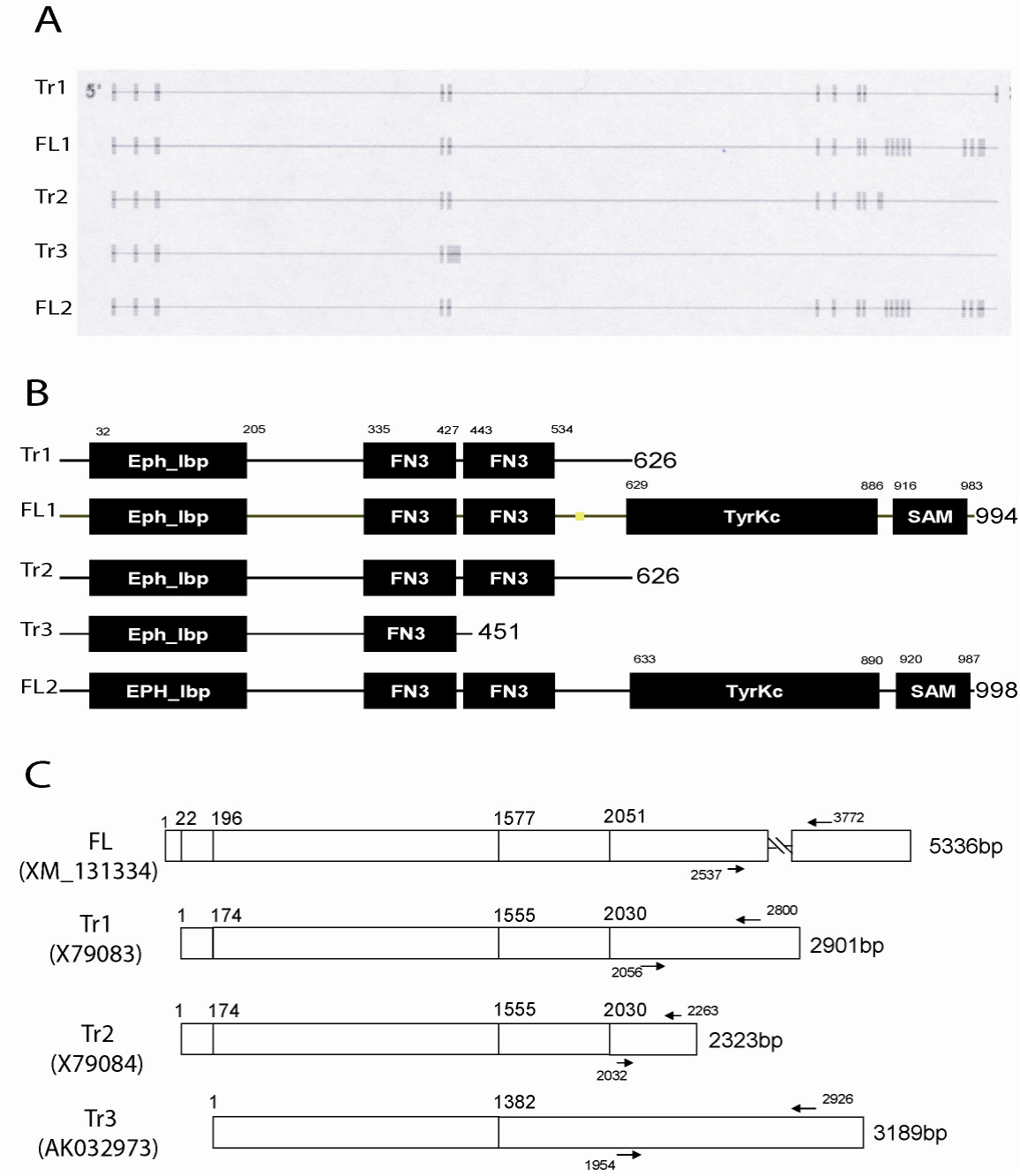

Fig.3.8: Schematic map of *EphA7* receptor variant transcripts and their predicted proteins. (A) The Celera sequence database expected five transcripts from *EphA7* locus. (B) Protein structure of EphA7 five variants and their length. Numbers above show the position in the protein sequence. (C) Sequence alignment among all variants mRNA, the corresponding accession number in Genebank, and the specific primers position which were against each variant 3′ UTR region (arrows and the number behind show primer position, numbers above show the position in the sequence).
Abbreviations: FL, EphA7-Full length; Tr1, Tr2, Tr3, EphA7 truncated 1, 2, 3; EPH_lbp, ephrin ligand binding domain; FN3, fibronectin III domain; TyrKc, tyrosine kinase domain, SAM, Sterile a-motif.

The novel truncated form (EphA7-Tr3, 451 amino acids) showed ephrin binding domain but only one fibronectin III domain, and very likely is not able to dock on the membrane (secreted?). It contains 2 amino acids at the end which are different from other variant forms (Fig.3.8B).

primers specific for each of the variants (but only for one of the full length transcripts) were designed: EphA7-FL, EphA7-Tr1, EphA7-Tr2, EphA7-Tr3, which are against each variant 3′ UTR region (Fig.3.8C). Specific probes for them were cloned by RT-PCR. In situ hybridization performed on tissue sections of developing mouse brain at ages E16.5, E17.5, E18.5 showed expression of all forms in the developing diencephalon. All of them were expressed in the whole of the dorsal thalamus, as well as very specifically in MBO, and in a group of cells alongside the mammillothalamic tract to the thalamus. EphA7-FL was the predominant expressed form during development in the diencephalons. The expression of all isoforms was very much decreased in the developing homozygotes, EphA7-FL (Fig.3.9); EphA7-Tr1 (Fig.3.10); EphA7-Tr2 (Fig.3.11); EphA7-Tr3 (Fig.3.12).

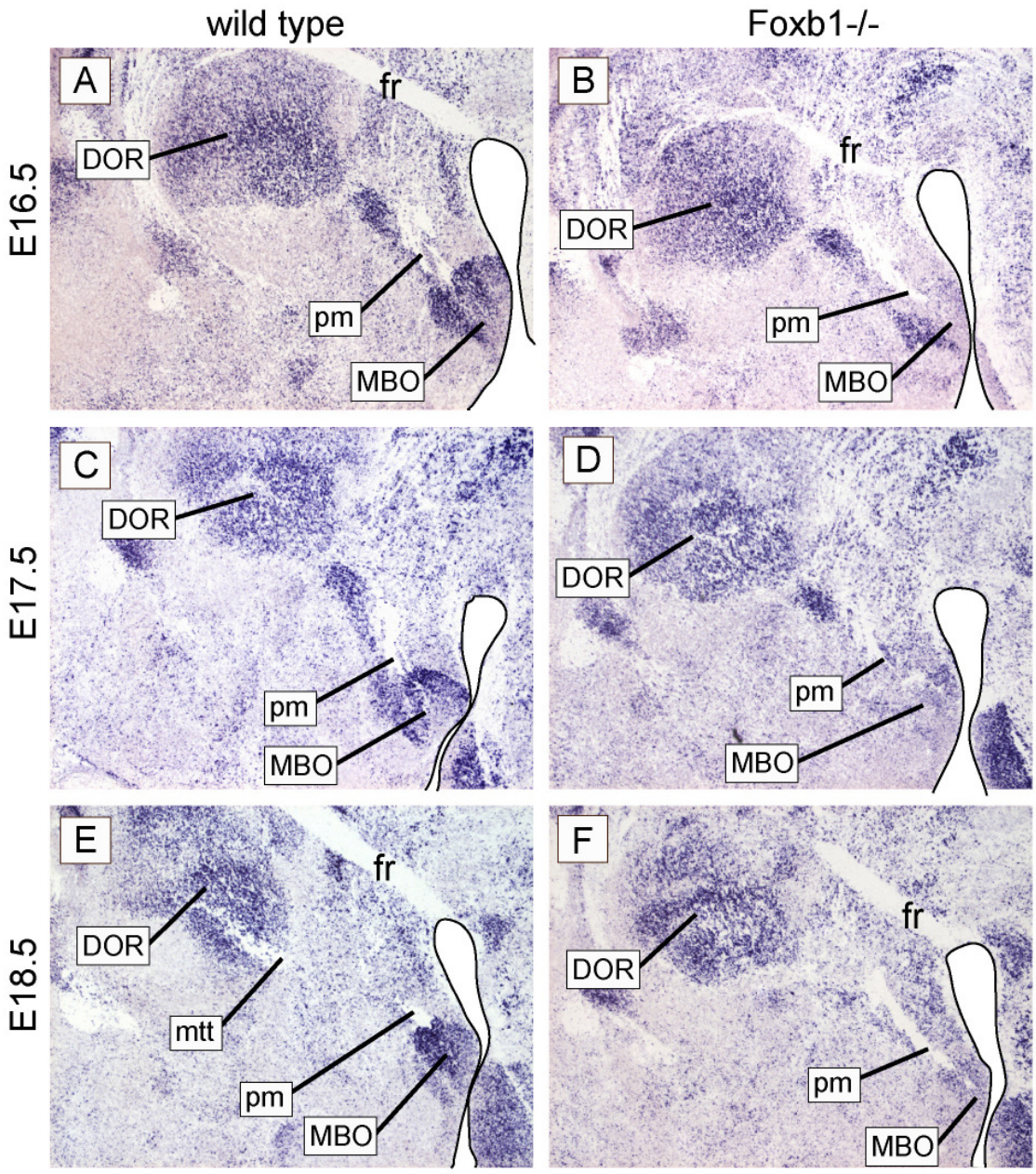

Fig.3.9: EphA7 full length (EphA7-FL) is strongly expressed in the wildtype developing diencephalon (A, C, E); its expression was very much reduced in the developing homozygous mammillary body (B, D, F). (A, B) EphA7-FL expression in E16.5 hypothalamus. In B, the expression was much decreased in mammillary body. (C, D) EphA7-FL expression in E17.5 hypothalamus. In D, the expression was much decreased in mammillary body. (E, F) EphA7-FL expression in E18.5 hypothalamus. In F, the expression was much decreased in mammillary body. In A, C, E, EphA7-FL strongly expressed in the dorsal thalamus, the patch of cells alongside mammillothalamic tract and mammillary body.
Abbreviations: DOR, dosal thalamus; mtt, mammillothalamic tract; pm, principal mammillary tract; MBO, mammillary body; fr, fasciculus retroflexus.

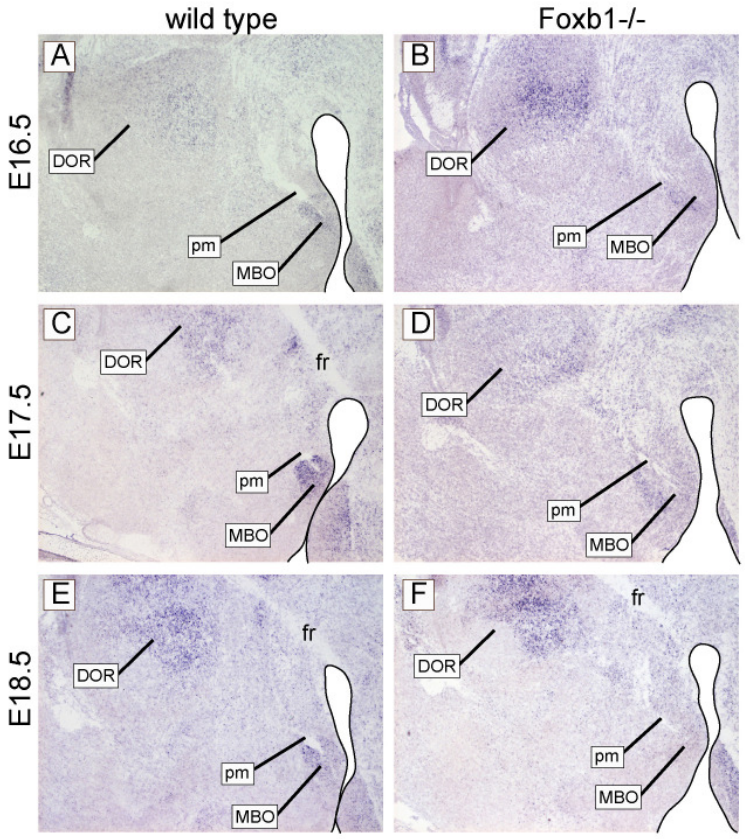

Fig.3.10: EphA7 truncated 1 (EphA7-Tr1), expressed in the developing diencephalon and the expression was very much reduced in the developing homozygous mammillary body. (A, B) EphA7-Tr1 expression on wild type (A) and homozygous (B) E16.5 hypothalamus. (C, D) On wild type (C) and homozygous (D) E17.5 hypothalamus. (E, F) On wild type (E) and homozygous (F) E18.5 hypothalamus. In A, C, E EphA7-Tr2 expressed in the dorsal thalamius, the patch of cells located alongside the mammillothalamic tract and mammillary body. In B, D, F, the expression was much decreased in mammillary body. DOR, dosal thalamus; mtt, mammillothalamic tract; pm, principal mammillary tract; MBO, mammillary body; fr, fasciculus retroflexus.

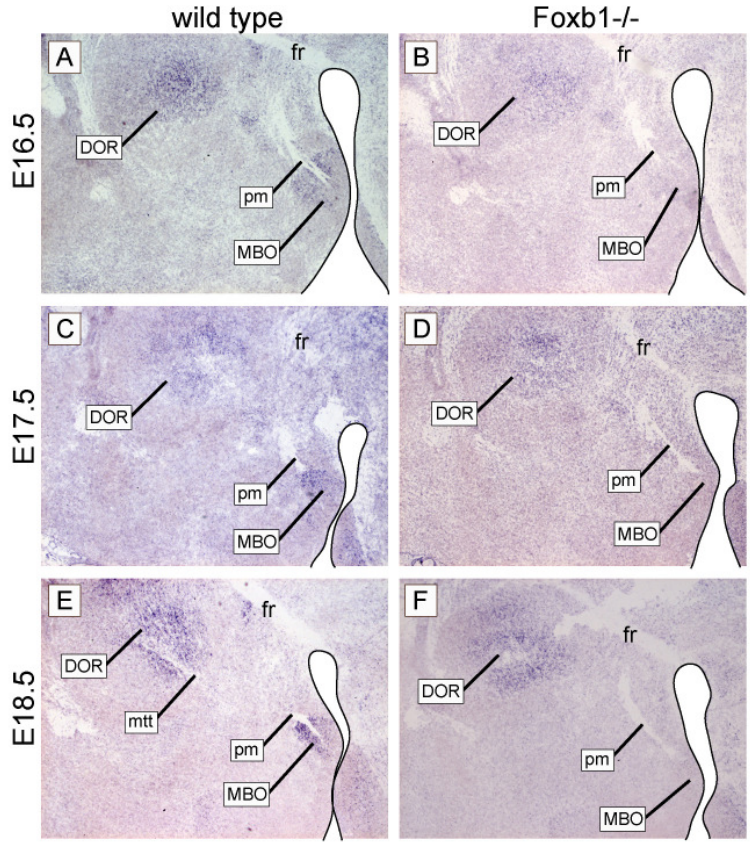

Fig.3.11: EphA7 truncated 2 (EphA7-Tr2) expressed in the developing diencephalon and the expression was very much reduced in the developing homozygous mammillary body. (A, B) EphA7-Tr2 expression on wild type (A) and homozygous (B) E16.5 hypothalamus. (C, D) On wild type (C) and homozygous (D) E17.5 hypothalamus. (E, F) On wild type (E) and homozygous (F) E18.5 hypothalamus. In A, C, E EphA7-Tr2 expressed in the dorsal thalamius, the patch of cells alongside mammillothalamic tract and mammillary body. In B, D, F, the expression was much decreased in mammillary body. DOR, dosal thalamus; mtt, mammillothalamic tract; pm, principal mammillary tract; MBO, mammillary body; fr, fasciculus retroflexus.

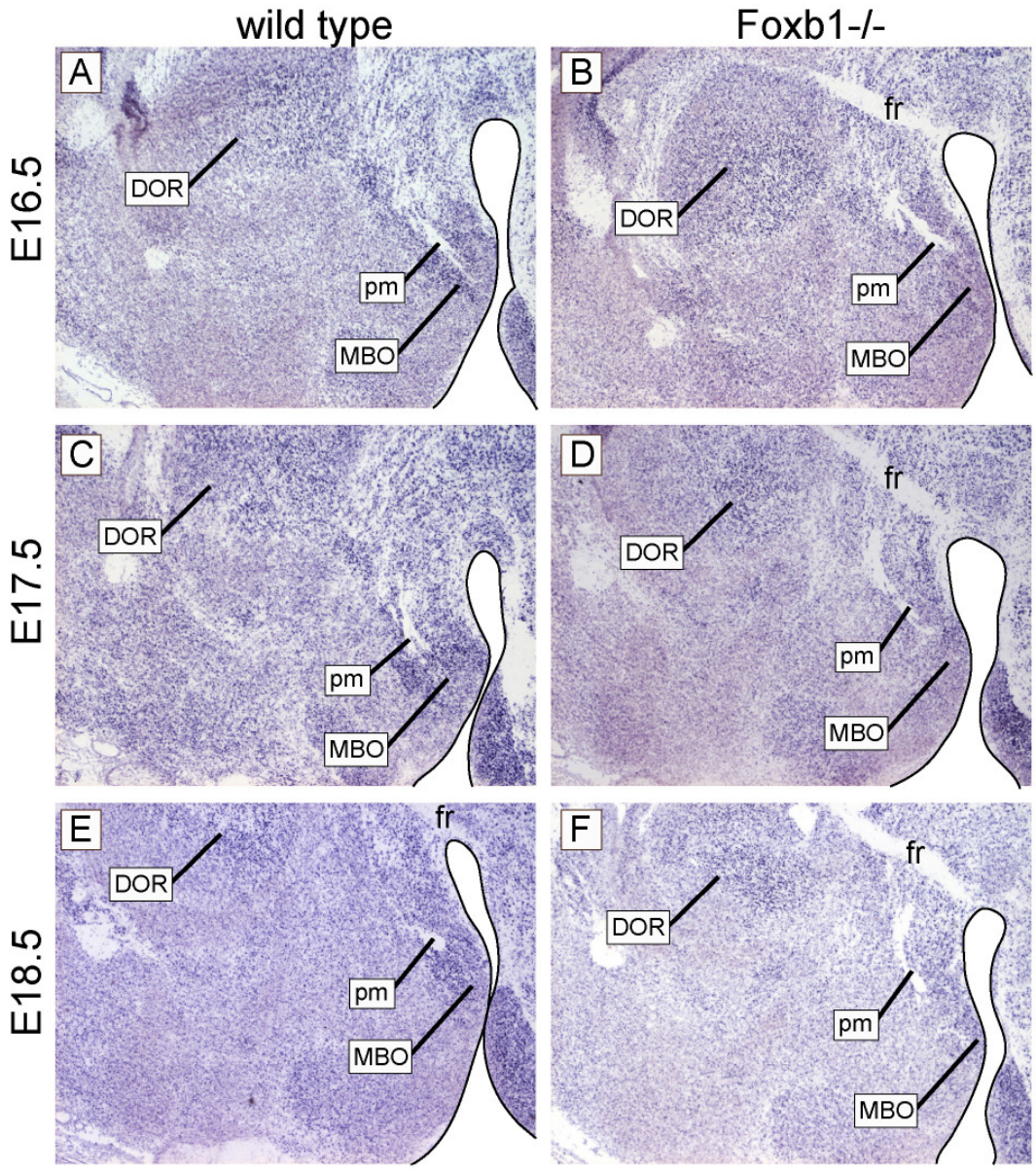

Fig.3.12: EphA7 truncated 3 (EphA7-Tr3) was expressed in the developing wildtype diencephalon (A, C, E) and the expression was very much reduced in the homozygous (B, D, F) mammillary body. (A, B) EphA7-Tr3 expression in E16.5 hypothalamus. (C, D) Expression in the 17.5 hypothalamus. (E, F) Expression in the E18.5 hypothalamus. In A, C, E, EphA7-Tr3 expressed in the dorsal thalamus, the patch of cells alongside mammillothalamic tract and mammillary body. In B, D, F, the expression was much decreased in mammillary body.
DOR, dosal thalamus; mtt, mammillothalamic tract; pm, principal mammillary tract; MBO, mammillary body; fr, fasciculus retroflexus.

3.2.3 All of the EphA7 isoforms were equally decreased in the Foxb1 mutant hypothalamus.

Next it was investigated if some of the isoforms were more affected than others by the *Foxb1* deficiency. Quantitative RT-PCR was used to determine the proportion of decrease in mRNA amount for each of the variants.

Caudal hypothalamus of E18.5 wild type and homozygous mouse fetuses was microdissected, and mRNA and cDNA were prepared from them. Then I used specific primers to amplify 75-150bp fragments of each of the variants in the two genotypes. Amplification was evident from all samples while the negative control (no template) responded appropriately. SYBR Green I dsDNA dye was used to monitor fluorescence. Amplification products were identified by melting curve profile analysis and confirmed by gel electrophoresis. Unknown sample concentration was optimized by the analysis of amplification plot (threshold cycle: C_T). The housekeeping gene e*longation factor 1 alpha* (*EF1α*) was used to normalize different cDNA samples amounts. The results showed a decrease of 20 to 55% for all of the isoforms in the mutant. (Fig.3.13).

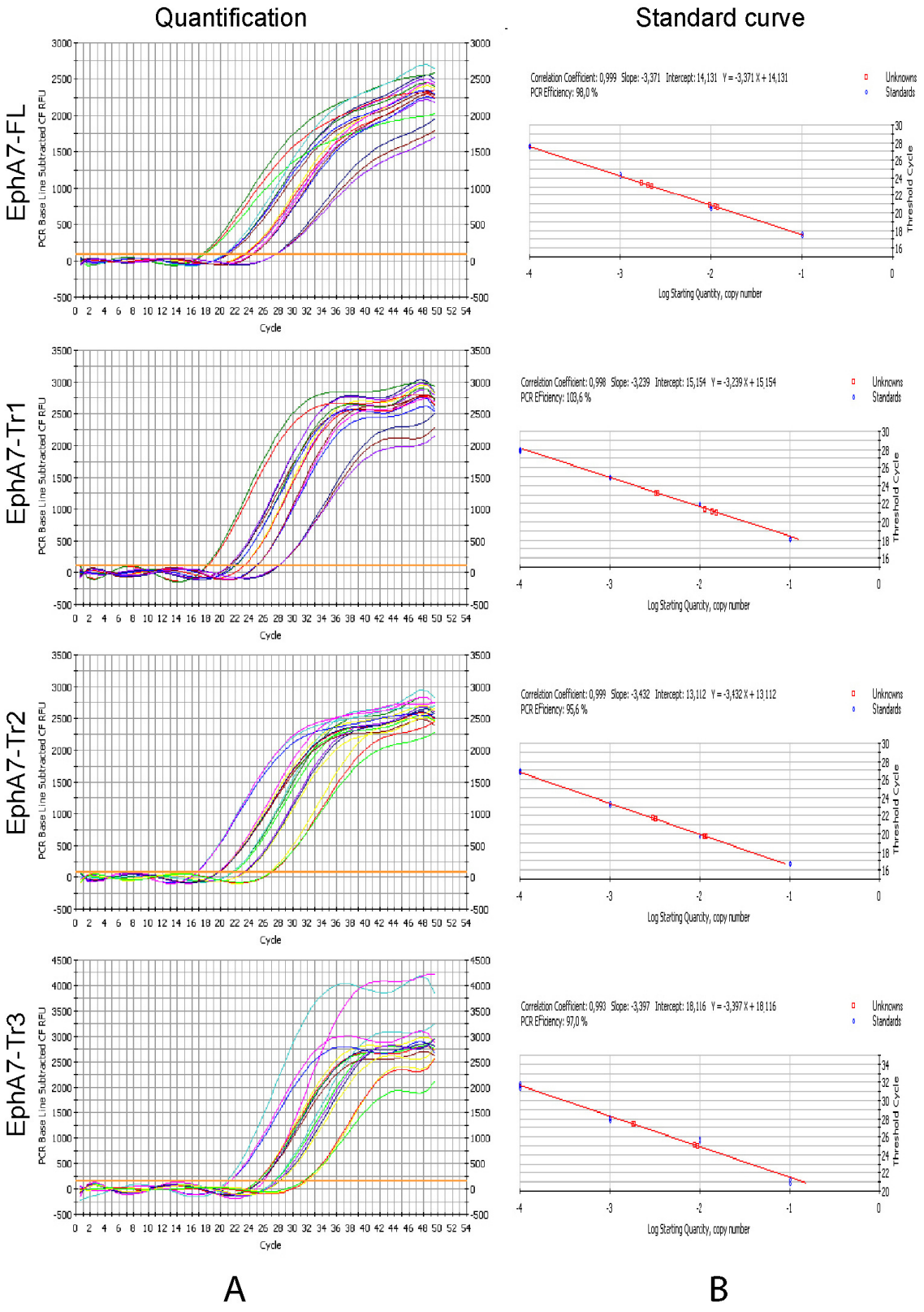
Quantification
Standard curve
EphA7-FL
EphA7-Tr1
EphA7-Tr2
EphA7-Tr3
PCR Base Line Subtracted CF RFU
Cycle
Correlation Coefficient: 0,999 Slope: -3,371 Intercept: 14,131 Y = -3,371 X + 14,131
PCR Efficiency: 98,0 %
Correlation Coefficient: 0,998 Slope: -3,239 Intercept: 15,154 Y = -3,239 X + 15,154
PCR Efficiency: 103,6 %
Correlation Coefficient: 0,999 Slope: -3,432 Intercept: 13,112 Y = -3,432 X + 13,112
PCR Efficiency: 95,6 %
Correlation Coefficient: 0,993 Slope: -3,397 Intercept: 18,116 Y = -3,397 X + 18,116
PCR Efficiency: 97,0 %
Unknowns
Standards
Threshold Cycle
Log Starting Quantity, copy number
A
B

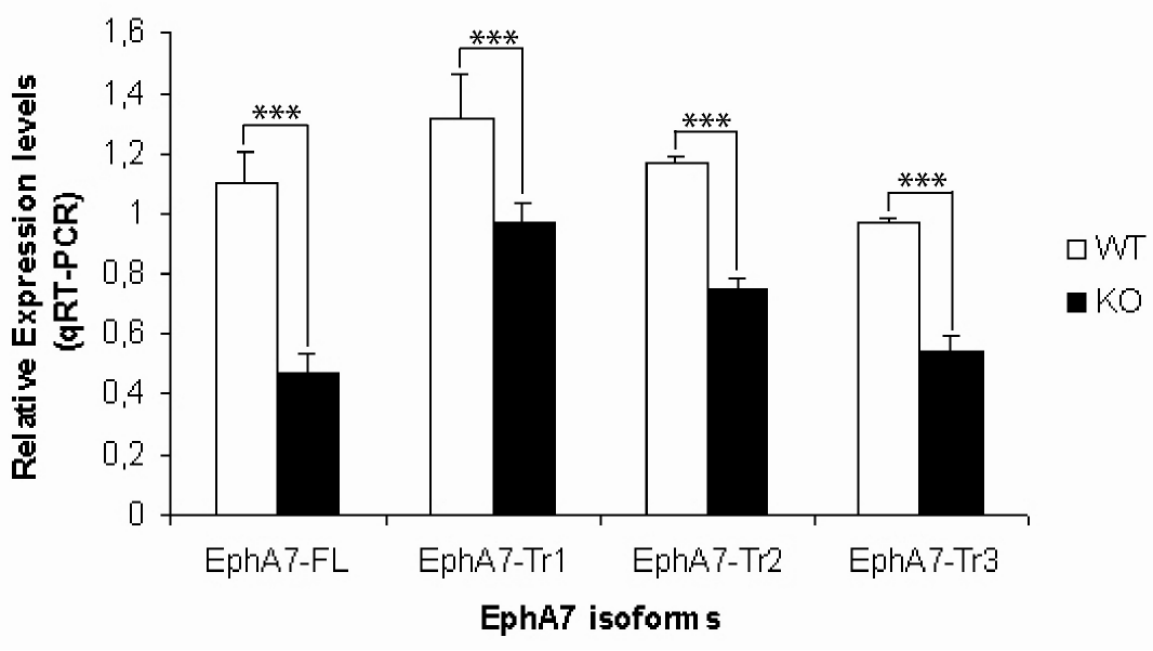

Fig. 3.13: Quantitative real-time PCR of *EphA7* isoforms (SYBR Green I assay). (A) Real-time amplification plots for EphA7-FL, EphA7-Tr1, EphA7-Tr2, EphA7-Tr3 genes. The chart showing a plot for each PCR reaction based upon its relative florescence unit (RFU). The cycle numbers (Cycle threshold, C_T) necessary to achieve the given level of florescence (horizontal level), Baseline subtraction is made at the lowest point where linear amplification of the PCR reactions is occurring. (B) The standard curve with each isoform was obtained by plotting of signals in (A) for four concentrations of standards (blue points, each concentration was examined in three or six replicates). Similarly, the unknown was analyzed in parallel replicates (Red points). (C) The relative expression of each isoform in wild type and homozygous hypothalamus after normalization with the control of *Ef1a* expression. EphA7-FL was 55% decreased in homozygous hypothalamus, other truncated forms were around 25% decreased in homozygous hypothalamus.

3.2.4 *Foxb1* can bind *EphA7* through putative binding sites as demonstrated by the One Hybrid Assay in Yeast

To judge from the axonal phenotype of the *Foxb1* mutant mouse, Foxb1 is part of the cis-regulatory genetic circuitry controlling axonal pathfinding in the diencephalon. In order to place *EphA7* more precisely in this circuitry, to find out if *EphA7* is under the direct control by the Foxb1 DNA-binding protein. The alternative hypothesis would be that *EphA7* expression is at the end of a chain of transcriptional regulation events starting with *Foxb1* but including one or more intermediate steps (i. e. transcription factors downstream Foxb1, etc.) before reaching *EphA7*.

In contrast to most helix–turn–helix proteins, forkhead proteins bind DNA as monomers (Pierrou et al., 1994). Their specific binding sites, which typically span 15–17bp, are asymmetrical. The sequence specificity has been determined for several representatives of this protein family

through selection of binding sites from pools of short, random-sequence duplexes (Pierrou et al., 1995). A seven-nucleotide core corresponds to the major groove base contacts made by the recognition helix (helix 3). For the majority of forkhead proteins, the core conforms to the RYMAAYA consensus (Overdier et al., 1994; Pierrou et al., 1994; Kaufmann and Knochel, 1996), where **R** stands for A or G; **Y** for C or T, and **M** for A or C). I used this seven nucleotide consensus as motif to search the 170kb *EphA7* genomic sequence (+ 10kb on either side), with the help of the Celera Database. I found out that some RYMAAYA sequences are present on the genomic sequence of *EphA7* with high frequency:

ATAAATA	is present	80	times on the genomic sequence of EphA7
ACAAACA	,,	46	,,
ACAAATA	,,	38	,,
GCAAACA	,,	28	,,
ATAAACA	,,	24	,,
ACCAATA	,,	15	,,
ATCAATA	,,	13	,,
GTAAAATA	,,	13	,,
GCAAATA	,,	12	,,
GTAAAACA	,,	12	,,
GTCAATA	,,	12	,,
ACCAACA	,,	10	,,
GCCAATA	,,	10	,,
ATCAACA	,,	7	,,
GCCAACA	,,	6	,,
GTCAACA	,,	3	,,

I selected the 6 RYMAAYA which were repeated with the highest frequency on *EphA7* genome for further investigation (in bold lettering in the above list). As a first approach to the question of the direct interaction of Foxb1 protein with these binding sites, I used a "One Hybrid" strategy on a yeast model (Matchmaker kit, Clontech) to detect which DNA element which Foxb1 protein can bind. First, I designed oligonucleotides based on the candidate binding sequences, and had them commercially synthesized. I gave them the names element 1 (E1), element 2 (E2), element 3 (E3), element 4 (E4), element 5 (E5) and element 6 (E6), respectively:

E1) A ATAAATA A ATAAATA AATA
E2) AATAAATACAAACA
E3) C ACAAACA AA ACAAACA CAC
E4) CA ATAAATACAAATA
E5) ACCA ATAAATAAAACAAATA
E6) CAA ACAAACA A ACAAACA AA

Next, three tandem copies were ligated into the EcoRI-SmaI sites (i. e. in front of the basal promoter) of plasmid vectors pHISi and pHISi-1 (which contains the yeast *HIS3* gene downstream of the multiple cloning sites and the minimal promoter of *HIS3locus*, so allowing HIS3-defective YM4271 yeast strain to grow on Histidine-deficient selection medium) and of plasmid vector pLacZi (which carries the LacZ reporter gene downstream of the minimal promoter of the yeast iso-1-cytochrome C gene (P_{cyc1}), and which is ready for integration in the *ura* locus). All vectors were from the Matchmaker Kit of Clontech. The constructs so generated were called pHISi-E1, E2, E3, E4, E5, E6, pHISi-1-E1, E2, E3, E4, E5, E6 and pLacZi-E1, E2, E3, E4, E5, E6 respectively. These constructs have now not only the minimal promoter but the tandem repeats upstream which should function as enhancers if it is true that they bind Foxb1. The reason why two different HIS vectors are used is that in some circumstances one of them gives higher background than the other (the backbones of these plasmid vectors are different). It is up to the researcher to determine which one will be more suitable for her experiments.
The constructs were then sequentially integrated into the genome of the YM4271 yeast strain to obtain two strains for each element (E). One of them was carrying pHISi-pLacZi-E (1-6) and the other pHISi-1-pLacZi-E (1-6).
The next step was to perform controls of the suitability of these vectors for the experiment: in the absence of Foxb1, the constructs are not supposed to activate expression of the survival reporter HIS3 or the blue reporter LacZ (ß-gal). Because of the basal promoter these vectors carry, the transformed yeast strain will be able to produce some HIS3 gene product and survive in deficient medium (leaky expression; background). 3-AT, a competitive inhibitor of the yeast HIS3 protein, eliminates this “leaky expression”. I performed a “leaking test” by culturing all strains on SD/-His, -Ura3, +15mM, 45mM and 60mM 3-AT selection plates. The purpose of this test is to find

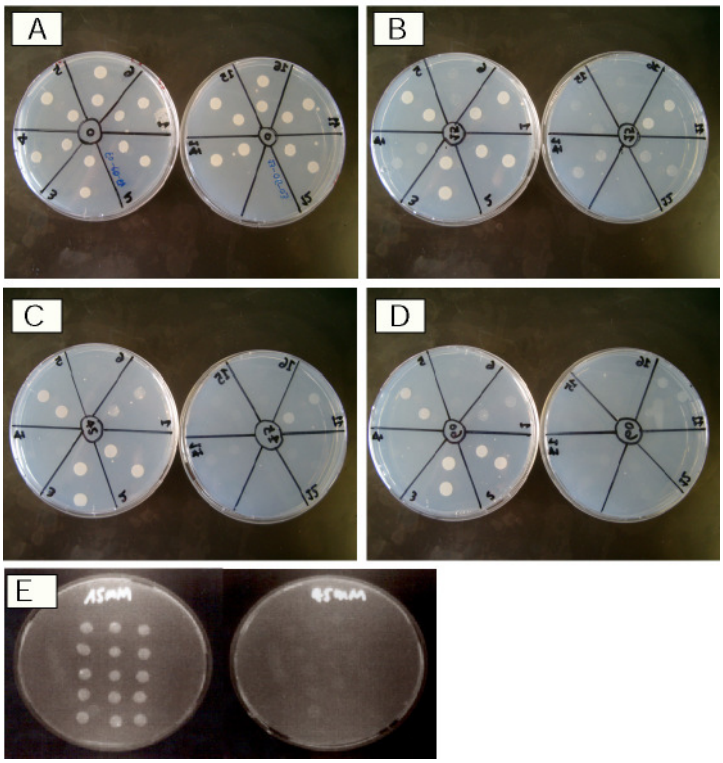

Fig.3.14: Test yeast pHISi-pLacZi-E (1-6) and pHISi-1-pLacZi-E (1-6) colonies for HIS 3 expression. (A) pHISi-pLacZi-E (1-6) (left plate), pHISi-1-pLacZi-E (1,2,4-6) (right plate), 0mM 3-AT. (B) pHISi-pLacZi-E (1-6) (left plate), pHISi-1-pLacZi-E (1,2,4-6) (right plate), 15mM 3-AT. pHISi-pLacZi-E4 could not grow in left B; pHISi-1-pLacZi-E2, 4, 5, 6 could not grow no the right plate. (C) pHISi-pLacZi-E (1-6) (left plate), pHISi-1-pLacZi-E (1,2,4-6) (right plate), 45mM 3-AT. pHISi-1-pLacZi-E1 could not grow on the right plate. (D) pHISi-pLacZi-E(1-6) (left plate), pHISi-pLacZi-E (1,2,4-6) (right plate), 60mM 3-AT. (E) pHISi-1-pLacZi-E3 could not grow on selection plate with 45mM 3-AT.

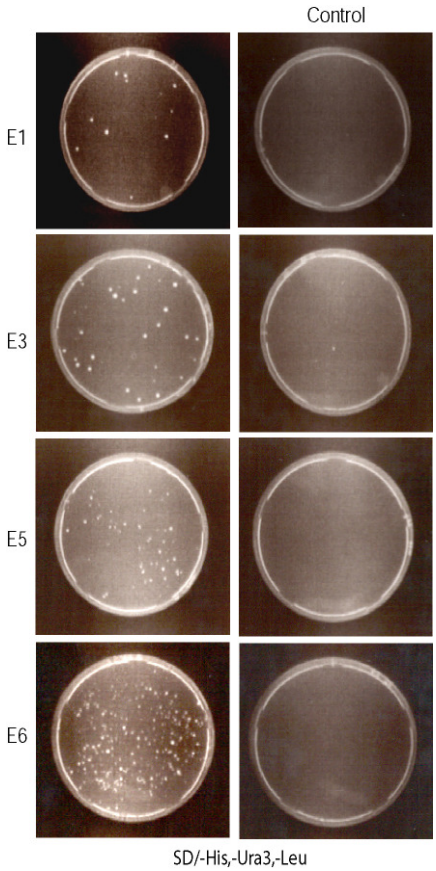

Fig.3.15: After the transformation of pGAD424-Foxb1 vector, the pHISi-1pLacZi-E1, E3, E5, E6 strains could grow on the SD plates with 15mM 3-AT. The control without pGAD424-Foxb1 could not grow.

out which strain has low background expression and which one is suitable for the experiment. pHISi- pLacZi-E4, pHISi-1-pLacZi-E1, E2, E3, E4, E5 E6 could not grow on the selection plate with 45mM 3-AT. (Fig.3.14). These were selected for the experiment. Then the background ß-gal (LacZ) expression of each strain was checked with ß-Gal filter assay: after 2 hours incubation, none of them turned blue (data not shown), indicating they were appropriate for the experiment.

Next *Foxb1* cDNA was cloned into the EcoRI-BamHI sites of the pGAD424 vector, this construct was called pGAD424-Foxb1. Transform pGAD424-Foxb1 into the pHISi-1pLacZi-E (1-6) strains respectively, growing them afterwards on minimal synthetic dropout (SD) plates (-His -Ura3, , -Leu). The strains carrying tandem repeats of E1, E3, E5, E6 were discovered that they could not grow on the SD plates (Fig.3.15).

To confirm the above results, the positive colonies were picked up and performed 3-AT assay according to standard protocol: the pHISi-1-pLacZi-E1 yeast strain transformed with pGAD424-Foxb1 did grow on SD plates supplemented with 45mM 3-AT; the pHISi-1-pLacZi-E3 yeast strain transformed with pGAD424-Foxb1 did grow on SD plates supplemented with 15mM of 3-AT; the pHISi-1-pLacZi-E5 yeast strain transformed with pGAD424-Foxb1 did grow on SD plates supplemented with 60mM of 3-AT; the pHISi-1-pLacZi-E6 yeast strain transformed with pGAD424-Foxb1 did grow on SD plates supplemented with 60mM 3-AT respectively. The control yeast strain without pGAD424-Foxb1 transformation did not grow at all on the SD plates supplemented with corresponding experimental concentration of 3-AT(Fig.3.16A). By a ß-gal filter assay, all positive colonies turned blue in about 30 minutes, however, the control did not turn blue in this period (Fig.3.16B). It was concluded that Foxb1 can bind the DNA sequences E1, E3, E5, and E6.

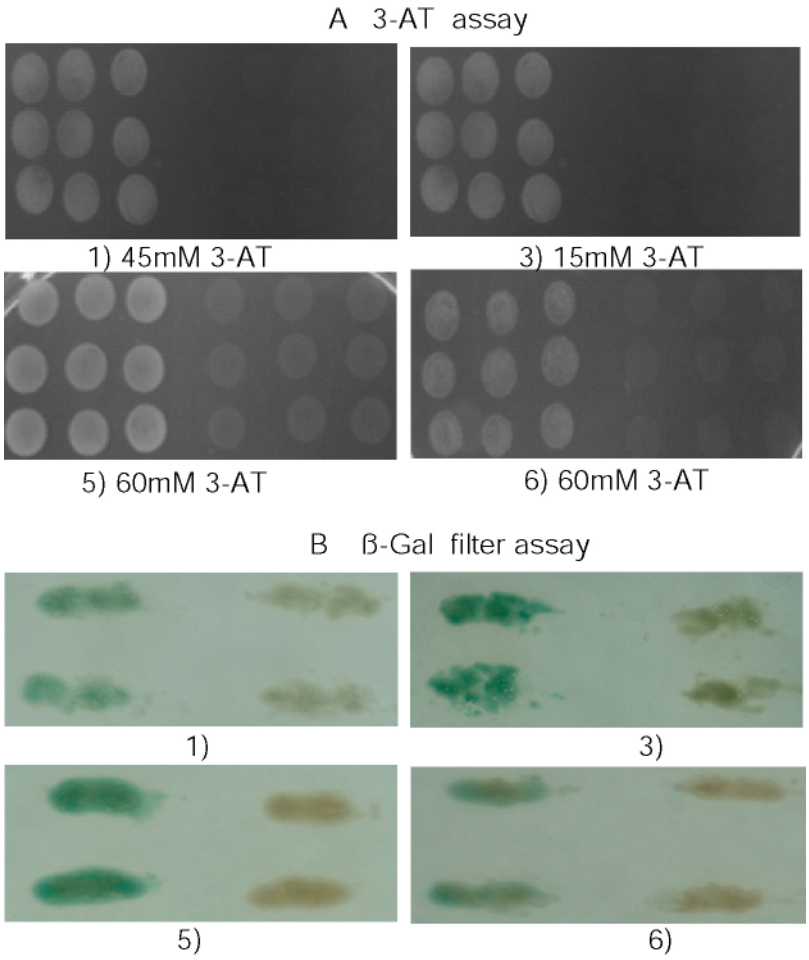

Fig.3.16: 3-AT assay and ß-Gal filter assay of positive colonies. (A) 3-AT assay. Positive colonies could grow on SD selection plates supplemented with relative concentration of 3-AT, the control without Foxb1 could not grow. (B) ß-Gal filter assay. Positive colonies turn blue in about 30 minutes, but the control remained unstained after that period of time.

3.2.5 Foxb1 can regulate gene expression through E1, E3, E5 and E6 in mammalian cells in culture

To investigate the ability of Foxb1 to regulate gene expression in mammalian cells through these binding sites, each of the Foxb1 binding sequences identified by One-Hybrid Assay was inserted into MCS sites upstream of SV40 promoter of pGL3-C (Promega) respectively, which carrys the luciferase reporter gene. Those four binding sites were called Ea, Eb, Ec, Ed and these constructs corresponded to Ea, Eb, Ec, Ed respectively.

In order to perform the experiments, in a system as biologically significant as possible, a cell line expressing Foxb1 endogenously was searched. The rationale was that, if the cells express Foxb1,

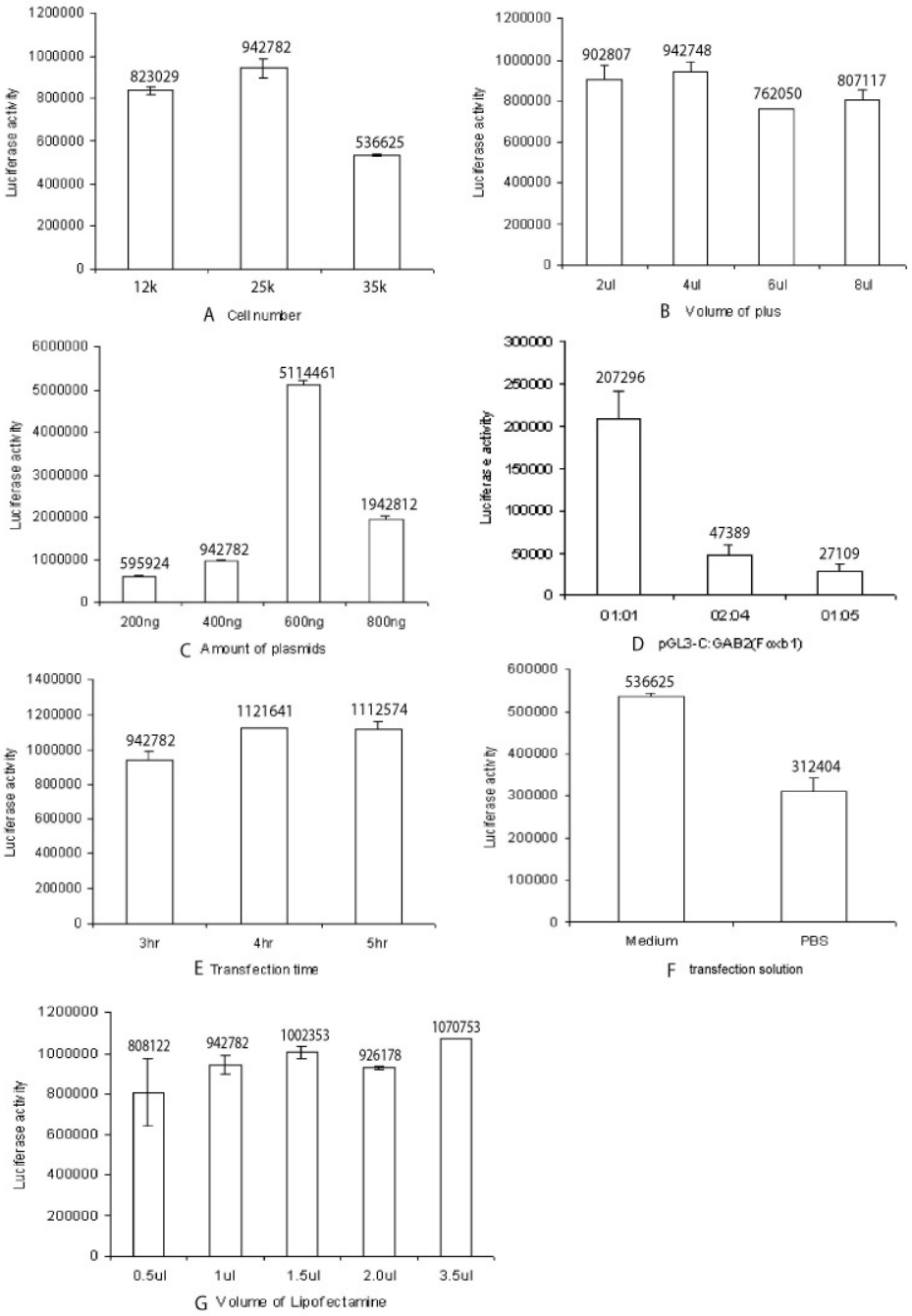

Fig.3.17: Optimization of transient co-transfection assay. (A) Co-transfection assay with different cells number. 25000 cells per well gave highest luciferase activity. (B) Co-transfection assay with different amount of PLUS reagent. 4ul of PLUS reagent per well gave highest luciferase activity. (C) Co-transfection assay with different total amount of plasmids. 600ng plasmids per well gave highest luciferase activity. (D).Co-transfection assay with different ratio of plasmids. The ratio 1:1 of Foxb1 expressing plasmid to reporter plasmid (total amount is 600ng) per well gave highest luciferase activity. (E) Co-transfection assay with different transfection time. 4 hours transfection gave highest luciferase activity. (F) Co-transfection assay with different solution. Growth medium without serum as transfection medium gave highest luciferase activity. (G) Co-transfection assay with different amount of Lipofectamine reagent. 1.5ul of Lipofectamine reagent per well gave highest luciferase activity.

they will probably have any (yet unknown) cofactors that Foxb1 needs to bind, etc. I chose the P19 cell line (ATCC No. CRL-1825), which was derived from an embryonal carcinoma induced in a C3H/He mouse, and it is pluripotential (McBurney and Rogers, 1982). This was confirmed by RT-PCR that these cells express Foxb1 endogenously (not shown). With these reporter constructs plus a vector constitutively expressing full-length Foxb1 under the control of the CMV promoter, (plus the TKß plasmid, expressing ß-gal, as transfection efficiency control) a series of standard transient cotransfection assays were performed in P19 cells to optimize transfection conditions. The optimal conditions were: in each well, 25000 cells, 600ng total amount of DNA, 1:1 of the ratio of Foxb1 expression plasmid to reporter plasmid, 4ul of "Plus" reagent, 1.5ul of "Lipofectamine" reagent, growth medium without serum as transfection medium, 4 hours transfection time (Fig.3.17). Use Ea, Eb, Ec, Ed and Foxb1 expressing plasmid with TKß to perform the transient co-transfection assay (See materials and methods). The luciferase activity was summarized in Table 3.1.

Table 3.1: Luciferase and ß-Gal activity after transfection with Ea, Eb, Ec, Ed constructs respectively

samples	Luciferase (Luc)	ß-Gal	Luc/ß-Gal (normalization)	Luc/ß-Gal (mean)
pGL3-C	328900	0,514	639883	612020
	307710	0,518	594035	
	354060	0,588	602143	
Ea (+ Foxb1)	183270	0,473	387463	355803
	209510	0,514	407607	
Eb (+ Foxb1)	95302	0,516	184694	172069
	115609	0,696	166105	
	128522	0,777	165408	
Ec (+ Foxb1)	51583	0,373	138292	138045
	53734	0,419	128243	
	81032	0,549	147599	
Ed (+ Foxb1)	71239	0,635	112187	106918
	63031	0,607	103840	
	58019	0,554	104727	
Ea (– Foxb1)	362430	0,623	581750	517426
	276580	0,504	548770	
	215940	0,512	421758	
Eb (– Foxb1)	294150	0,686	428790	512337
	371010	0,649	571664	
	261840	0,488	536557	
Ec (– Foxb1)	175620	0,513	342339	305884
	150243	0,492	305372	
	106087	0,393	269941	
Ed (– Foxb1)	136006	0,55	247284	271397
	213980	0,608	351941	
	98885	0,46	214967	

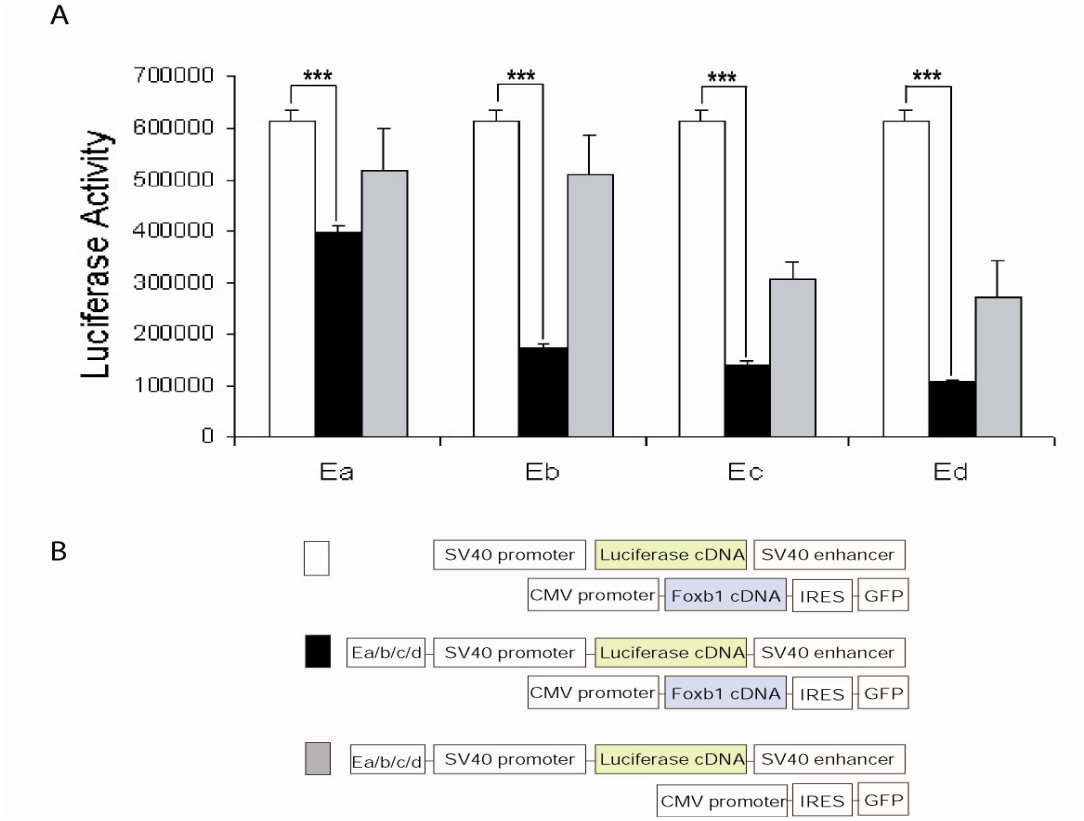

Fig.3.18: (A) Foxb1 inhibits transcription of reporter gene luciferase through putative binding sites Ea, Eb, Ec, Ed. (B) Schematic structure of each construct and the combination of each co-transfection.

These results seemed to indicate that Foxb1 was exerting an inhibitory influence on reporter expression (This was done three times). This was contradictory with the results of DNA microarray, the ISH and Q-PCR, which showed clear decrease of *EphA7* expression in the mutant, indicating that Foxb1 is an activator. One possible explanation for the disagreement was that the short stretches of putative binding sequence for Foxb1 were not enough to elicit the full natural regulatory function of the protein. Perhaps if placed in their genomic context, the binding sequences would give results more according to what the ISH showed.

Since the stretches of DNA sequence used for binding of regulatory factors are very important for correct development and hence for survival, it is usually assumed that biologically relevant putative binding sites will be found in those parts of the genome that are conserved between different species. The Celera Database was used to find the putative Foxb1 binding sites on human-mouse conserved portions of the genomic sequence of EphA7. A large conserved fragment with numerous Foxb1 binding sites was found on the 3′ flanking region of *EphA7* genomic sequence from 161,073bp to 163,969bp. This large conserved genomic fragment was

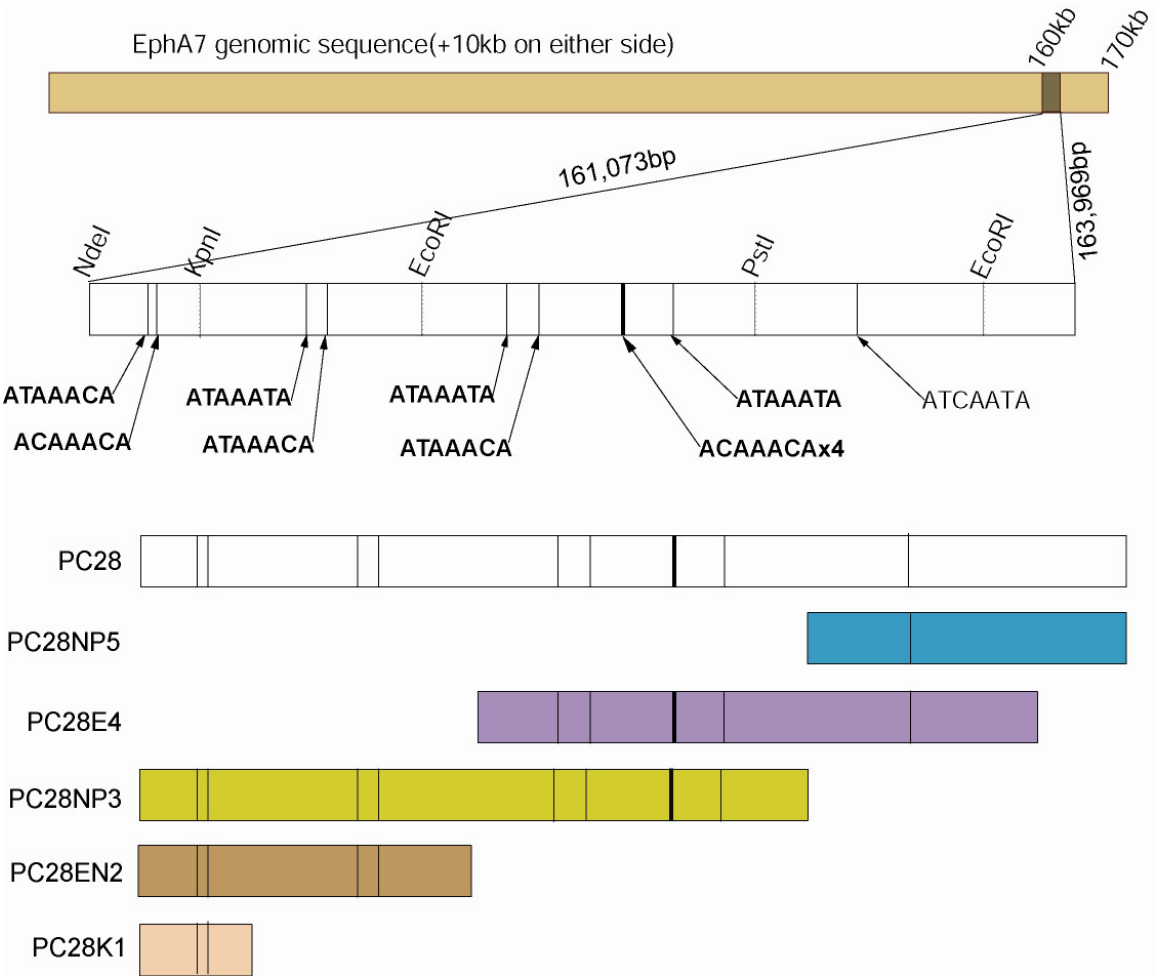

Fig.3.19: 3′ flanking conserved *EphA7* genomic fragment and the different smaller fragments generatead from it. Nde, KpnI, EcoRI, PstI, are the corresponding restriction enzyme digestion sites.

cloned by long-range PCR using as template a BAC clone RP230134E11 (Invitrogen) containing *EphA7*.

The PCR product was confirmed to contain the desired fragment by restriction enzyme digestion and agarose gel electrophoresis, as is usual. Several reporter gene constructs were generated from this big fragment, in which different lengths of 3′ flanking sequence were contained upstream of the SV40 promoter in pGL3-C (Promega), which has reporter gene luciferase following the promoter. Reporter constructs designated PC28, PC28NP5, PC28E4, PC28NP3, PC28EN2, PC28K1 plasmids contained 2896bp, 935bp, 1700bp, 1943bp, 896bp, 336bp 3′ flanking sequences of *EphA7*, respectively (Fig.3.19).

Then a transient cotransfection assay was used again to investigate the ability of Foxb1 to regulate reporter expression through the EphA7 genomic domains. The luciferase activity was summarized in Table 3.2, Table, 3.3, Table 3.4 respectively. Interestingly, Foxb1 can

Table 3.2 Luciferase and ß-Gal activity after transfection with pC28, pC28NP5 constructs respectively.

samples	Luciferase (Luc)	ß-Gal	Luc/ß-Gal (normalization)	Luc/ß-Gal (mean)
pGL3-C	5,20E+04	0,285	1,82E+05	1,86E+05
	7,09E+04	0,335	2,12E+05	
	5,00E+04	0,321	1,56E+05	
	4,05E+04	0,267	1,52E+05	
	5,65E+04	0,305	1,85E+05	
	3,45E+04	0,152	2,27E+05	
pC28 (+ Foxb1)	1,07E+05	0,437	2,45E+05	2,95E+05
	1,49E+05	0,37	4,03E+05	
	1,29E+05	0,356	3,62E+05	
	9,98E+04	0,37	2,70E+05	
	8,29E+04	0,36	2,30E+05	
	8,62E+04	0,33	2,61E+05	
pC28 (-Foxb1)	6,83E+04	0,293	2,33E+05	2,00E+05
	6,79E+04	0,306	2,22E+05	
	7,28E+04	0,341	2,13E+05	
	5,95E+04	0,34	1,75E+05	
	6,71E+04	0,343	1,96E+05	
	4,98E+04	0,305	1,63E+05	
pC28NP5 (+Foxb1)	5,20E+05	0,503	1,03E+06	8,56E+05
	5,02E+05	0,482	1,04E+06	
	4,72E+05	0,509	9,27E+05	
	4,45E+05	0,478	9,31E+05	
	3,42E+05	0,431	7,94E+05	
	1,50E+05	0,367	4,09E+05	
pC28NP5 (-Foxb1)	9,44E+04	0,285	3,31E+05	3,27E+05
	8,71E+04	0,333	2,62E+05	
	9,62E+04	0,335	2,87E+05	
	9,13E+04	0,345	2,65E+05	
	1,45E+05	0,334	4,34E+05	
	1,45E+05	0,378	3,84E+05	

Table 3.3 Luciferase and ß-Gal activity after transfection with pC28E4 construct.

samples	Luciferase (Luc)	ß-Gal	Luc/ß-Gal (normalization)	Luc/ß-Gal (mean)
pGL3-C	23627	0,158	149538	142397
	31670	0,280	113107	
	52819	0,321	164545	
pC28E4 (+Foxb1)	73088	0,291	251162	343155
	189910	0,464	409289	
	171960	0,466	369013	
pC28E4 (-Foxb1)	187280	0,476	393445	422535
	195470	0,454	430551	
	183210	0,413	443608	

Table 3.5 Luciferase and ß-Gal activity after transfection with pC28K1, pC28EN2, pC28NP3 constructs respectively.

samples	Luciferase (Luc)	ß-Gal	Luc/ß-Gal (normalization)	Luc/ß-Gal (mean)
pGL3-C	1,53E+05	0,569	2,69E+05	2,66E+05
	1,48E+05	0,533	2,78E+05	
	1,78E+05	0,66	2,70E+05	
	1,68E+05	0,596	2,82E+05	
	8,70E+04	0,43	2,02E+05	
	1,06E+05	0,36	2,94E+05	
pC28K1 (+Foxb1)	7,80E+04	0,44	1,77E+05	1,79E+05
	7,80E+04	0,361	2,16E+05	
	7,20E+04	0,395	1,82E+05	
	6,10E+04	0,378	1,61E+05	
	7,40E+04	0,422	1,75E+05	
	3,30E+04	0,204	1,62E+05	
pC28K1 (-Foxb1)	5,69E+04	0,268	2,12E+05	2,00E+05
	6,62E+04	0,343	1,93E+05	
	6,00E+04	0,289	2,08E+05	
	6,10E+04	0,397	1,54E+05	
	7,80E+04	0,339	2,30E+05	
	7,10E+04	0,351	2,02E+05	
pC28EN2 (+Foxb1)	9,01E+03	0,296	3,04E+04	2,89E+04
	9,13E+03	0,331	2,76E+04	
	9,77E+03	0,347	2,81E+04	
	8,79E+03	0,326	2,70E+04	
	1,03E+04	0,351	2,93E+04	
	1,09E+04	0,355	3,07E+04	
pC28EN2 (-Foxb1)	1,16E+04	0,31	3,74E+04	3,74E+04
	1,19E+04	0,298	3,99E+04	
	1,27E+04	0,345	3,68E+04	
	1,07E+04	0,398	2,69E+04	
	1,41E+04	0,334	4,22E+04	
	1,29E+04	0,515	2,50E+04	
pC28NP3 (+Foxb1)	1,61E+05	0,321	5,02E+05	4,90E+05
	1,25E+05	0,261	4,79E+05	
pC28NP3 (-Foxb1)	1,18E+05	0,235	5,02E+05	5,63E+05
	1,58E+05	0,303	5,21E+05	
	1,47E+05	0,284	5,18E+05	
	1,88E+05	0,303	6,20E+05	
	2,11E+05	0,322	6,55E+05	

differentially regulate these genomic domains in p19 cells (Fig.3.20). Foxb1 activates reporter gene expression through PC28, PC28NP3, PC28E4, PC28NP5. The most significant activation was observed from PC28NP5. PC28NP5 has a potential Foxb1 binding site ATCAATA, which was not shown in yeast one hybrid results. However, Foxb1 indeed was able to repress reporter gene expression through PC28K1 and PC28EN2. These experiments demonstrate that Foxb1 can activate gene expression on mouse cells through binding sites in certain genomic regions of *EphA7*.

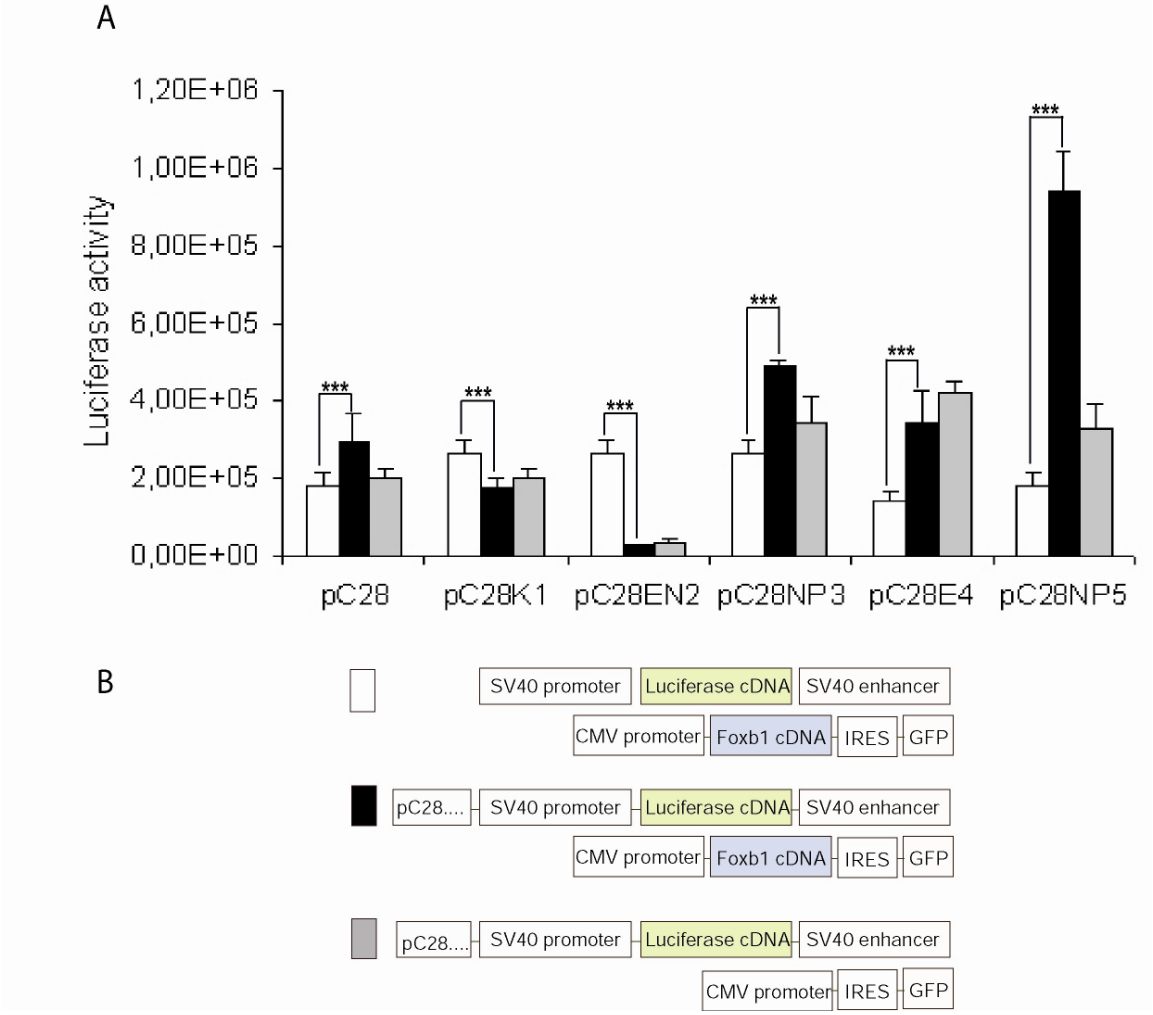

Fig.3.20: Foxb1 can differentially regulate 3′ flanking conserved *EphA7* genomic fragments in p19 cells. (A) Foxb1 activates reporter gene luciferase expression through PC28, PC28NP3, PC28E4, PC28NP5. Foxb1 represses reporter gene luciferase expression through PC28K1 and PC28EN2. (B) The schematic structure of each construct and the combination of each cotransfection..

3.2.6 Electrophoretic Mobility Shift Assays ("Band Shift") show that Foxb1 can bind Ea, Ec, Ed, Ee

As a final experiment in order to support the hypothesis of direct interaction between Foxb1 and *EphA7*, I wanted to show that the protein Foxb1 can bind to the candidate genomic fragment *in vitro*. To this end, I first produced His-tagged Foxb1 recombinant protein (see Materials and Methods). I confirmed specific Foxb1 protein expression by western blotting with Ni-NTA AP conjugate and by the size on SDS-PADE gel after purification. One band of the right size (42kD) was specifically detected on the blot (Fig.3.21).

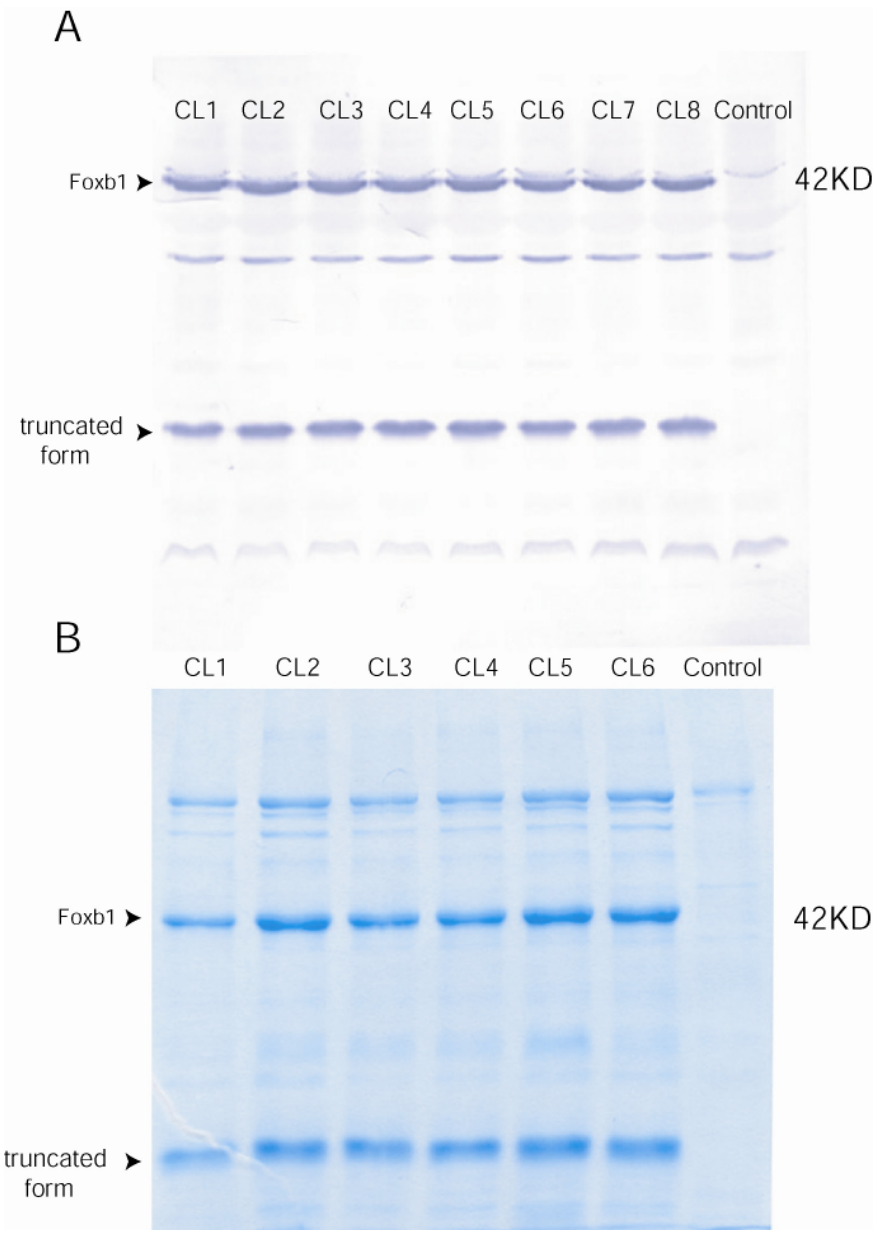

Fig.3.21: Expression and purification of Foxb1 protein in *E.Coli*. (A) Foxb1 protein (42KD) was expressed from pQE31 in XL1 blue cells and detected by Alkaline Phosphatase staining solution used for the western blots with Ni-NTA AP (upper arrowhead). There was another band which might be a truncated form (17KD) (lower arrowhead). CL, cell lysate from different single clone; control, without Foxb1 protein. (B) Foxb1 protein was purified using Ni-NTA Agarose with the indicated imidazole concentrations in the wash and elution steps. Protein (42KD) was visualized by Coomassie staining (arrowhead). CL, the protein was purified from different single clone; the control, without Foxb1 protein in the cells.

A binding assay was performed by incubating the recombinant protein together with end-labeled oligonucleotides carrying each the sequence of one of the putative binding sites Ea, Ec, Ed identified by One-Hybrid Assay and Ee (not identified by One-hybrid Assay, but shown in the fragment of PC28NP5 which was observed the most significant activation in transient co-transfection assay) (with the help of DIG Gel Shift Kit, 2nd Generation, Cat. No. 3353591, Roche). Finally, the incubated samples were seperated by polyacrylamide gel electrophoresis (PAGE). As shown in Fig.3.22, Ea, Ec, Ed and Ee form complexes with Foxb1 protein. The specificities of these complexes were confirmed by being competed off when unlabeled corresponding elements were included in the reaction. And the negative control element did not form the complex with Foxb1 under the same condition.

The oligonucleotides are:

Ea: GTGACAGTTGT ATAAATAAATAAATA AACG
Ec: GTGACAGTTGT ATAAATAAACAAATA AACG
Ed: GTGACAGTTGT ACAAACAAACAAACA AACG
Ee: GTGACAGTTGT CCTAATCAACACTAT AACG
Econ: GTGACAGTTGT CAGTTGTACAGTTGT AACG

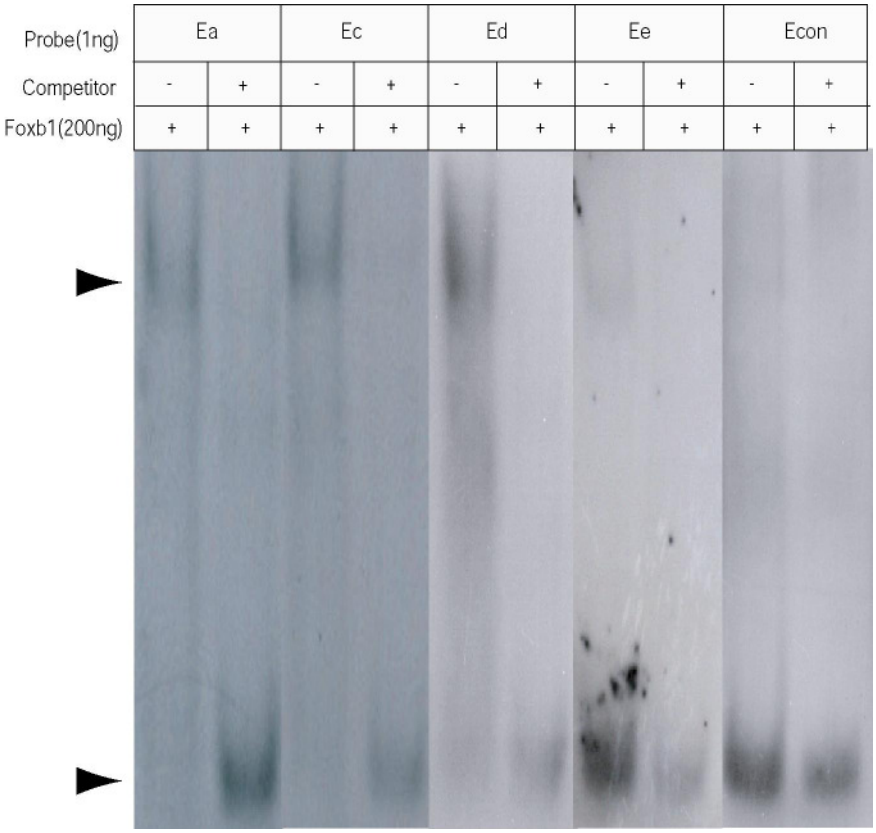

Fig.3.22: DIG Gel Shift Assay with Foxb1 protein and oligonucleotides, the Foxb1 protein specifically bound the sites on Ea, Ec, Ed, Ee oligonucleotides. Gel mobility shift assays were performed with the Foxb1 protein and Foxb1 putative binding oligonucleotides. The reaction components were separated on an 8% native polyacrylamide gel, then transferred to a nylon membrane by electroblot. DIG-labeled moieties were detected in a chemiluminescent assay (CSPD substrate, about 20 min exposure, X-ray film). Lane 1: DIG-labeled Ea oligonuleotide (1ng) after incubation with 200ng Foxb1protein. Lane 2: Same as lane 1, except the incubations also contained increasing amounts of unlabeled nucleotide Ea (125-fold) Lane 3, 4: Same as lane 1 and 2, except the oligo is Ec. Lane 5, 6: Same as lane 1 and 2, except the oligo is Ed, lane 7, 8: Same as lane 1 and 2, except the oligo is Ee. Lane 9, 10: Same as lane 1 and 2, except the oligo is Econ, Upper band, protein oligonucleotide complex (arrowhead); lower band, unbound oligonucleotide (arrowhead).

4 DISCUSSION

Genetics as a science tries to find out how genes influence the development and physiology of the organism. The main approach of the geneticist is the study of mutant phenotypes. In order to learn more about the way in which genes influence axonal navigation, the brain phenotype of a mouse line carrying a mutation in transcription factor gene *Foxb1* was studied. Since the gene and its mutant phenotype were already well characterized, this work went one step further, trying to find out through which other genes (effector genes) Foxb1 influences axonal navigation in the developing diencephalon. Starting with a high-throughput, genomic approach (DNA microarray analysis), and going through a series of "filtering" steps, one candidate gene (tyrosine kinase receptor EphA7) was isolated, known to be involved in axonal navigation in other systems. Several quantitative and non-quantitative techniques were used to demonstrate that its expression is reduced in the *Foxb1* mutant, to prove the biological plausibility of this gene as a Foxb1 downstream candidate and to demonstrate that its expression is directly regulated by Foxb1. Although EphA7 might of course be not the only Foxb1 downstream gene involved in the axonal phenotype under study, its identification as a *bona fide* effector in the Foxb1 signaling cascade is a major contribution to the analysis of axonal pathfinding in the central nervous system.

4.1 The Microarray Approach and Validation of Microarray Data

4.1.1 Microarray data: issues of consistency/reliability, need for validation

Justification of DNA Microarray Approach. Previous attempts of this group to find genes whose expression is altered in the Foxb1 mutant by manual in situ hybridization with probes for candidate genes gleaned from the literature proved a very slow process which did not give any results. The "guessing approach" (guessing probable candidates from the literature on brain development) has thus been inefficient and disappointing. At this point, we felt that large-scale analysis of gene expression in brain using microarray technology had the potential to elucidate molecular changes in gene transcription regulation event.

Reliability. Although it can be said that DNA microarray analysis of expression is in its beginnings, the literature dealing with potential problems of consistency and reliability of the data generated by this technique is already sizable [see the review in (Chuaqui et al., 2002)]. The main reasons for these concerns are probably the lack of experience with this novel approach, and the large data sets that the technique generates. In general terms, the questions that arise are two: are these data accurate? and: are they biologically relevant? We will deal with the second question below. As for the accuracy of the data, factors like not perfectly reproducible dissections, DNA amplification protocols and other can influence the repeatability of each individual result. A measure of the variability of the data sets generated by this approach can be given by the following summary of our DNA microarray results: the first hybridization of DNA microarrays gave 31 genes whose expression was changed in the mutant vs. the wild type. When we hybridized DNA microarrays a second time with a probe obtained from the same pool of mRNA, we obtained 120 genes changed, while only 9 of them were common to the two hybridizations. The third hybridization, with a probe from new, more precise dissections of the mammillary body, found 160 genes changed, and 5 genes coincided between the three hybridizations (were found to be changed in the three data sets).

Validation Methods. As was already clear from the literature, validation of the DNA microarray data by independent methods was essential. A consensus seems to be building among DNA microarray practitioners about validation methods (Rajeevan et al., 2001; Barlow and Lockhart, 2002; Chuaqui et al., 2002), with Quantitative Polymerase Chain Reaction (Q-PCR) and in situ hybridization (ISH) being the most widely used and recommended.

ISH is able to show spatial localization of expression and even relatively large quantitative changes in expression (although admitedly not being a quantitative technique). The main advantage of ISH is of course the spatial localization, because the complex anatomical organization of the brain necessitates a method with high spatial resolution. 57 genes were analyzed by in situ hybridization. Of these, 50 (88%) yielded detectable in situ hybridization signals in the brain. Of which, 30 (61%) showed signal in MBO, but, among these, only 10 showed MBO specific expression and the rest were genes with ubiquitous expression (including of course MBO expression). From the point of view of the comparison between wild type and mutant tissue, among all 57 genes we tested, 7 cases (13%) were fully consistent with DNA microarray data, 4 of them decreased in the mutant, and 3 of them increased. Maybe because probe design and hybridization parameters for each gene in the microarray, it is possible that the actual false negative and false positive rate is lower than we observed.

Q-PCR is an independent technique that provides greater accuracy in terms of individual gene targets and should ideally be used to confirm results from microarray (Sgroi et al., 1999; Rajeevan et al., 2001; Elkahloun et al., 2002; Mimmack et al., 2004). 30 genes were validated by Q-PCR. Of them 8 (27%) were consistent with microarray data, but, intriguingly, 73% of the Q-PCR results show coincidence with the ISH data. Nonreproducibility of microarray results does not necessarily mean that these results are invalid, however, because outbreed mouse genetic background, differences in tissue harvesting, RNA secondary structures, splice variants, complex poly A tails, low transcript expression, and many other factors can influence both microarray and Q-PCR results.

Summary. In this project, DNA microarrays pointed at a relatively small number of possible candidate genes (57), although with "low confidence". Considering that the mouse genome (as well as the human) is believed to have some 30.000 protein-coding genes (Lander et al., 2001; Waterston et al., 2002), this is not a bad approximation. On the basis of this relatively small group of genes, and by applying other more laborious techniques (less high-throughput than the DNA microarrays), I narrowed down the list to only a small, experimentally approachable, number of genes.

4.1.2 Microarray data: Issues of biological validation

The next issues of importance were those of "biological validation" and "narrowing down to hypothesis-driven research".

Biological validation. In other words, what matters in this type of analysis is not so much the confirmed quantitative variation in the expression of a gene, as the significance of the role of that gene in the particular process under study. This means that the mere fact that expression of a gene changes in the mutant in comparison with the wild type does not mean that the gene is directly responsible for the mutant phenotype. In the particular case of the mutant phenotype of a transcription factor, it is obvious that quantitative expression changes do not imply that the gene is directly under the control of the particular transcriptional regulator of interest. One first indication that a certain candidate is actually important is given by the function of the protein codified. Functional data gathered from the literature, databases, etc., are an essential. In the present study, it was immediately obvious that EphA7 was an important candidate, since it belongs to a much-researched family of tyrosine kinase receptors which, together with their specific ligands (the ephrins), have a major involvement in axonal guidance [the original literature is too complex and extensive, see (Wilkinson, 2001; Dickson, 2002; Knoll and Drescher, 2002; Kullander and Klein, 2002) for reviews]. Together with the very strong and specific expression of EphA7 in the wild type MBO, and the validated decrease in expression in the mutant, the functional data made of this particular gene an outstanding candidate. But perhaps the most important biological validation for a receptor is the availability of specific ligand(s) in the precise region and at the precise time when the mutant phenotype appears. The expression data on ephrin A5, whose mRNA was detected by us in the dorsal and ventral thalamus around E18.5, were definitive from this point of view: EphA7 was from that moment on a candidate with high probability of being involved in the axonal guidance model under study.

Narrowing down. Genomic or "high-throughput" projects present a peculiar problem, which is intimately related to the question of biological validation. These projects make available to the biologist huge quantitative data sets of the kind previously available only to astrophysicists and the like (e. g. automatic readings from radiotelescopes, etc.) These are novel problems for the biologist, and are causing much excitement, commentary and discussion [see for instance (Smalheiser, 2002; Weinstein, 2002; Kell and Oliver, 2004; Steinhauser et al., 2004)]. Although extreme positions have been announced, between partisans of the "omic" (genomic, proteomic, cellomic, etc.) research and seriously skeptical, "hypothesis-driven" practitioners (Allen, 2001), a consensus seems to be building around a "synergism" of both kinds of approach [see for instance (Weinstein, 2002)]. It is maybe not too much of a simplification to describe this synergistic process as a series of cycles, whereby "classical" scientific thinking about very complex systems and processes generates questions which prompt researchers to produce large amounts of "omic" data, and then again hypothesis are needed to make the data into information. The paradigm that

underlies most biological research seems to be a molecular version of the "Domino Effect": one molecule pushes (interacts with) another, which pushes the next, etc. According to this, we could summarize: high-throughput methods let us know the number of dominoes, and hypotheses place each domino in its place in the chain. Since the experimental confirmation that is the aim of much hypothesis-driven research cannot usually be carried out for very large numbers of molecules and / or processes, the "classical" part of the cycle we just described includes a first step of "narrowing down" to those data (genes, etc.) perceived as important or perhaps simply more accessible to experimental manipulation. The biological validation (see above) is an essential part of this process: faced with a large group of genes potentially involved in our favorite biological problem, we focus on those genes (on that gene) we can make sense of on the basis of the functional information at hand. Again, in the case of the present study, focusing on EphA7 was the most logical next step.

4.1.3 Biological plausibility of EphA7 as a candidate to be involved in the Foxb1 axonal phenotype

The reported function of EphA7 matches the phenotype under study. Examination of axonal development in the diencephalon of Foxb1 mutants has revealed an axonal navigation failure starting around E18.5: mtt axons are not able to enter their target, the dorsal thalamus (Alvarez-Bolado et al., 2000). A large number of molecules have been showed to be involved in the process of axonal guidance from their site of origin to their target area, such as the netrins and their receptors (Dcc and Unc5), the semaphorins and the neurophilin and plexin receptors, the Slits and Robos, as well as the ephrins, which interact with receptor tyrosine kinases of the Eph family [a subject abundantly reviewed, see especially (Tessier-Lavigne and Goodman, 1996; Mueller, 1999; Dickson, 2002)]. After the discovery of the first biochemically characterized ephrin (Cheng and Flanagan, 1994) 10 years ago, numerous contributions have appeared underlining the importance of their receptor-ligand interactions in the development of topographically organized axonal projections such as retinotectal projection (Cheng and Flanagan, 1994; Drescher et al., 1995).

EphA7 is expressed in the MBO at the onset of the phenotype. The full length form of EphA7, as well as all its shorter isoforms, are appropriately and very specifically expressed in the cells of origin of the mtt (the MBO neurons) as well as in the group of cells alongside the mtt tract at least from E16.5 to E18.5 (the age of onset of the mutant phenotype), as we have shown by ISH. Expression of all of them is reduced in the mutant.

Appropriate ligands are expressed in the region at the onset of the phenotype. The tyrosine kinase receptor EphA7 binds the five known cell-attached ephrin-A ligands (Wilkinson, 2001). We have shown by ISH that, on E18.5, ephrin A1-A3 are widely expressed in the brain (including the diencephalon), and ephrin A5 has very specific diencephalic expression pattern, complementary with that of EphA7 (ephrin A4 was not expressed in the brain at this age). On the basis of these results, an involvement of EphA7 / ephrin A in mammillary axonal navigation is probable.

4.1.4 EphA7 in the developing mammillothalamic tract: a mechanistic hypothesis

The players. In order to hypothesize a plausible mechanistic explanation for the formation of the mtt and the appearance of the mutant phenotype, I will first enumerate the key molecular and cellular players:

1) Full length and truncated EphA7. Most experimental evidence indicates that the Eph family exerts its function by a repellent mechanism, although there are some reports of an adhesive or permissive function of Eph receptors and ligands (Dickson, 2002; Kullander and Klein, 2002). The truncated (non-signalling) and full length (signalling) isoforms of EphA7 have been shown to serve different functional roles (Holmberg et al., 2000). Since truncated forms bind the ligand without signalling to the interior of the cell (they are missing the tyrosine kinase domain), they act as adhesive factors; the full length protein, however, upon binding to the ligand, starts a signalling pathway leading to repulsion (Holmberg et al., 2000). By means of specific antibodies, it has been shown that, in the MBO, the truncated forms of EphA7 are positioned in the cell body membrane, while the full length protein is found in the membrane of the tip of the axons (Ciossek et al., 1999; Rogers et al., 1999).

2) The ephrin ligands. Ephrin-As can be secreted and act as soluble factors although in principle associated with the cell membrane through GPI (Guan and Rao, 2003). The surrounding cells of the diencephalon, as we have shown here, express ephrin A5, which presumably repel the growing mtt axons preventing them to stray from the right pathway.

3) The EphA7 "bridge". Here we have shown that there is a small group of cells expressing EphA7 in the region between MBO and dorsal thalamus. By E16.5, these cells form a "bridge" spanning the distance later to be covered by the mtt axons. We have shown that, at E18.5, the mtt actually follows the pathway formed by those cells in order to reach the target region (dorsal thalamus).

A plausible scenario. Therefore, we would have EphA7-displaying axonal growth cones (the developing mtt) advancing on a "bridge" or "carpet" of equally EphA7-displaying cells. But why

are the mtt growth cones not repelled by secreted ephrin A5, and what has the EphA7 "bridge" to do with this? In principle, that EphA7-displaying axons navigate on top of EphA7-displaying cells seems counterintuitive: a receptor interacts with a receptor? The concept of "masking" by Eph receptors offers a possible explanation to these questions. It has been shown that areas of the brain expressing high amounts of Eph receptors can bind soluble ephrin ligands (secreted by other cell groups) with such efficiency that they act as "sinks" for those ligands, effectively "masking" their repulsive activity (Sobieszczuk and Wilkinson, 1999; Helmbacher et al., 2000). The same "masking" concept has been seen to work for Sema3F (ligand) and its receptor neuropilin2 in the developing brainstem (Watanabe et al., 2004). A plausible scenario could be as follows: The nascent mtt, expressing EphA7 and therefore sensitive to the repulsive power of ephrins, presumably obeying to a powerful soluble attractant secreted by the anterior dorsal thalamus, has to navigate through an area of intense expression of ephrins. It does so by growing on top of an elongated group of cells (a "bridge") leading from the branching point to the dorsal thalamus (target region). These cells express EphA7 which acts as a sink for ephrins, effectively masking their repulsive effect for as long as the axons do not stray from the straight path to the target region. In *Foxb1*-deficient mutants, EphA7 expression is severely reduced in the MBO (but not in the bridge, which is intact in the mutant since it does not express *Foxb1*), making the mtt axons less sensitive to the repulsive ephrins, and allowing them to stray, perhaps following inappropriate rostral attractants meant for axons of different origin. In this way, by combining our original observations and current concepts in the field, we have, first, contributed to explain our results, and second, generated a complex hypothesis that can be further explored by future studies.

Matching phenotypes? An obvious question here would be: do we expect the EphA7 mutant phenotype then to match the Foxb1 phenotype in the diencephalon? Two reasons seem to indicate that the reasonable answer is "no". 1) Foxb1 is a transcription factor, i. e., it regulates the expression of other genes, probably several of them; alteration of only one of its effectors (EphA7 in this case), is not likely to reproduce all details of the Foxb1 mutant phenotype; 2) The Eph receptor and the ephrin families of genes are very numerous (14 different receptors and eight ligands so far, all of which are widely expressed in the central and peripheral nervous systems during development and in the adult) and they bind each other promiscuously [reviewed for instance by (Drescher, 1997; Flanagan and Vanderhaeghen, 1998; Kullander and Klein, 2002) and many others], which gives this system a high degree of functional redundancy, particularly in regions where, like the developing diencephalon, several members of these gene families are coexpressed.

4.2 *EphA7* as a Direct Target of Foxb1 protein

4.2.1 Direct interaction

Once the search had narrowed down to this particular candidate, the problem became quite different. Now the hypothesis "EphA7 expression in MBO is controlled by Foxb1" demanded experimental confirmation or falsification. The first straightforward step to be taken was to find if putative binding sites for Foxb1 were present on conserved regions of the genomic sequence of EphA7. Since the binding sites of Foxb1 are not yet known, experiments destined to find out this information would seem to be the next step. However, Fox proteins seem to have very conserved binding requirements through the whole gene family (Carlsson and Mahlapuu, 2002), and so a consensus binding site for Fox proteins has been defined. The binding DNA sequence specificity has been determined for several representatives of forkhead family through selection of binding sites from pools of short, random-sequence duplexes (Pierrou et al., 1995). A seven-nucleotide core corresponds to the major groove base contacts made by the recognition helix (helix 3). For the majority of forkhead proteins, the core conforms to the RYMAAYA (R _ A or G; Y _ C or T; M _ A or C) consensus (Kaufmann and Knochel, 1996). Since every Fox gene whose binding requirements have been analyzed binds to the consensus sequence RYMAAYA, it was logical to use this consensus in order to investigate the possibility of direct interaction between Foxb1 protein and EphA7 genomic sequence. It was encouraging to find out that, on the EphA7 receptor genomic sequence170kb (+ 10kb on either side), RYMAAYA sequences can be found with high frequency (here it is also interesting to mention that I could not find on EphA7 any DNA binding sites for transcription factor Pax6: not every combination of nucleotides is present on conserved regions of every gene). Here again, although at a different scale, bioinformatics made available for me a relatively large amount of data: the large number of RYMAAYA sequences on EphA7. Consequently, the next step was again to narrow down this data set by focusing on consensus sequences showing high frequency on the genome and clustering together. The new hypothesis was "Foxb1 is able to bind to these sequences". In order to test it, I used the three standard methods accepted in the field as proof of direct interaction. I used Yeast One-Hybrid Assay and Electrophoretic Mobility Shift Assay (EMSA) in order to prove that the RYMAAYA sites that I selected on the EphA7 genomic sequence do bind Foxb1, and I used cotransfection on cultured cells in order to prove that Foxb1 not only binds to those sequences but is able to influence EphA7 transcription through them. Both the yeast one-hybrid system (Liao and Fang, 2000; Sieweke, 2000) and the EMSA (or band shift assay) (Lane et al., 1992; Rippe et al., 2001) are

highly stringent, widely utilized methods to identify the recognition site of a transcription protein. Perhaps not surprisingly, these two methods gave the most clear-cut (and indeed positive) results: Foxb1 protein is able to bind to the RYMAAYA sequences found on EphA7.

4.2.2 Is Foxb1 an activator or a repressor of EphA7 transcription?

The next question, if through this binding Foxb1 is able to influence EphA7 transcription, is perhaps the last occurrence in this study of the "Biological Significance Question" discussed above, now narrowed down to the final test. To answer it I relied on the cotransfection approach, routinely used for this type of questions and well accepted in the field of molecular and cell biology (Claudio, 1992; Hauser et al., 1995; Zhang and Danielsen, 2001). However, as a reflection of the huge complexity of intact living cells as opposed to the oversimplification of in vitro assays, the results of these experiments were at first contradictory or paradoxal (instead of the expected activation we found evidence of repression of *EphA7* by Foxb1). Forkhead proteins have been shown to act mostly as transcriptional activators but not exclusively so: *trans*-repression has been reported for FoxC2, -D2, -D3, and -G1 and, in *C. elegans,* the forkhead protein LIN-31 is thought to act as either repressor or activator, depending on its phosphorylation in response to MAP kinase signaling (Carlsson and Mahlapuu, 2002). Even so, the repressor role of Foxb1 in the context of this study contradicted our DNA microarray, ISH and Q-PCR results. The problem could be that we were oversimplifying again. Foxb1 does not bind to isolated RYMAAYA sequences, but to RYMAAYA sequences embedded in a genomic context, that is, surrounded by other sequences which can be the target of DNA binding proteins acting as cofactors or modifiers of Foxb1 function. Like many other transcription factors, forkhead proteins often contain several activating regions, and these can be found in any location relative to the DNA binding domain. Little is known about the mechanisms through which forkhead proteins interact with the transcriptional machinery. *In vitro,* FOXF2 binds the general transcription factors TBP and TFIIB, and in cotransfection experiments, FOXF2 acts synergistically with TFIIB (Carlsson and Mahlapuu, 2002). Accordingly, my cotransfection experiments using long stretches of genomic sequence rather than "pure" RYMAAYA sequences were able to show Foxb1 as activator, in agreement with our data previously obtained by other methods.

4.2.3 Foxb1 as modulator of EphA7 transcription

However, EphA7 receptor expression did not disappear completely in Foxb1 null mutant.

Higher eukaryotes exploits signal integration and combinational control to a great degree. One case to illustrate this strategy is human interferon-ß gene, three signals are integrated to switch on

that gene (Ptashne and Gann, 2002).Studies of the EphA7 genomic sequence has identified a huge number of transcription factor binding sites both proximal and further downstream. This suggested that factor may modulate other transcription factors by direct interaction and by blocking their binding at the promoter. EphA7 receptor genome is 170kb and quite long, how might enhancer-binding proteins and their associated coactivators establish a productive interaction with the cognate promoter? Looping between the enhancer and promoter has been an attractive and popular hypothesis (Wang and Giaever, 1988; Blackwood and Kadonaga, 1998).

5 ABBREVIATIONS

3-AT	3-amino-1,2,4-triazole
amp	Ampicillin
BAC	Bacterial artificial chromosome
bp	Base pairs
CMV	Cytomegalovirus
CNS	Central nervous system
cDNA	Complementary DNA
C_T	Threshold cycle
DAB	Diaminobenzidine
DEPC	Diethylpyrocarbonate
DI	Diencephalon
DMSO	Dimethylsulfoxide
DNA	Deoxyribonucleic acid
DNase	Deoxyribonuclease
dsDNA	Double-strain DNA
dNTP	Deoxynucleotide
DIG	Digoxygenin
DTT	Dithiotheitol
E	Embryonic day
EDTA	Ethylene diamine tetraacetic acid
EF1a	Elonggation factor 1a
EMSA	Electrophoretic mobility shift assay
Fig.	Figure
Fox	Forkhead box
GluR2/3	Glutamine receptor 2 or 3
GPI	Glycosylphosphatidylinostitol
HB	Hindbrain
HEPES	N-2-hydroxyethylpiperazine-N'-2-ethane-sulfonic acid
ISH	*In situ* hybridization
IPTG	Isopropyl-ß-thiogalactopyranoside
kb	Kilo base
LB	Lauria-Bertani medium
LiAC	Lithium Acetate
LiCl	Lithium Chloride

M	mol/liter
MB	Midbrain
MBO	Mammillary body
mL	Milliliter
mM	Millimol
min	Minutes
mRNA	Messager RNA
NaAc	Sodium Acetate
NBT	Nitro-blue tetrazolium
NMR	Nuclear magnetic resonance
NTE	Sodium tris EDTA
P	Postnatal day
PAGE	Polyacrylamide gel electrophoresis
PBS	Phosphate buffered saline
PFA	Paraformaldehyde
PCR	Polymerase chain reaction
Q-PCR	Quantitative real-time PCR
RNA	Ribonucleic acid
RNase	Ribonuclease
rpm	Revolutions per minute
RTK	Receptor tyrosine kinase
RT	Reverse transcriptase
SD	Minimal synthetic dropout medium
SDS	Sodiumdodecylsulfate
SLR	Signal log ratio
SQ	Start quantity
SSC	Saline-sodium citrate buffer
TAE	Tris-acetate-EDTA
Taq	*Thermus aquaticus*
TBS	Tris borate EDTA
TEMED	N,N,N',N'-tetramethylethylenediamine
TNT	Tris sodium tween
Tris	Tris[hydroxymethyl]-aminomethane
U	Unit (Enzyme)
UTR	Untranslated region
Vs.	Versus
X-Gal	5-bromo-4-chloro-3-indolyl-ß-galactosidas

6 LITERATURE

Allen JF (2001) In silico veritas. Data-mining and automated discovery: the truth is in there. EMBO Rep 2:542-544.

Altschul SF, Gish W, Miller W, Myers EW, Lipman DJ (1990) Basic local alignment search tool. J Mol Biol 215:403-410.

Alvarez-Bolado G, Swanson LW (1996) Developmental Brain Maps: Structure of the Embryonic Rat Brain. Amsterdam: Elsevier.

Alvarez-Bolado G, Cecconi F, Wehr R, Gruss P (1999) The fork head transcription factor Fkh5/Mf3 is a developmental marker gene for superior colliculus layers and derivatives of the hindbrain somatic afferent zone. Brain Res Dev Brain Res 112:205-215.

Alvarez-Bolado G, Zhou X, Voss AK, Thomas T, Gruss P (2000) Winged helix transcription factor Foxb1 is essential for access of mammillothalamic axons to the thalamus. Development 127:1029-1038.

Ang SL, Wierda A, Wong D, Stevens KA, Cascio S, Rossant J, Zaret KS (1993) The formation and maintenance of the definitive endoderm lineage in the mouse: involvement of HNF3/forkhead proteins. Development 119:1301-1315.

Barlow C, Lockhart DJ (2002) DNA arrays and neurobiology--what′s new and what′s next? Curr Opin Neurobiol 12:554-561.

Bartley TD, Hunt RW, Welcher AA, Boyle WJ, Parker VP, Lindberg RA, Lu HS, Colombero AM, Elliott RL, Guthrie BA, et al. (1994) B61 is a ligand for the ECK receptor protein-tyrosine kinase. Nature 368:558-560.

Blackshaw S, Fraioli RE, Furukawa T, Cepko CL (2001) Comprehensive analysis of photoreceptor gene expression and the identification of candidate retinal disease genes. Cell 107:579-589.

Blackwood EM, Kadonaga JT (1998) Going the distance: a current view of enhancer action. Science 281:61-63.

Bolz J, Castellani V (1997) How do wiring molecules specify cortical connections? Cell Tissue Res 290:307-314.

Bourguignon C, Li J, Papalopulu N (1998) XBF-1, a winged helix transcription factor with dual activity, has a role in positioning neurogenesis in Xenopus competent ectoderm. Development 125:4889-4900.

Brazma A, Vilo J (2000) Gene expression data analysis. FEBS Lett 480:17-24.

Canteras NS, Swanson LW (1992) The dorsal premammillary nucleus: an unusual component of the mammillary body. Proc Natl Acad Sci U S A 89:10089-10093.

Carlsson P, Mahlapuu M (2002) Forkhead transcription factors: key players in development and metabolism. Dev Biol 250:1-23.

Cheng HJ, Flanagan JG (1994) Identification and cloning of ELF-1, a developmentally expressed ligand for the Mek4 and Sek receptor tyrosine kinases. Cell 79:157-168.

Chuaqui RF, Bonner RF, Best CJ, Gillespie JW, Flaig MJ, Hewitt SM, Phillips JL, Krizman DB, Tangrea MA, Ahram M, Linehan WM, Knezevic V, Emmert-Buck MR (2002) Post-analysis follow-up and validation of microarray experiments. Nat Genet 32 Suppl:509-514.

Ciossek T, Ullrich A (1997) Identification of Elf-1 and B61 as high affinity ligands for the receptor tyrosine kinase MDK1. Oncogene 14:35-43.

Ciossek T, Lerch MM, Ullrich A (1995a) Cloning, characterization, and differential expression of MDK2 and MDK5, two novel receptor tyrosine kinases of the eck/eph family. Oncogene 11:2085-2095.

Ciossek T, Millauer B, Ullrich A (1995b) Identification of alternatively spliced mRNAs encoding variants of MDK1, a novel receptor tyrosine kinase expressed in the murine nervous system. Oncogene 10:97-108.

Ciossek T, Ullrich A, West E, Rogers JH (1999) Segregation of the receptor EphA7 from its tyrosine kinase-negative isoform on neurons in adult mouse brain. Brain Res Mol Brain Res 74:231-236.

Clark KL, Halay ED, Lai E, Burley SK (1993) Co-crystal structure of the HNF-3/fork head DNA-recognition motif resembles histone H5. Nature 364:412-420.

Claudio T (1992) Stable expression of heterologous multisubunit protein complexes established by calcium phosphate- or lipid-mediated cotransfection. Methods Enzymol 207:391-408.

Collective TABPWG (2004) Expression profiling--best practices for data generation and interpretation in clinical trials. Nat Rev Genet 5:229-237.

Courey A (2001) Regulator transcription factors and *cis*-regulatory regions, in Transcription factor, edited by L locker,. BIOS scientific publisher LTD: Oxford, UK.

Dent CL, Smith MD, Latchman DS (1999) The DNA Mobility Shift Assay. In: Transcription Factors. A Practical Approach (Latchman DS, ed), pp 1-26. Oxford: Oxford University Press.

Diaz E, Ge Y, Yang YH, Loh KC, Serafini TA, Okazaki Y, Hayashizaki Y, Speed TP, Ngai J, Scheiffele P (2002) Molecular analysis of gene expression in the developing pontocerebellar projection system. Neuron 36:417-434.

Dickson BJ (2002) Molecular mechanisms of axon guidance. Science 298:1959-1964.

Docherty K (1996) Gene Transcription. DNA Binding Proteins. Chichester: John Wiley & Sons.

Dou C, Ye X, Stewart C, Lai E, Li SC (1997) TWH regulates the development of subsets of spinal cord neurons. Neuron 18:539-551.

Drescher U (1997) The Eph family in the patterning of neural development. Curr Biol 7:R799-807.

Drescher U, Bonhoeffer F, Muller BK (1997) The Eph family in retinal axon guidance. Curr Opin Neurobiol 7:75-80.

Drescher U, Kremoser C, Handwerker C, Loschinger J, Noda M, Bonhoeffer F (1995) In vitro guidance of retinal ganglion cell axons by RAGS, a 25 kDa tectal protein related to ligands for Eph receptor tyrosine kinases. Cell 82:359-370.

Elble RC, Pauli BU (2001) Tumor suppression by a proapoptotic calcium-activated chloride channel in mammary epithelium. J Biol Chem 276:40510-40517.

Elkahloun AG, Gaudet J, Robinson GS, Sgroi DC (2002) In situ gene expression analysis of cancer using laser capture microdissection, microarrays and real time quantitative PCR. Cancer Biol Ther 1:354-358.

Ellis J, Liu Q, Breitman M, Jenkins NA, Gilbert DJ, Copeland NG, Tempest HV, Warren S, Muir E, Schilling H, et al. (1995) Embryo brain kinase: a novel gene of the eph/elk receptor tyrosine kinase family. Mech Dev 52:319-341.

Ernstsson S, Betz R, Lagercrantz S, Larsson C, Ericksson S, Cederberg A, Carlsson P, Enerback S (1997) Cloning and characterization of freac-9 (FKHL17), a novel kidney-expressed human forkhead gene that maps to chromosome 1p32-p34. Genomics 46:78-85.

Fairall L, Schwabe J (2001) DNA binding by transcription factor, in Transcription factor, edited by J Locker. BIOS scientific publishers LTD: Oxford, UK.

Flanagan JG, Vanderhaeghen P (1998) The ephrins and Eph receptors in neural development. Annu Rev Neurosci 21:309-345.

Frisen J, Yates PA, McLaughlin T, Friedman GC, O'Leary DD, Barbacid M (1998) Ephrin-A5 (AL-1/RAGS) is essential for proper retinal axon guidance and topographic mapping in the mammalian visual system. Neuron 20:235-243.

Gale NW, Flenniken A, Compton DC, Jenkins N, Copeland NG, Gilbert DJ, Davis S, Wilkinson DG, Yancopoulos GD (1996a) Elk-L3, a novel transmembrane ligand for the Eph family of receptor tyrosine kinases, expressed in embryonic floor plate, roof plate and hindbrain segments. Oncogene 13:1343-1352.

Gale NW, Holland SJ, Valenzuela DM, Flenniken A, Pan L, Ryan TE, Henkemeyer M, Strebhardt K, Hirai H, Wilkinson DG, Pawson T, Davis S, Yancopoulos GD (1996b) Eph receptors and ligands comprise two major specificity subclasses and are reciprocally compartmentalized during embryogenesis. Neuron 17:9-19.

Gandhi R, Elble RC, Gruber AD, Schreur KD, Ji HL, Fuller CM, Pauli BU (1998) Molecular and functional characterization of a calcium-sensitive chloride channel from mouse lung. J Biol Chem 273:32096-32101.

Geschwind DH, Ou J, Easterday MC, Dougherty JD, Jackson RL, Chen Z, Antoine H, Terskikh A, Weissman IL, Nelson SF, Kornblum HI (2001) A genetic analysis of neural progenitor differentiation. Neuron 29:325-339.

Gilbert S (1997) Developmental biology, 5th Edition. Sunderland, Massachusettes: Sinauer Associates.

Giulietti A, Overbergh L, Valckx D, Decallonne B, Bouillon R, Mathieu C (2001) An overview of real-time quantitative PCR: applications to quantify cytokine gene expression. Methods 25:386-401.

Griffin RS, Mills CD, Costigan M, Woolf CJ (2003) Exploiting microarrays to reveal differential gene expression in the nervous system. Genome Biol 4:105.

Guan KL, Rao Y (2003) Signalling mechanisms mediating neuronal responses to guidance cues. Nat Rev Neurosci 4:941-956.

Hauser CA, Westwick JK, Quilliam LA (1995) Ras-mediated transcription activation: analysis by transient cotransfection assays. Methods Enzymol 255:412-426.

Hellqvist M, Mahlapuu M, Samuelsson L, Enerback S, Carlsson P (1996) Differential activation of lung-specific genes by two forkhead proteins, FREAC-1 and FREAC-2. J Biol Chem 271:4482-4490.

Hellqvist M, Mahlapuu M, Blixt A, Enerback S, Carlsson P (1998) The human forkhead protein FREAC-2 contains two functionally redundant activation domains and interacts with TBP and TFIIB. J Biol Chem 273:23335-23343.

Helmbacher F, Schneider-Maunoury S, Topilko P, Tiret L, Charnay P (2000) Targeting of the EphA4 tyrosine kinase receptor affects dorsal/ventral pathfinding of limb motor axons. Development 127:3313-3324.

Herzig U, Cadenas C, Sieckmann F, Sierralta W, Thaller C, Visel A, Eichele G (2001) Development of high-throughput tools to unravel the complexity of gene expression patterns in the mammalian brain. Novartis Found Symp 239:129-146; discussion 146-159.

Holmberg J, Clarke DL, Frisen J (2000) Regulation of repulsion versus adhesion by different splice forms of an Eph receptor. Nature 408:203-206.

Jiang Y, Harlocker SL, Molesh DA, Dillon DC, Stolk JA, Houghton RL, Repasky EA, Badaro R, Reed SG, Xu J (2002) Discovery of differentially expressed genes in human breast cancer using subtracted cDNA libraries and cDNA microarrays. Oncogene 21:2270-2282.

Jin C, Marsden I, Chen X, Liao X (1999) Dynamic DNA contacts observed in the NMR structure of winged helix protein-DNA complex. J Mol Biol 289:683-690.

Kaestner KH, Schutz G, Monaghan AP (1996) Expression of the winged helix genes fkh-4 and fkh-5 defines domains in the central nervous system. Mech Dev 55:221-230.

Kaestner KH, Knochel W, Martinez DE (2000) Unified nomenclature for the winged helix/forkhead transcription factors. Genes Dev 14:142-146.

Kaufmann E, Knochel W (1996) Five years on the wings of fork head. Mech Dev 57:3-20.

Kaufmann E, Muller D, Knochel W (1995) DNA recognition site analysis of Xenopus winged helix proteins. J Mol Biol 248:239-254.

Kell DB, Oliver SG (2004) Here is the evidence, now what is the hypothesis? The complementary roles of inductive and hypothesis-driven science in the post-genomic era. Bioessays 26:99-105.

Knoll B, Drescher U (2002) Ephrin-As as receptors in topographic projections. Trends Neurosci 25:145-149.

Kullander K, Klein R (2002) Mechanisms and functions of Eph and ephrin signalling. Nat Rev Mol Cell Biol 3:475-486.

Kume T, Deng KY, Winfrey V, Gould DB, Walter MA, Hogan BL (1998) The forkhead/winged helix gene Mf1 is disrupted in the pleiotropic mouse mutation congenital hydrocephalus. Cell 93:985-996.

Labosky PA, Winnier GE, Sasaki H, Blessing M, Hogan BL (1996) The chromosomal mapping of four genes encoding winged helix proteins expressed early in mouse development. Genomics 34:241-245.

Labosky PA, Winnier GE, Jetton TL, Hargett L, Ryan AK, Rosenfeld MG, Parlow AF, Hogan BL (1997) The winged helix gene, Mf3, is required for normal development of the diencephalon and midbrain, postnatal growth and the milk-ejection reflex. Development 124:1263-1274.

Lai E, Clark KL, Burley SK, Darnell JE, Jr. (1993) Hepatocyte nuclear factor 3/fork head or "winged helix" proteins: a family of transcription factors of diverse biologic function. Proc Natl Acad Sci U S A 90:10421-10423.

Lander ES, Linton LM, Birren B, Nusbaum C, Zody MC, Baldwin J, Devon K, Dewar K, Doyle M, FitzHugh W, Funke R, Gage D, Harris K, Heaford A, Howland J, Kann L, Lehoczky J, LeVine R, McEwan P, McKernan K, Meldrim J, Mesirov JP, Miranda C, Morris W, Naylor J, Raymond C, Rosetti M, Santos R, Sheridan A, Sougnez C, Stange-Thomann N, Stojanovic N, Subramanian A, Wyman D, Rogers J, Sulston J, Ainscough R, Beck S, Bentley D, Burton J, Clee C, Carter N, Coulson A, Deadman R, Deloukas P, Dunham A, Dunham I, Durbin R, French L, Grafham D, Gregory S, Hubbard T, Humphray S, Hunt A, Jones M, Lloyd C, McMurray A, Matthews L, Mercer S, Milne S, Mullikin JC, Mungall A, Plumb R, Ross M, Shownkeen R, Sims S, Waterston RH, Wilson RK, Hillier LW, McPherson JD, Marra MA, Mardis ER, Fulton LA, Chinwalla AT, Pepin KH, Gish WR, Chissoe SL, Wendl MC, Delehaunty KD, Miner TL, Delehaunty A, Kramer JB, Cook LL, Fulton RS, Johnson DL, Minx PJ, Clifton SW, Hawkins T, Branscomb E, Predki P, Richardson P, Wenning S, Slezak T, Doggett N, Cheng JF, Olsen A, Lucas S, Elkin C, Uberbacher E, Frazier M, et al. (2001) Initial sequencing and analysis of the human genome. Nature 409:860-921.

Lane D, Prentki P, Chandler M (1992) Use of gel retardation to analyze protein-nucleic acid interactions. Microbiol Rev 56:509-528.

Latchman DS (1999) Transcription Factors. A Practical Approach. Oxford: Oxford University Press.

Liao M, Fang F (2000) [Yeast one-hybrid system--one effective method studying DNA-protein interaction]. Zhongguo Yi Xue Ke Xue Yuan Xue Bao 22:388-391.

Lockhart DJ, Winzeler EA (2000) Genomics, gene expression and DNA arrays. Nature 405:827-836.

Lockhart DJ, Barlow C (2001) Expressing what′s on your mind: DNA arrays and the brain. Nat Rev Neurosci 2:63-68.

Marthiens V, Padilla F, Lambert M, Mege RM (2002) Complementary expression and regulation of cadherins 6 and 11 during specific steps of motoneuron differentiation. Mol Cell Neurosci 20:458-475.

Mayanil CS, George D, Freilich L, Miljan EJ, Mania-Farnell B, McLone DG, Bremer EG (2001) Microarray analysis detects novel Pax3 downstream target genes. J Biol Chem 276:49299-49309.

McBurney MW, Rogers BJ (1982) Isolation of male embryonal carcinoma cells and their chromosome replication patterns. Dev Biol 89:503-508.

Mills JC, Roth KA, Cagan RL, Gordon JI (2001) DNA microarrays and beyond: completing the journey from tissue to cell. Nat Cell Biol 3:E175-178.

Mimmack ML, Brooking J, Bahn S (2004) Quantitative polymerase chain reaction: validation of microarray results from postmortem brain studies. Biol Psychiatry 55:337-345.

Mirnics K, Pevsner J (2004) Progress in the use of microarray technology to study the neurobiology of disease. Nat Neurosci 7:434-439.

Mitchell PJ, Tjian R (1989) Transcriptional regulation in mammalian cells by sequence-specific DNA binding proteins. Science 245:371-378.

Mori T, Wanaka A, Taguchi A, Matsumoto K, Tohyama M (1995) Localization of novel receptor tyrosine kinase genes of the eph family, MDK1 and its splicing variant, in the developing mouse nervous system. Brain Res Mol Brain Res 34:154-160.

Mueller BK (1999) Growth cone guidance: first steps towards a deeper understanding. Annu Rev Neurosci 22:351-388.

Mutch DM, Berger A, Mansourian R, Rytz A, Roberts MA (2001) Microarray data analysis: a practical approach for selecting differentially expressed genes. Genome Biol 2:PREPRINT0009.

Nagy A, Gertsenstein M, Vintersten K, Behringer R (2002) Manipulating the mouse embryo: a laboratory manual, 3rd Edition. Cold Spring Harbor: Cold Spring Harbor Laboratory Press.

Nakamoto M, Cheng HJ, Friedman GC, McLaughlin T, Hansen MJ, Yoon CH, O′Leary DD, Flanagan JG (1996) Topographically specific effects of ELF-1 on retinal axon guidance in vitro and retinal axon mapping in vivo. Cell 86:755-766.

Overdier DG, Porcella A, Costa RH (1994) The DNA-binding specificity of the hepatocyte nuclear factor 3/forkhead domain is influenced by amino-acid residues adjacent to the recognition helix. Mol Cell Biol 14:2755-2766.

Pabo CO, Sauer RT (1992) Transcription factors: structural families and principles of DNA recognition. Annu Rev Biochem 61:1053-1095.

Pani L, Overdier DG, Porcella A, Qian X, Lai E, Costa RH (1992) Hepatocyte nuclear factor 3 beta contains two transcriptional activation domains, one of which is novel and conserved with the Drosophila fork head protein. Mol Cell Biol 12:3723-3732.

Park S, Frisen J, Barbacid M (1997) Aberrant axonal projections in mice lacking EphA8 (Eek) tyrosine protein kinase receptors. Embo J 16:3106-3114.

Pierrou S, Enerback S, Carlsson P (1995) Selection of high-affinity binding sites for sequence-specific, DNA binding proteins from random sequence oligonucleotides. Anal Biochem 229:99-105.

Pierrou S, Hellqvist M, Samuelsson L, Enerback S, Carlsson P (1994) Cloning and characterization of seven human forkhead proteins: binding site specificity and DNA bending. Embo J 13:5002-5012.

Ptashne M, Gann A (2002) Genes & Signals. Cold Spring Harbor, New York: Cold Spring Harbor Laboratory Press.

Radyushkin KA, Anokhin KV, Meyer B, Jiang Q, Alvarez-Bolado G, Gruss P (2005) Genetic ablation of the mammillary bodies in the Foxb1 mutant mouse leads to selective deficit of spatial working memory. Eur J Neurol *(in press)*.

Rajeevan MS, Vernon SD, Taysavang N, Unger ER (2001) Validation of array-based gene expression profiles by real-time (kinetic) RT-PCR. J Mol Diagn 3:26-31.

Ramalho-Santos M, Yoon S, Matsuzaki Y, Mulligan RC, Melton DA (2002) "Stemness": transcriptional profiling of embryonic and adult stem cells. Science 298:597-600.

Read M (1996) Protocols. Electrophoretic Mobility Shift Assay. In: Gene Transcription. DNA Binding Proteins (Docherty K, ed), pp 6-33. Chichester: John Wiley & Sons.

Rippe RA, Brenner DA, Tugores A (2001) Techniques to measure nucleic acid-protein binding and specificity. Nuclear extract preparations, DNase I footprinting, and mobility shift assays. Methods Mol Biol 160:459-479.

Risold PY, Swanson LW (1995) Evidence for a hypothalamothalamocortical circuit mediating pheromonal influences on eye and head movements. Proc Natl Acad Sci U S A 92:3898-3902.

Risold PY, Thompson RH, Swanson LW (1997) The structural organization of connections between hypothalamus and cerebral cortex. Brain Res Brain Res Rev 24:197-254.

Rogers JH, Ciossek T, Ullrich A, West E, Hoare M, Muir EM (1999) Distribution of the receptor EphA7 and its ligands in development of the mouse nervous system. Brain Res Mol Brain Res 74:225-230.

Roskies AL, O′Leary DD (1994) Control of topographic retinal axon branching by inhibitory membrane-bound molecules. Science 265:799-803.

Roux J, Pictet R, Grange T (1995) Hepatocyte nuclear factor 3 determines the amplitude of the glucocorticoid response of the rat tyrosine aminotransferase gene. DNA Cell Biol 14:385-396.

Sambrook J, Russell DW (2001) Molecular Cloning. A Laboratory Manual, 3rd Edition Edition. Cold Spring Harbor: Cold Spring Harbor Laboratory Press.

Sandberg R, Yasuda R, Pankratz DG, Carter TA, Del Rio JA, Wodicka L, Mayford M, Lockhart DJ, Barlow C (2000) Regional and strain-specific gene expression mapping in the adult mouse brain. Proc Natl Acad Sci U S A 97:11038-11043.

Schuddekopf K, Schorpp M, Boehm T (1996) The whn transcription factor encoded by the nude locus contains an evolutionarily conserved and functionally indispensable activation domain. Proc Natl Acad Sci U S A 93:9661-9664.

Schulte D, Cepko CL (2000) Two homeobox genes define the domain of EphA3 expression in the developing chick retina. Development 127:5033-5045.

Sgroi DC, Teng S, Robinson G, LeVangie R, Hudson JR, Jr., Elkahloun AG (1999) In vivo gene expression profile analysis of human breast cancer progression. Cancer Res 59:5656-5661.

Shoemaker DD, Linsley PS (2002) Recent developments in DNA microarrays. Curr Opin Microbiol 5:334-337.

Sieweke M (2000) Detection of transcription factor partners with a yeast one hybrid screen. Methods Mol Biol 130:59-77.

Smalheiser NR (2002) Informatics and hypothesis-driven research. EMBO Rep 3:702.

Sobieszczuk DF, Wilkinson DG (1999) Masking of Eph receptors and ephrins. Curr Biol 9:R469-470.

St-Arnaud R (1998) Transcriptional regulation during mesenchymal cell differentiation: the role of coactivators. Crit Rev Eukaryot Gene Expr 8:191-202.

Steinhauser D, Junker BH, Luedemann A, Selbig J, Kopka J (2004) Hypothesis-driven approach to predict transcriptional units from gene expression data. Bioinformatics 20:1928-1939.

Talukder AH, Muramatsu T, Kaneda N (1997) A novel truncated variant form of Ebk/MDK1 receptor tyrosine kinase is expressed in embryonic mouse brain. Cell Struct Funct 22:477-485.

Tan PB, Lackner MR, Kim SK (1998) MAP kinase signaling specificity mediated by the LIN-1 Ets/LIN-31 WH transcription factor complex during C. elegans vulval induction. Cell 93:569-580.

Tessier-Lavigne M, Goodman CS (1996) The molecular biology of axon guidance. Science 274:1123-1133.

Tjian R, Maniatis T (1994) Transcriptional activation: a complex puzzle with few easy pieces. Cell 77:5-8.

Valenzuela DM, Rojas E, Griffiths JA, Compton DL, Gisser M, Ip NY, Goldfarb M, Yancopoulos GD (1995) Identification of full-length and truncated forms of Ehk-3, a novel member of the Eph receptor tyrosine kinase family. Oncogene 10:1573-1580.

Vann SD, Aggleton JP (2003) Evidence of a spatial encoding deficit in rats with lesions of the mammillary bodies or mammillothalamic tract. J Neurosci 23:3506-3514.

Visel A, Thaller C, Eichele G (2004) GenePaint.org: an atlas of gene expression patterns in the mouse embryo. Nucleic Acids Res 32 Database issue:D552-556.

Wang B, Weidenfeld J, Lu MM, Maika S, Kuziel WA, Morrisey EE, Tucker PW (2004) Foxp1 regulates cardiac outflow tract, endocardial cushion morphogenesis and myocyte proliferation and maturation. Development 131:4477-4487.

Wang JC, Giaever GN (1988) Action at a distance along a DNA. Science 240:300-304.

Wang T, Brown MJ (1999) mRNA quantification by real time TaqMan polymerase chain reaction: validation and comparison with RNase protection. Anal Biochem 269:198-201.

Watanabe Y, Toyoda R, Nakamura H (2004) Navigation of trochlear motor axons along the midbrain-hindbrain boundary by neuropilin 2. Development 131:681-692.

Waterston RH, Lindblad-Toh K, Birney E, Rogers J, Abril JF, Agarwal P, Agarwala R, Ainscough R, Alexandersson M, An P, Antonarakis SE, Attwood J, Baertsch R, Bailey J, Barlow K, Beck S, Berry E, Birren B, Bloom T, Bork P, Botcherby M, Bray N, Brent MR, Brown DG, Brown SD, Bult C, Burton J, Butler J, Campbell RD, Carninci P, Cawley S, Chiaromonte F, Chinwalla AT, Church DM, Clamp M, Clee C, Collins FS, Cook LL, Copley RR, Coulson A, Couronne O, Cuff J, Curwen V, Cutts T, Daly M, David R, Davies J, Delehaunty KD, Deri J, Dermitzakis ET, Dewey C, Dickens NJ, Diekhans M, Dodge S, Dubchak I, Dunn DM, Eddy SR, Elnitski L, Emes RD, Eswara P, Eyras E, Felsenfeld A, Fewell GA, Flicek P, Foley K, Frankel WN, Fulton LA, Fulton RS, Furey TS, Gage D, Gibbs RA, Glusman G, Gnerre S, Goldman N, Goodstadt L, Grafham D, Graves TA, Green ED, Gregory S, Guigo R, Guyer M, Hardison RC, Haussler D, Hayashizaki Y, Hillier LW, Hinrichs A, Hlavina W, Holzer T, Hsu F, Hua A, Hubbard T, Hunt A, Jackson I, Jaffe DB, Johnson LS, Jones M, Jones TA, Joy A, Kamal M, Karlsson EK, et al. (2002) Initial sequencing and comparative analysis of the mouse genome. Nature 420:520-562.

Wehr R, Mansouri A, de Maeyer T, Gruss P (1997) Fkh5-deficient mice show dysgenesis in the caudal midbrain and hypothalamic mammillary body. Development 124:4447-4456.

Weigel D, Jackle H (1990) The fork head domain: a novel DNA binding motif of eukaryotic transcription factors? Cell 63:455-456.

Weigel D, Jurgens G, Kuttner F, Seifert E, Jackle H (1989) The homeotic gene fork head encodes a nuclear protein and is expressed in the terminal regions of the Drosophila embryo. Cell 57:645-658.

Weigelt J, Climent I, Dahlman-Wright K, Wikstrom M (2001) Solution structure of the DNA binding domain of the human forkhead transcription factor AFX (FOXO4). Biochemistry 40:5861-5869.

Weinstein JN (2002) ′Omic′ and hypothesis-driven research in the molecular pharmacology of cancer. Curr Opin Pharmacol 2:361-365.

Wilkinson DG (2000) Topographic mapping: organising by repulsion and competition? Curr Biol 10:R447-451.

Wilkinson DG (2001) Multiple roles of EPH receptors and ephrins in neural development. Nat Rev Neurosci 2:155-164.

Xu Q, Alldus G, Macdonald R, Wilkinson DG, Holder N (1996) Function of the Eph-related kinase rtk1 in patterning of the zebrafish forebrain. Nature 381:319-322.

Yao J, Lai E, Stifani S (2001) The winged-helix protein brain factor 1 interacts with groucho and hes proteins to repress transcription. Mol Cell Biol 21:1962-1972.

Zhang S, Danielsen M (2001) Cotransfection assays and steroid receptor biology. Methods Mol Biol 176:297-316.

Zhao X, Lein ES, He A, Smith SC, Aston C, Gage FH (2001) Transcriptional profiling reveals strict boundaries between hippocampal subregions. J Comp Neurol 441:187-196.

Zhou R (1998) The Eph family receptors and ligands. Pharmacol Ther 77:151-181.

Zirlinger M, Kreiman G, Anderson DJ (2001) Amygdala-enriched genes identified by microarray technology are restricted to specific amygdaloid subnuclei. Proc Natl Acad Sci U S A 98:5270-5275.

CURRICULUM VITAE

Name: **Qiuhong Jiang**
Date of birth: Dec 8th, 1972
Place of birth: Hunan, China

Address: Schierholz-Str. 5A,
30655, Hannover

Contact: Telephone: 0511/5359102; 0175-6392416
email: qiuhong.jiang@mpihan.mpg.de

Education and Professional Experience

Sep/1991-Jun/1995 **Bachelor of Science** (Biology)
Xiangtan Teacher University, China

Sep/1995-Jun/1998 **Master of Science** (Biochemistry)
Thesis: "Purification of ribosome inactivating protein from plant seeds"
Northwest Agriculture University, China

Sep/1998-Jun/1999 **PhD Preparation Course** (Advanced Biochemistry)
Chinese Academy of Sciences, Shanghai, China

Jun/1998-April/2002 **Staff Scientist** (state key laboratory of Molecular Biology)
Shanghai Institute of Biochemistry and Cell Biology, Chinese Academy of Sciences

May/2002-present **PhD Student**
MPI of Experimental Endocrinology, Hannover, Germany
Topic: "Role of *Foxb1* in transcriptional control of axonal pathfinding"
Supervisors: Dr. G. Alvarez-Bolado (MPI), Prof. Dr. W. Müller (MHH)

PUBLICATIONS

Jiang, Q. and Alvarez-Bolado, G. *Transcription factor Foxb1 influences mammillo-thalamic tract development cell autonomously through control of EphA7 expression.* (In preparation)

Radyushkin, K.A., Anokhin, K. V., Meyer, B., **Jiang, Q.,** Alvarez-Bolado, G. and Gruss, P. (2005) *Genetic ablation of the mammillary bodies in the Foxb1 mutant mouse leads to selective deficit of spatial working memory*. Eur. J. Neurol. (in press)

ERKLÄRUNG

Hereby I declare that I did all of the work described in this thesis myself and that I indicated all means that were used and help that was provided by others. The results included in this work were never used for another thesis (e.g. Diploma) and, except the indicated partial publications, have not been published otherwise.

Hannover, 28. September 2004

(Qiuhong Jiang)